VARIOUS
HYBRID MICROWAVE/MIC COMPONENT DEVELOPMENTS

ILLUSTRATIONS (U)

TABLES (U)

ACKNOWLEDGMENTS (U)

(U) The authors acknowledge the significant contributions made by Mr. Allen Podell to the initial phases of the work presented in this report. The new W coupler concept and "proximity-effect" 3-dB quadrature hybrid are primarily results of his physical insight.

(U) The valuable contributions of Mr. Joe Hunt, Mr. York Sato, and Mr. Helmut Moessner in the fabrication and testing of the components are also acknowledged.

(U) The anticipated difficulty from diode breakage during assembly was not experienced for the three switches constructed, although a total of eight diodes per switch was used. Better switch performance, particularly lower losses and greater isolation, could be obtained by using the improved construction techniques that were developed after the DPDT switches were completed. In many applications, a similar switch design with one diode per arm would have adequate isolation characteristics and would be much easier to fabricate because of the reduced complexity.

5. SPDT Switch (U)

(U) The design of the SPDT switch derives easily from the DPDT switch design. It was concluded that for the DPDT switch, placing all diodes in the shunt configuration provides the best compromise for performance, manufacturability, and integration into monolithic circuits. This conclusion also applies to the SPDT switch. In addition, all other design techniques and criteria developed are influenced to a greater extent by the choice of the microstrip medium than by the switch configuration, so those outlined for the DPDT switch apply equally well to the SPDT switch.

6. Frequency Translator (U)

(U) To avoid spurious responses in a broadband frequency translator, some means for providing resistive loading of the "switched-out" transmission-line sections is required. The use of DPDT switches to simultaneously select the phase-shift bits and to terminate the temporarily unused transmission-line elements is the most effective technique for providing the desired spurious free operation. Therefore, a microstrip DPDT switch is a critical element in the frequency translator.

(U)
In the microstrip medium, realization of the phase-shifter part of the frequency-translator circuit is also critical. Broadband C-section phase shifters require relatively tightly coupled line sections. Because the coupling that can be achieved with edge-coupled microstrip is limited in the practical case, better performance can be achieved by using 45° sections throughout. That is, for the 90° bit, two 45° sections in tandem would be used and the 180° bit would be made up of four 45° C-sections.

(U) Implementation of the frequency translator also requires successful integration of several additional microstrip components including diode biasing circuits, blocking capacitors, 50-ohm terminations, and transmission-line crossovers. All of the necessary components have been successfully demonstrated over the frequency band of interest, with the exception of the transmission-line crossover. Additional effort would be required to develop a suitable transmission-line crossover and to demonstrate a completed frequency-translator model.

7. Circulators (U)

(U) The circulators supplied by Western Microwave are constructed in the stripline, rather than the microstrip medium, and are therefore of questionable use in monolithic circuits.

8. Limiter Detector (U)

(U) A design for a limiter detector is worked out in Section IV; however, no units were tested to determine its ultimate power-handling capability.

2. Electrical Properties (U)

(U) The major difference between quartz and sapphire is the relative dielectric constant as shown in Table II-1.

Table II-1

(U) DIELECTRIC-MATERIAL CHARACTERISTICS (U)

Parameter	Subtrate			
	Quartz	Sapphire	Beryllia	Alumina
Dielectric constant	3.78	10.55 $\|\|$ to c-axis	6.5	9.7
Loss tangent	0.0004	0.0002	0.0005	0.0002
Thermal conductivity (cal/cm/°C/s)	0.0035	0.08	0.5	0.05
Thermal expansion	0.55×10^{-6}	5.8×10^{-6}	7×10^{-6}	8×10^{-6}
Dielectric attenuation (dB/wavelength)	0.01	0.005	0.013	0.005

(U) The lower dielectric constant of quartz is an advantage when conductor losses are considered. Figure II-1 shows the ratio of the microstrip conductor width to the dielectric substrate thickness (w/h) as a function of the relative dielectric constant of the material. For a 50-ohm line, the conductor width on quartz is 2.4 times the width on sapphire for equal dielectric thicknesses. At P-band wavelengths, the dielectric losses are small compared to conductor losses for both quartz and sapphire, so that the total loss per unit length is approximately 2.4 times as great for sapphire as for quartz. However, the loss per wavelength is more meaningful for circuit components constructed from multiples of quarter-wave line lengths such as couplers and matching networks. Because the effective wavelength is less for sapphire than for quartz, the loss per effective wavelength compares more favorably and is approximately 1.33 times as great for sapphire as for quartz.

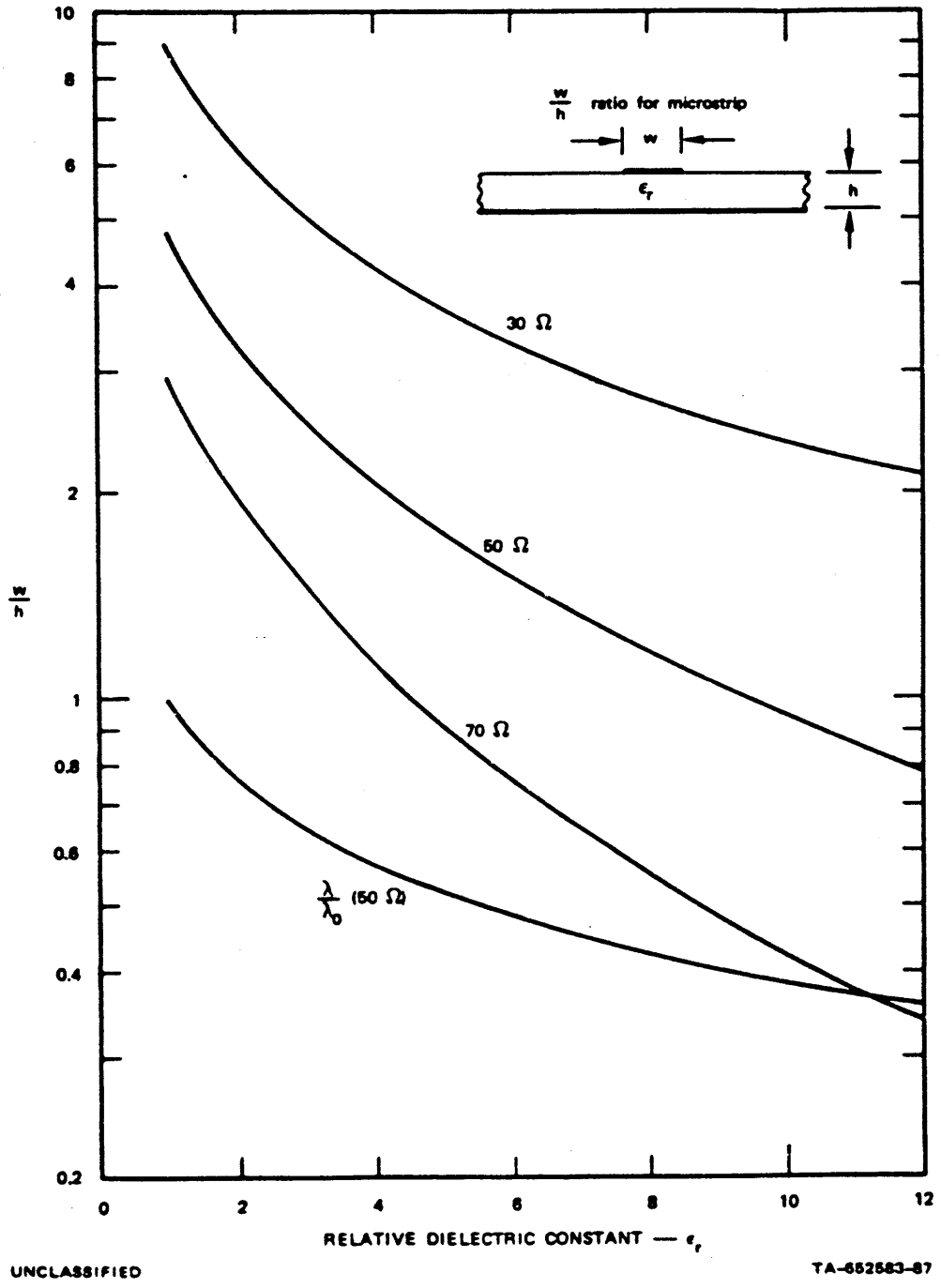

FIGURE II-1 w/h RATIO FOR MICROSTRIP (U)

(U)

Estimates of the loss for 50-ohm lines of gold conductors 1 μm thick (five skin depths at 18 GHz) on 0.010-inch-thick substrates are shown in Figure II-2.

C. Selection of Substrate Material and Thickness (U)

1. A Critical Component (U)

(U) On considerations of loss alone, the quartz substrate is slightly superior to sapphire. However, the 3-dB hybrid is a critical component and its design constraints must be factored into the choice of substrate material. In Section III-B, the 3-dB hybrid design is discussed, and it is determined that the most optimum approach is a tandem connection of two 8.3-dB couplers. Figure II-3 shows relative layouts for an 8.3-dB coupler on two thicknesses of both sapphire and quartz. For each substrate thickness, the differences in geometry are due entirely to the differences in dielectric constant.

2. Form Factor (U)

(U) The choice between substrate material and substrate thickness must be considered together. Two of the main determining factors are the width of the gap between the coupled arms and the form factor of the overall coupler layout. For substrate thicknesses of 0.025 inch, the form factor, denoted by ℓ/w in Figure II-3, is on the order of 2 for both quartz and sapphire. Experience has shown that couplers with form factors less than 3 or 4 tend to require more empirical adjustment than those with larger form factors. For smaller form factors, the couplings at the ends of the coupler constitute a larger percentage of the total coupling. The current distributions at the coupler ends, due to the geometrical discontinuities, result in coupling and impedance factors

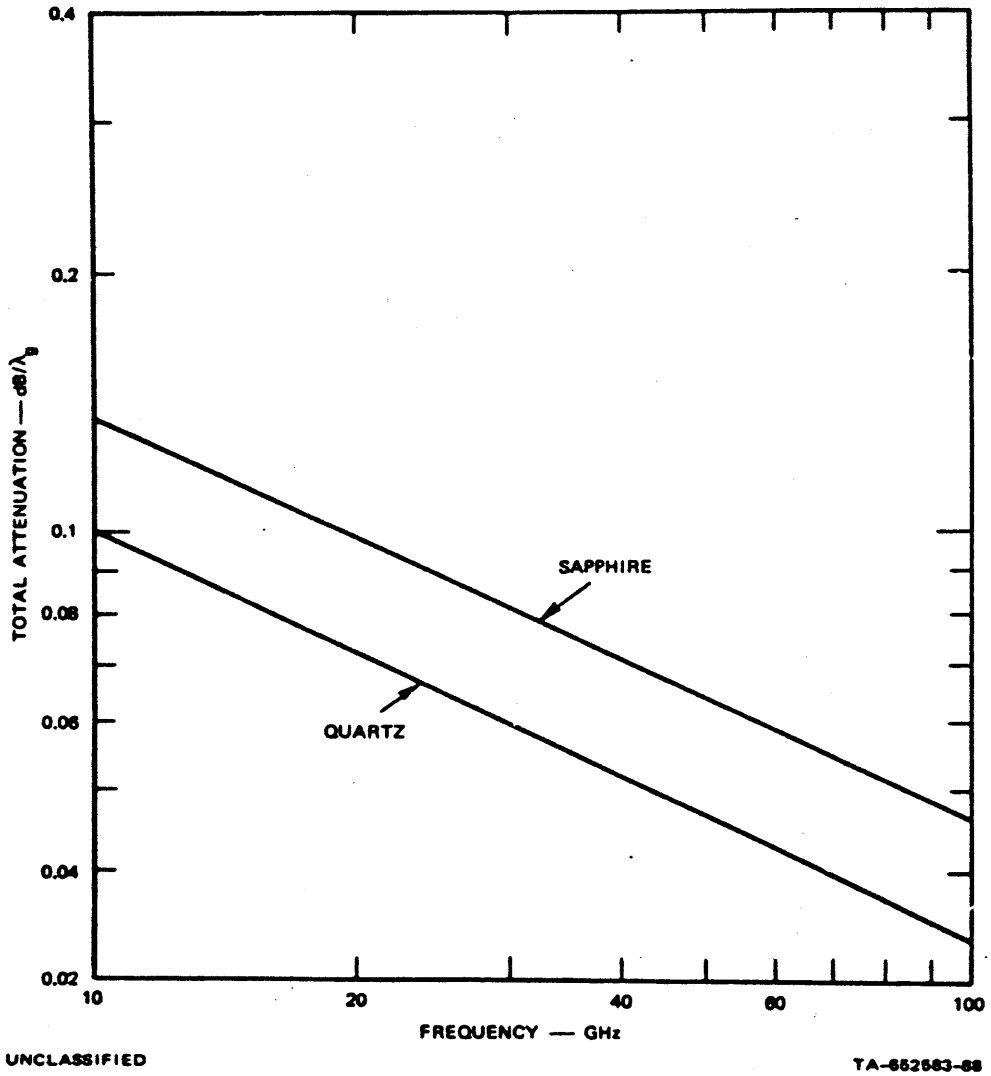

FIGURE II-2 ATTENUATION OF 50-ohm MICROSTRIP (U)

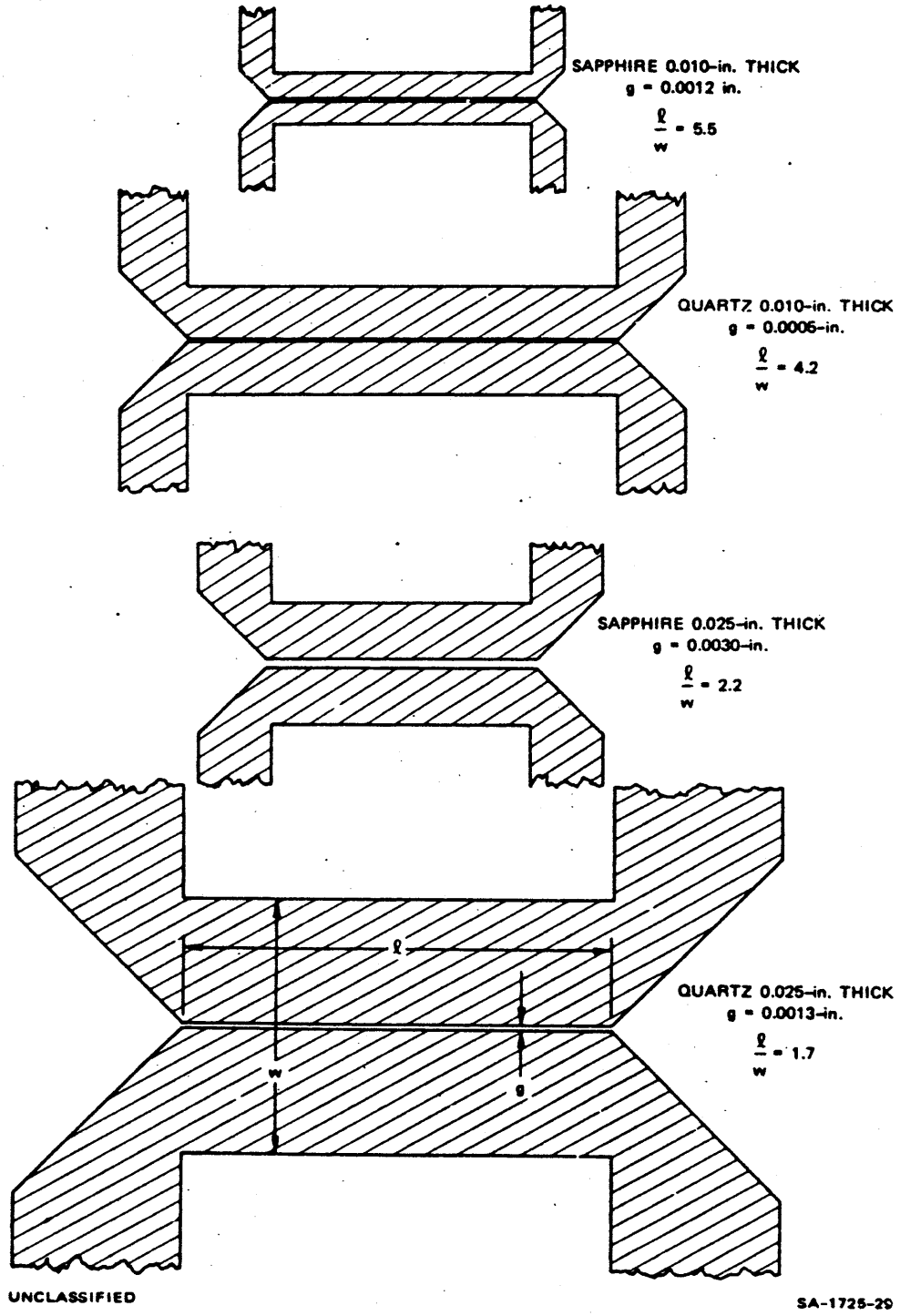

FIGURE II-3 COMPARISON OF P-BAND COUPLER DESIGNS ON SAPPHIRE AND QUARTZ SUBSTRATES · (U)

(U)

that can deviate considerably from those determined from the standard design theory based on the current and field distributions of uniformly coupled, long lines. Substantial changes in the coupler geometry are often required for compensation of the end effects.

(U) For single-section couplers of form factors on the order of 2 or less, the parasitic coupling between the input lines to the coupler becomes significant due to the unavoidable proximity of the input lines joining to the coupler ends. In multisection couplers of low form factor, the transitions between sections and the end effects combine so that compensation is extremely difficult. Because of these difficulties and to avoid excessive empirical adjustment of coupler geometries, form factors of 4 or larger are desired. Therefore a 0.010-inch substrate thickness was selected as the best for the component developments. As shown later, the thinner substrate also provides greater margin against conversion to unwanted modes.

3. Coupled-Gap Width (U)

(U) As shown in the example of Figure II-3 for an 8.3-dB coupler, the required gap between the coupled lines on the 0.010-inch-thick quartz substrate is 0.0005 inch. For a multisection 8.3-dB coupler, the coupling factor of the center section must be on the order of 6 dB, which would require a gap somewhat less than 0.0005 inch. With present technology, gaps on the order of 0.0005 inch represent about the lower limit that can be achieved on a routine basis in production. Therefore, the use of quartz is judged to be marginal, and sapphire is the best choice.

4. Higher-Order Modes (U)

(U) The major mode of propagation in the microstrip structure is recognized as a quasi-TEM mode since the pure TEM mode is not a true solution to Maxwell's equations. Other modes of propagation can exist on a microstrip structure; the most significant are surface-wave modes of both the transverse electric (TE) and the transverse magnetic (TM) types. These modes can interact with the quasi-TEM mode at higher frequencies and for relatively thick substrates. Specifically, either type of mode can efficiently couple energy from the quasi-TEM mode when its phase velocity is nearly equal to the TEM-mode phase velocity. Since the TE and TM waves are loosely bound to the substrates, this energy is easily lost by radiation. Additional dispersion in the microstrip mode also occurs. In addition, surface-wave modes are easily excited by any discontinuities on the microstrip line.

(U) The lowest-order transverse electric surface-wave mode (designated as TE_1) has a lower cutoff frequency given by[1]*

$$f_{c(TE_1)} = \frac{c_o}{4h\sqrt{\epsilon_r - 1}}$$

where

c_o = Free-space velocity of light

h = Dielectric substrate thickness

ϵ_r = Relative dielectric constant of dielectric material.

As the frequency increases above f_c, the phase velocity of the TE_1 mode decreases until it equals the phase velocity of the quasi-TEM mode, and at about twice f_c the coupling between modes is at a maximum. Figure II-4 shows $f_{c(TE_1)}$ for a range of substrate thicknesses. It is clear that

*(U) References are listed at the end of the report.

(U)

limitations due to the TE_1 surface mode do not become significant for either quartz or sapphire substrates until frequencies substantially above P-band are approached.

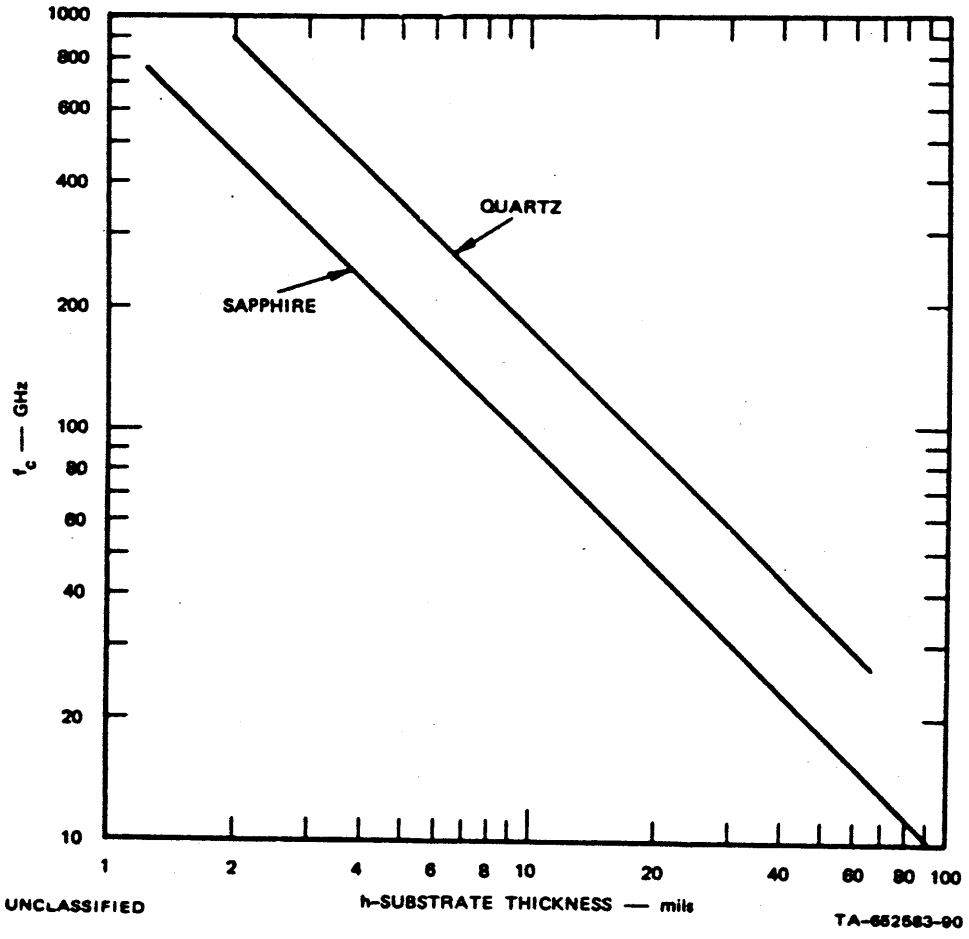

FIGURE II-4 MICROSTRIP TE_1-MODE CUTOFF FREQUENCY (U)

(U) Theoretically, the lowest-order transverse magnetic surface-wave mode (TM_0) can propagate at zero frequency on an infinite ground plane. For a finite-sized ground plane, this mode has a cutoff frequency, but very low frequencies can propagate. The frequency of maximum coupling for the TM_0 mode is given by

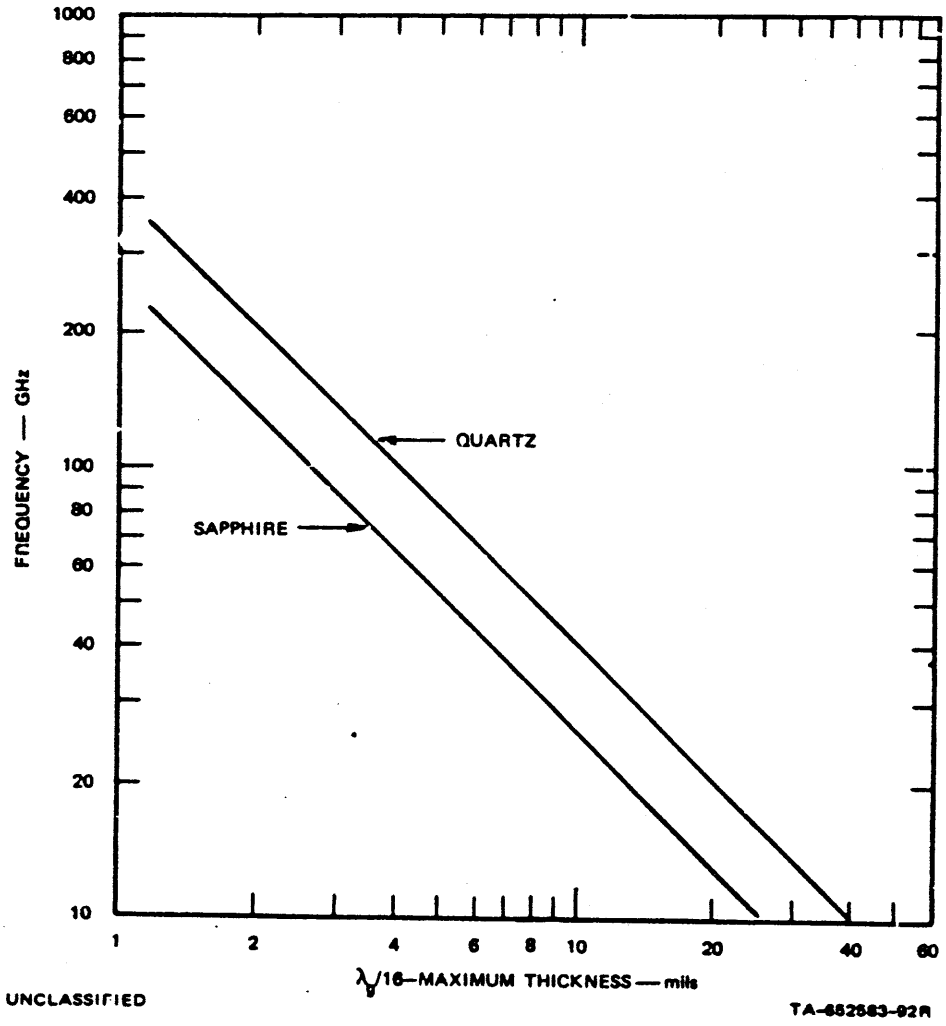

FIGURE II-6 MAXIMUM MICROSTRIP SUBSTRATE THICKNESS (U)

(U) The desired ripple performance cannot be obtained over the band of interest with a single-section coupler: therefore, multisection coupler configurations must be considered.

2. Multisection Couplers (U)

(U) Couplers comprised of two sections are ruled out at this point, because of undesirable phase characteristics. Three-section couplers with identical end sections possess the required symmetry and provide more than adequate ripple bandwidth.

(U) The coupling characteristics for several three-section designs are shown in Figure III-2. The smallest ripple shown is ± 0.1 dB and easily meets the desired performance. Table III-1 shows the coupling factors required for the designs in Figure III-2. The center sections must be very tightly coupled while the end sections are loosely coupled. For edge-coupled microstrip, the maximum coupling that can be achieved with practical approaches is about 6 dB, so that the desired 3-dB hybrid cannot be realized with a single, multisection coupler of the microstrip configuration.

3. Tandem-Connected Couplers (U)

(U) Two tandem-connected couplers each with an 8.34-dB overall coupling factor can be used for the desired 3-dB hybrid realization. Three-section, 8.34-dB couplers are within the capabilities of the present microstrip technology and provide a viable approach to the realization of the 3-dB hybrid.

(U) To proceed with a design, it is necessary to determine a method of specifying the ripple characteristic of the component 8.34-dB couplers, given the desired ripple characteristic of the composite 3-dB

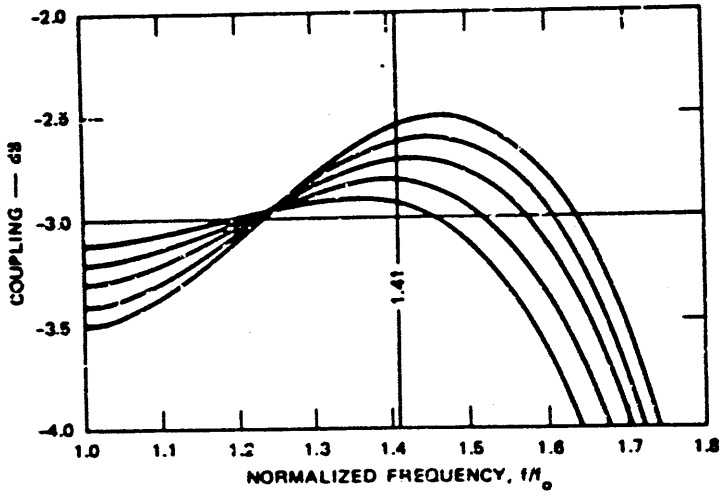

FIGURE III-2 COUPLING AS A FUNCTION OF FREQUENCY FOR FIVE THREE-SECTION TEM-MODE COUPLERS HAVING 3 dB AVERAGE COUPLING. Source: Ref. 2. (U)

Table III-1

(U) DESIGN PARAMETERS FOR THREE-SECTION, 3-dB TEM-MODE COUPLERS (U)

Ripple (dB)	Coupling (dB)	
	End Sections	Center Section
± 0.1	16.2	1.65
± 0.2	14.7	1.51
± 0.3	13.5	1.39
± 0.4	12.6	1.30
± 0.5	11.9	1.23

(U)

hybrid. The relationship between the component and composite coupling characteristics for perfect, matched, tandem-connected couplers is given by Young:[3]

$$\theta = \sin^{-1}(|k|) \quad \text{(for each component coupler)}$$

$$|k'| = \sin(2\theta) \quad \text{(for composite coupler)}$$

where k is the voltage coupling coefficient for each component coupler, and k' is the resulting voltage coupling coefficient for the composite hybrid. These relationships are shown graphically in Figure III-3. The abcissa corresponds to the coupling of each component coupler in dB and the ordinate corresponds to the coupling and transmission of the composite coupler. The curve labeled "C" is the coupling of the composite coupler, and the curve labeled "T" is the transmission of the direct path through the composite coupler. For example, for a component coupling of 8 dB, the composite coupling is 2.74 dB and the transmission of the composite coupler is 3.31 dB. Thus, the power split between the output arms of the composite coupler may be determined through the use of Figure III-3, if the coupling characteristic of the component coupler is known. Figure III-3 is applicable at any frequency where the sum of the output powers at the coupled and direct ports equals the input power (matched condition).

(U) The slope of the curve labeled C in Figure III-3 is less than unity, indicating that the change in dB of the composite coupling will always be less than the change in dB of the component coupling. The magnitude of the slope of the curve labeled T for the transmission is less than unity above a component coupling value of about 7.8 dB, indicating that for small ripple values of less than about 0.5 dB, the resulting ripple of the composite coupler is slightly less than for the component couplers. Thus, the component couplers should be designed with the same ripple characteristics as desired in the composite coupler.

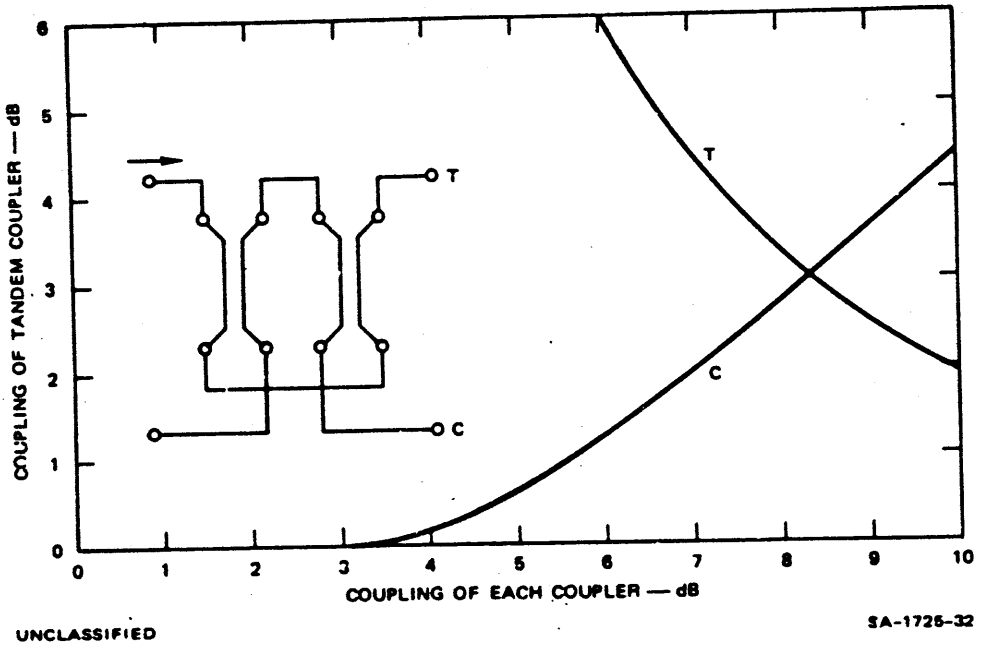

FIGURE III-3 IDENTICAL TANDEM-CONNECTED COUPLERS (U)

(U) Several three-section, 8.34-dB coupler designs are shown in Figure III-4. The design parameters are plotted in Figure III-5 to facilitate interpolation. Any ripple value between ± 0.1 and ± 0.25 dB meets both the bandwidth and ripple design goals.

4. Basic 3-dB Hybrid Microstrip Design (U)

(U) The required layout for the three-section, tandem-connected 3-dB hybrid is depicted in Figure III-6. To minimize interaction between the two individual 8.34-dB couplers, the minimum spacing should be four or five times the width of a 50-ohm line.

(U) The hybrid layout in Figure III-6 introduces two features worthy of emphasis at this point. The first is the wiggly center section that is used to counteract the effects of the velocity inequality of the

(U)

even and odd modes inherent in the microstrip configuration. It is impractical to wiggle the end sections because of the relatively large spacing required. However, it is effective to overcompensate the center section somewhat in order to achieve an overall effect of velocity equalization for the entire hybrid.

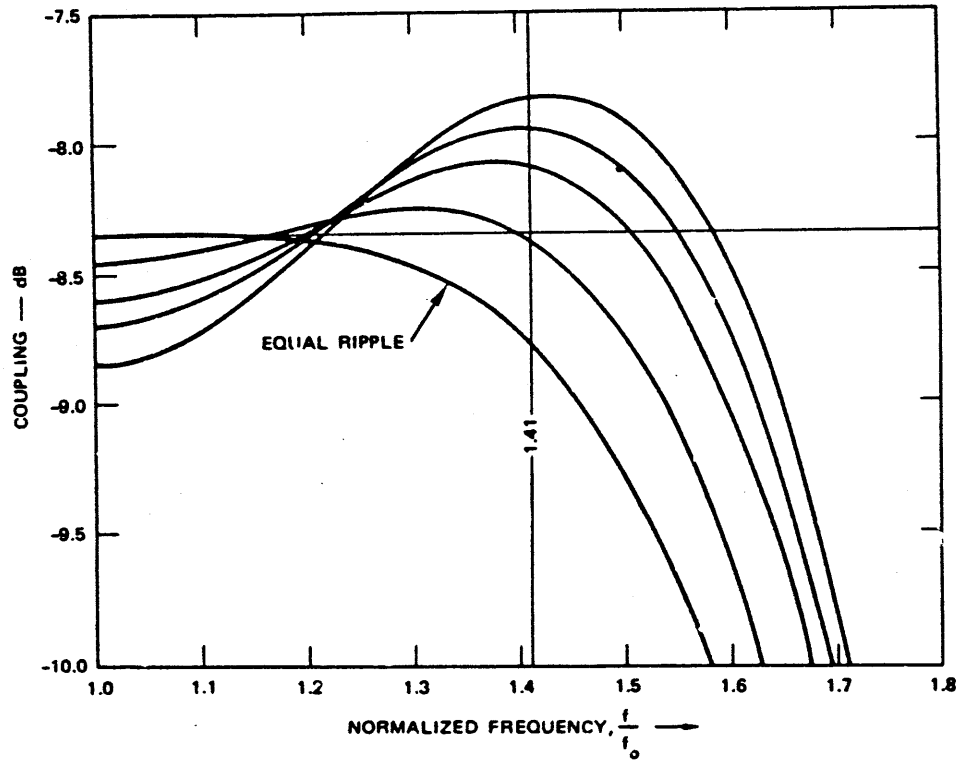

FIGURE III-4 COUPLING AS A FUNCTION OF FREQUENCY FOR FIVE THREE-SECTION TEM-MODE COUPLERS HAVING 8.34 dB AVERAGE COUPLING (U)

(U) The second important feature is the crossovers at the center of each center section. Crossovers are required in order to achieve the necessary connections between the appropriate ports of the individual couplers, and they are placed at the geometrical center of each coupler to maintain symmetry and subsequently the phase integrity of the composite coupler over the entire band.

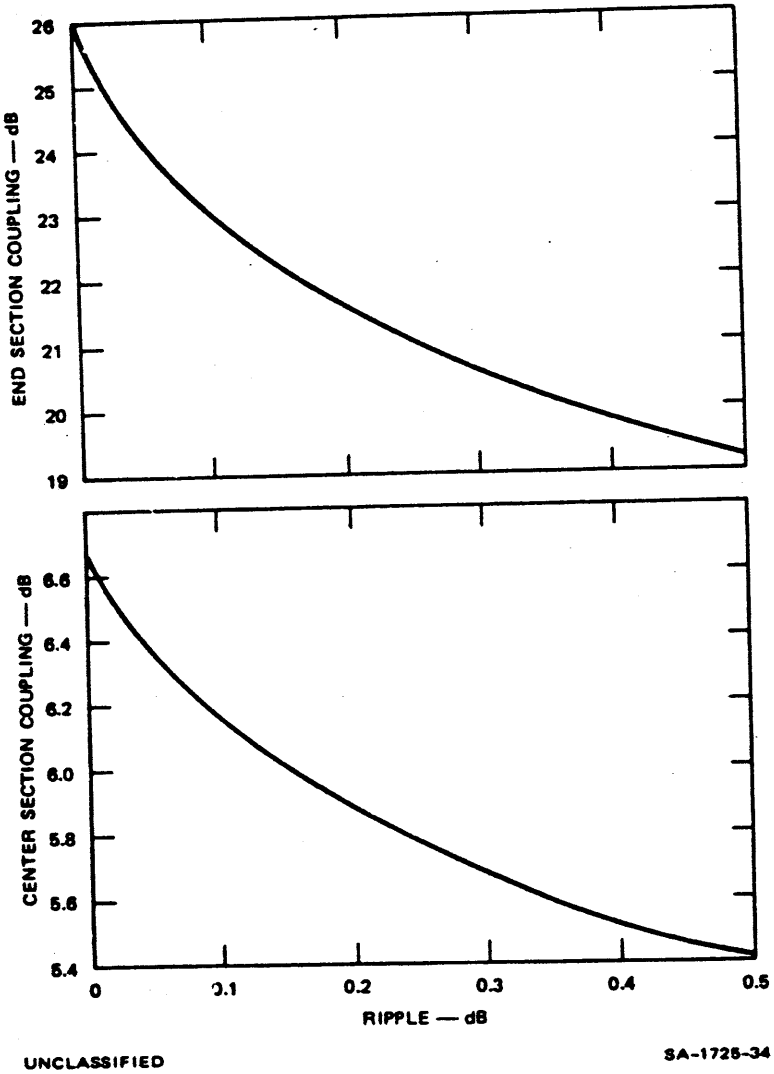

FIGURE III-5 COUPLING FACTORS FOR THREE-SECTION, 8.3432-dB COUPLER (U)

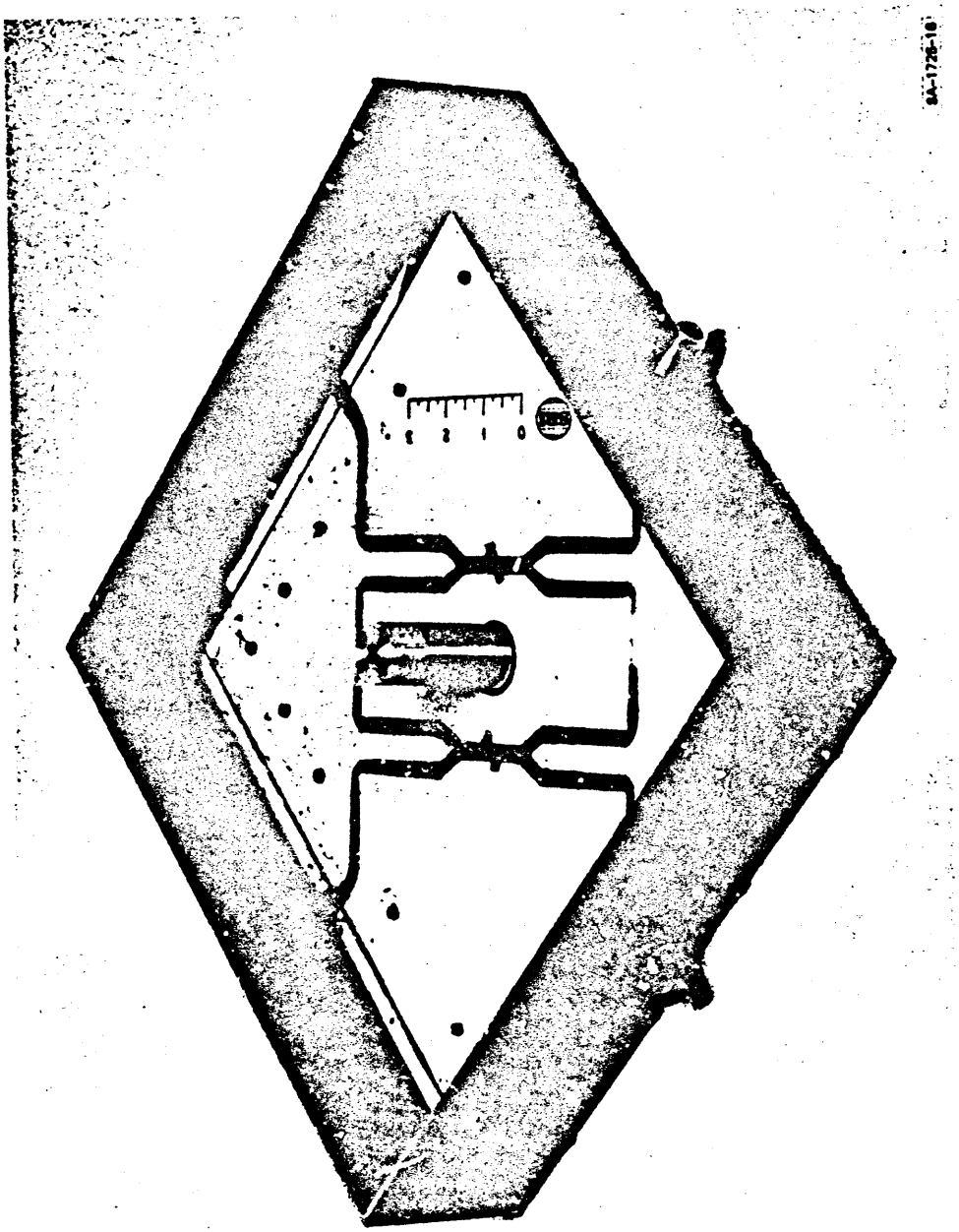

FIGURE III-7 25:1 SCALE MODEL OF THREE-SECTION, 3-dB MICROSTRIP HYBRID. Dielectric slab is 1/4 inch thick; ϵ_r = 10; conductor width = 1/4 inch. (U)

UNCLASSIFIED

(U) The scale model is enclosed in a box (top cover not shown in Figure III-7) simulating the final test enclosure including the mode suppressor at the center of the coupler layout. The mode suppressor is a conductive pin connecting the top and bottom ground planes and is necessary because the cavity formed by the box is large enough to resonate at the fundamental mode within the band of operation of the hybrid.

(U) For the measured performance of the scale model shown in Figure III-8, Port 1 is the input port; the subscripts on the S-parameters have the following meaning:

1 = Input port

2 = Direct output port

3 = Coupled output port

4 = Isolated port.

The return loss was greater than 20 dB over the range of measurement, so the VSWR is not shown in Figure III-8. The isolation is 20 dB or greater over the band, so that the maximum phase deviation from the quadrature relationship between the two outputs must be one degree or less.[5]

(U) Two sets of coupling characteristics are shown in Figure III-8--the top set shows the coupling with the top part of the enclosing box open as shown in Figure III-7. The middle set of data shows the coupling characteristics, with the cover in place, that are comparable to the coupling characteristic of the P-band unit discussed in Section III-E (see Figure III-11). Comparison of the two sets of coupling data in Figure III-8 illustrates the effects of "distant" ground planes on sensitive microstrip circuits such as couplers. The top ground plane is nine times farther from the circuit than the bottom ground plane for the case shown; however, presence or absence of the top ground plane results in a change of 0.1 to 0.2 dB in critical performance characteristics.

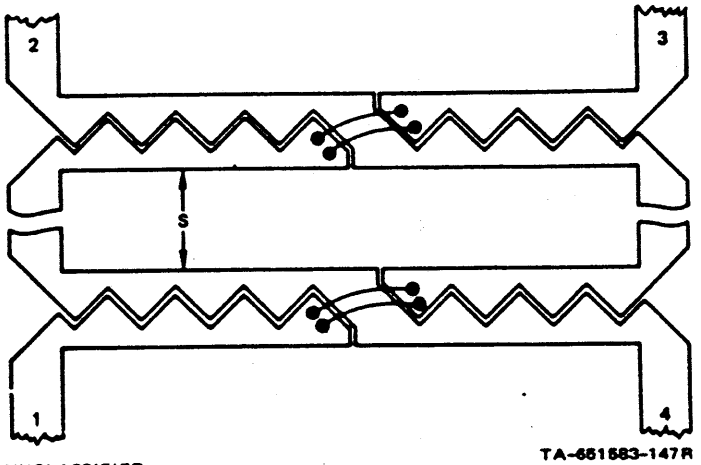

FIGURE III-13 3-dB HYBRID COUPLER WITH VARIABLE SPACING (U)

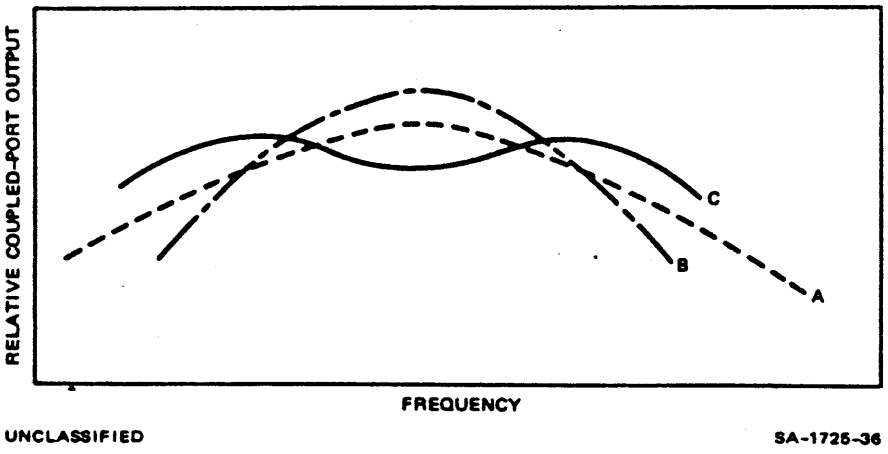

FIGURE III-14 TYPICAL COUPLING CHARACTERISTICS (U)

(U) To test the hypothesis that the proximity coupling possesses an equivalent, independent phase relationship with respect to the normal couplings, the interconnecting lines between the two couplers were increased from a relatively short length to about one-half wavelength long at midband. The resulting coupling characteristic was depressed at midband and enhanced at the band edges as depicted by Curve C in Figure III-14, indicating that the proximity coupling has been reversed in sign with respect to the normal couplings. Preliminary results indicated that the desired performance could be obtained with two single-section couplers with properly phased proximity coupling. Initially, the possibility of broadbanding a tandem connection of two single couplers rather than using two three-section couplers was very attractive.

G. Proximity 3-dB Hybrid Design (U)

(U) The final topology of the proximity, 3-dB hybrid is depicted in Figure III-15. The initial design consisted of two standard 8.3-dB wiggly couplers connected with phasing lines one-half wavelength long at midband spaced two 50-ohm linewidths apart. The approach used to arrive at the optimized configuration was substantially empirical from that point. Circuit adjustments were made on the 25:1 scale model shown in Figure III-16 during observation of the electrical response over the band of interest.

(U) Referring to Figure III-15 the basic microstrip conductor width, w_o, determines the system impedance of Z_o = 50 ohms. The conductors denoted by K are the direct interconnections between the two 8.3-dB couplers. Bends in the conductor strips are optimally mitered (M_1, M_2) to minimize the reactive discontinuity in the transmission line.

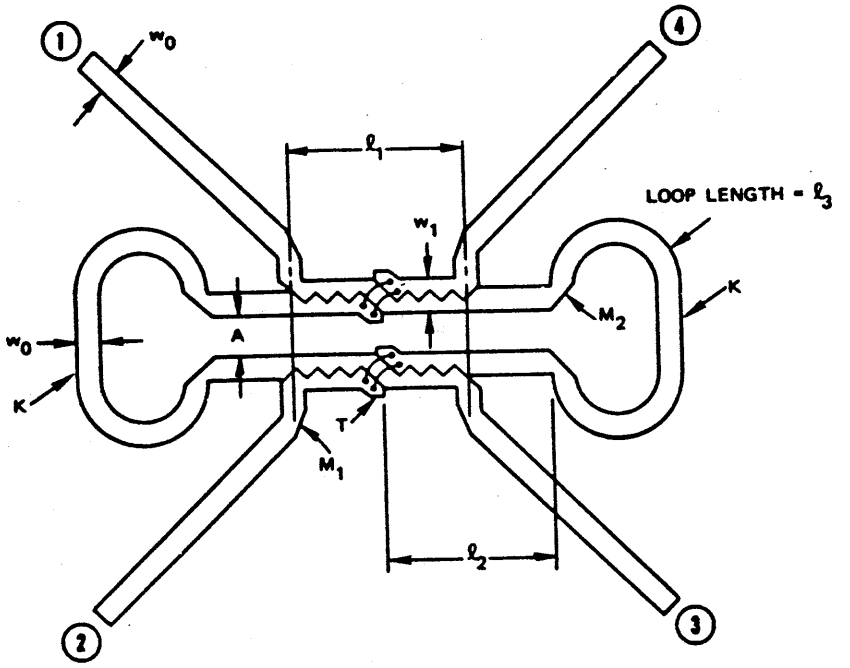

FIGURE III-15 CONDUCTOR PATTERN FOR 3-dB HYBRID BROADBANDED BY PROXIMITY COUPLING OF TANDEM-CONNECTED 8.3-dB COUPLER (U)

(U) The principal coupling in the hybrid occurs across the wiggly gap having an effective interaction length ℓ_1. Separately, each coupler would give somewhat tighter coupling than 8 dB. The final gap width was determined empirically. Data from earlier work of Podell[6] suggested appropriate wiggle angles, and the dimension w_1 was determined from the data of Bryant and Weiss.[4] A pair of bonded wires provides the crossover at the center of each coupler, needed for the correct topology of the hybrid. The capacitive tabs, T, determined empirically, roughly compensate for the inductance of the bridging wires, and are mechanically advantageous in the bonding operation. The length ℓ_1 is close to one-quarter the midband wavelength (for the even mode of propagation), and was adjusted to make the coupling characteristic symmetrical about the midband frequency.

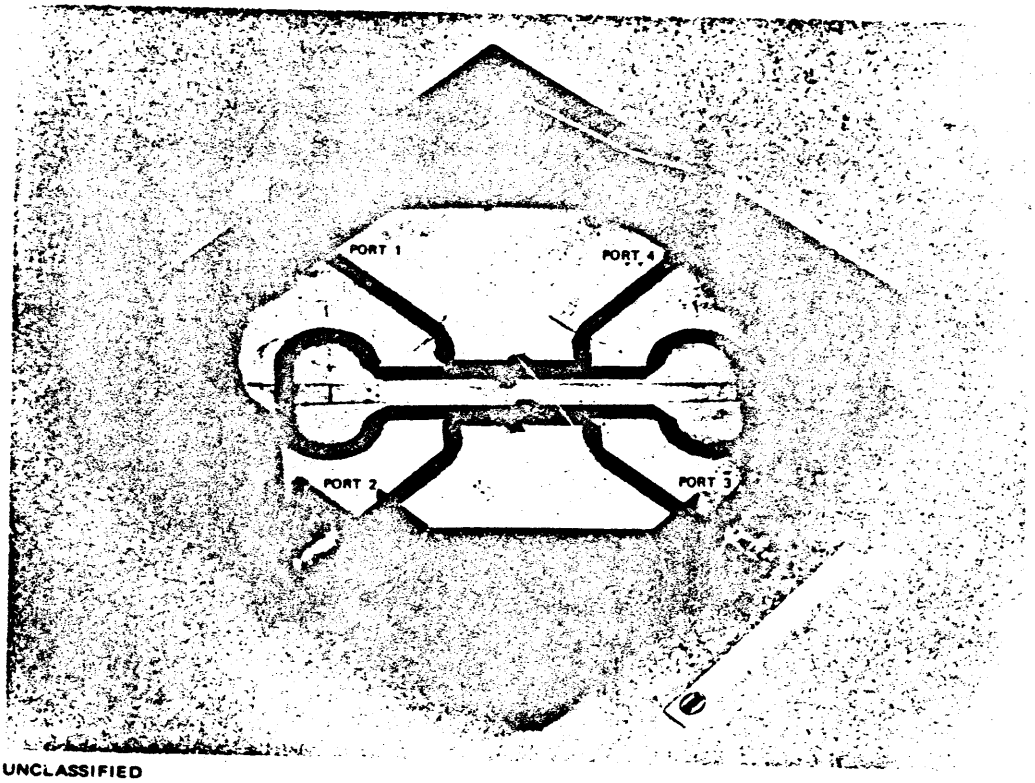

UNCLASSIFIED

FIGURE III-16 25:1 SCALE MODEL OF 3-dB MICROSTRIP HYBRID. Dielectric slab is 1/4 inch thick; ϵ_r = 10; conductor width = 1/4 inch. (U)

(U) The auxiliary proximity coupling occurs across the gap of width A. It appears that this coupling is largely, though probably not entirely, due to the innermost two of the four parallel conductor strips in any one cross section. This fact may explain why correct performance required the lengths ℓ_2 and ℓ_1 to be approximately one-quarter rather than one-eighth wavelength at midband. The delay-line length, ℓ_3, is close to one-half wavelength at midband. Correct adjustment of ℓ_3 (and of $\ell_2 + \ell_3 \approx$ 3/4 midband wavelength) is indicated by having the "dimple" in Curve C of Figure III-14 centered at the midband frequency in the

(U)

of unequal coefficients of attenuation in the odd and even modes of propagation. The following table summarizes the characteristics of the completed hybrids:

	Design Goal	Prototype	Test Unit
Maximum amplitude imbalance (dB)	0.5	1.0	1.2
Minimum isolation (dB)	20.0	20.0	13.0
Maximum VSWR	1.3	1.35	1.65
Maximum insertion loss (dB)	0.7	0.2	2.0

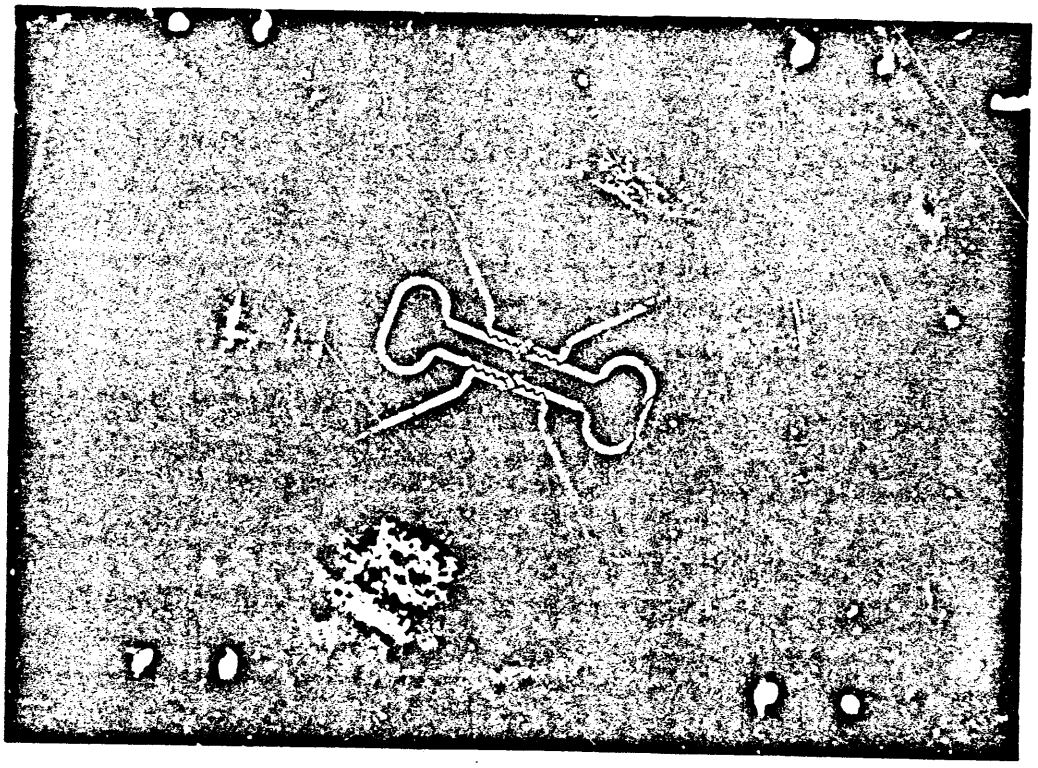

UNCLASSIFIED

SA-1725-39

FIGURE III-19 CLOSE-UP OF PRINTED CIRCUIT OF FIGURE III-18. Wiggled gap = 0.00088 inch; disc diameter = 0.375 inch. (U)

(U) Representative performance curves (from Test Unit X3-2) are shown in Figure III-20. The overall downward change of about 2 dB in the coupling characteristic is due to increasing dissipation loss in the coupler, since both S_{21} and S_{31} are comparably affected. However, the apparent rate of increase of loss is greater than would be predicted by the square root of the frequency dependence. This effect arises from the method of attachment of the substrate in the test box and is due to deterioration of the chromium gold ground-plane conductor. Significantly better performance was obtained on the three-section, 3-dB hybrid using an improved substrate attachment method. (See Figure X-1 and the discussion in Section X.) The same substrate attachment technique applied to the proximity coupler can be expected to result in a comparable improvement in the loss performance, and it is estimated that the loss would be on the order of only 0.5 dB, as was obtained for the three-section, 3-dB hybrid.

(U) The amplitude imbalance for these test units might be decreased if the prototype performance also showed less imbalance--e.g., 0.5 dB instead of 1.0 dB.* However, after adjustment of the prototype, the sensitivity to tolerances would probably limit the reproducibility of test-unit performance, and improved imbalance might not result.

(U) As mentioned above, the main cause of directivity deterioration is unequal odd- and even-mode dissipation. For the hybrid in question, the odd-mode attenuation is estimated to be at least an order of magnitude greater than that of the even mode, and the directivity could then be as low as 13 dB.

---

*(U) During the development, the design goal was incorrectly read as "± 0.5 dB" instead of "0.5 dB total."

(U)

(3) The two previous limitations combine to produce a third. Only couplers with three sections or less are practical in edge-coupled microstrip. This also implies that the maximum bandwidth that can be obtained in the microstrip medium is about 3:1. Therefore, wider bandwidths will be achieved using a different technique--stripline, for example.

(U)

reflections are not caused by impedance steps, as they are in the case of conventional parallel-line couplers. They are caused by shunt capacitances for the odd mode and by series inductances for the even mode, as indicated by the prototype circuits shown in Figure IV-5.

(U) The even-mode reflection coefficient for either type of coupler is the negative of the odd-mode reflection coefficient; hence they cancel in the input arm and the coupler as a whole is reflectionless.

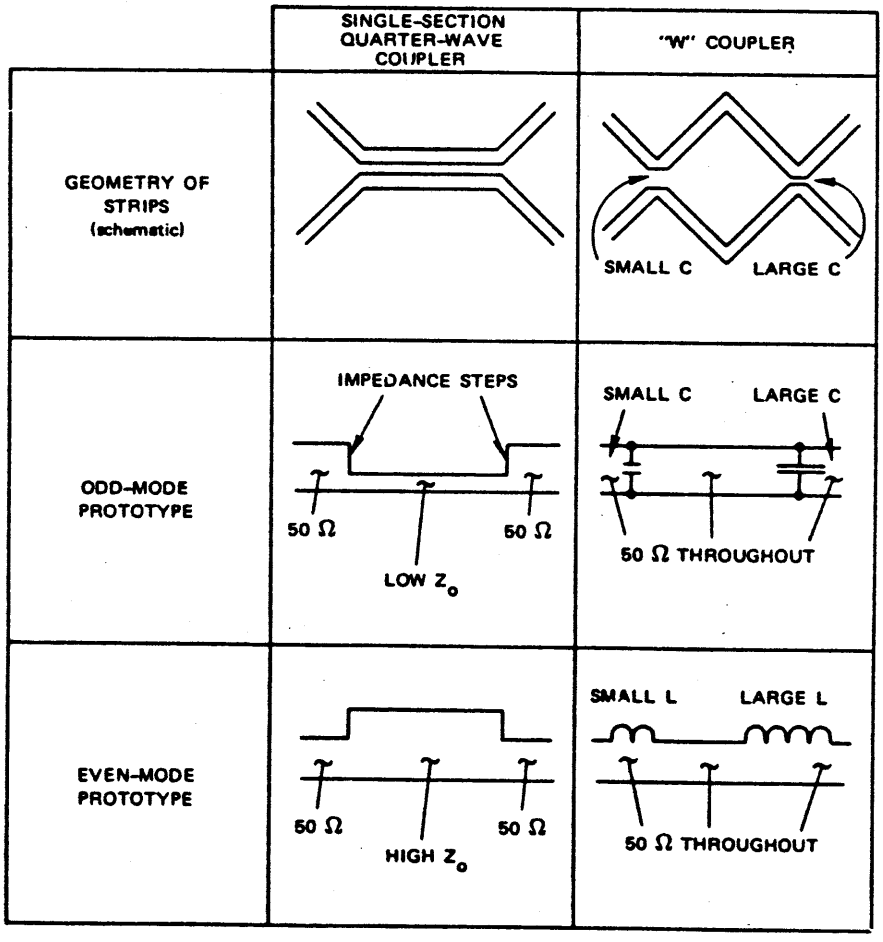

FIGURE IV-5 GEOMETRY AND PROTOTYPE CIRCUITS FOR W COUPLER AND CONVENTIONAL QUARTER-WAVE COUPLER (U)

(U)

However, in the backward-coupled arm the even- and odd-mode inputs are out of phase since there is no actual input there; hence, their reflected components add up, which explains the backward coupling of these couplers. The even- and odd-mode reflection coefficients are of opposite sign because the even- and odd-mode prototype circuits are duals of each other for both the W coupler and the conventional quarter-wave coupler.

(U) The coupling is a function of the reflection from each discontinuity in the prototype circuit, be it impedance step or shunt capacitance. For the case of shunt capacitance, the reflection coefficient due to each capacitance increases with frequency (since the susceptance increases with frequency). The principal reflection is due to the larger capacitance. If the smaller capacitance were zero, then the reflection coefficient, and therefore the coupling factor (for a weak coupler), would increase nearly linearly with frequency. The small capacitance is spaced one-quarter wavelength away at some frequency, f_m, greater than the midband frequency, f_o, but less than the upper band edge, f_u. The reflection from the small C subtracts from the reflection from the large C at f_m, but as the spacing departs from 90°, the two reflections (from the large C and the small C, respectively) are no longer 180° out of phase (for example, at the band edges they will be almost in quadrature). Thus, at the band edges, the small C has less effect on the total reflection coefficient, as indicated in Figure IV-6. The dashed straight lines in Figures IV-6(a), (b), and (c) correspond to the case where the small C is zero (that is, when there is only one discontinuity). The solid curves indicate the composite responses due to both Cs. Figure IV-6(a) corresponds to small C smaller than optimum, and Figure IV-(c) to small C larger than optimum, while Figure IV-6(b) corresponds to the situation in which small C is just right, since it results in an "equal-ripple" coupling between the lower band edge, f_ℓ,

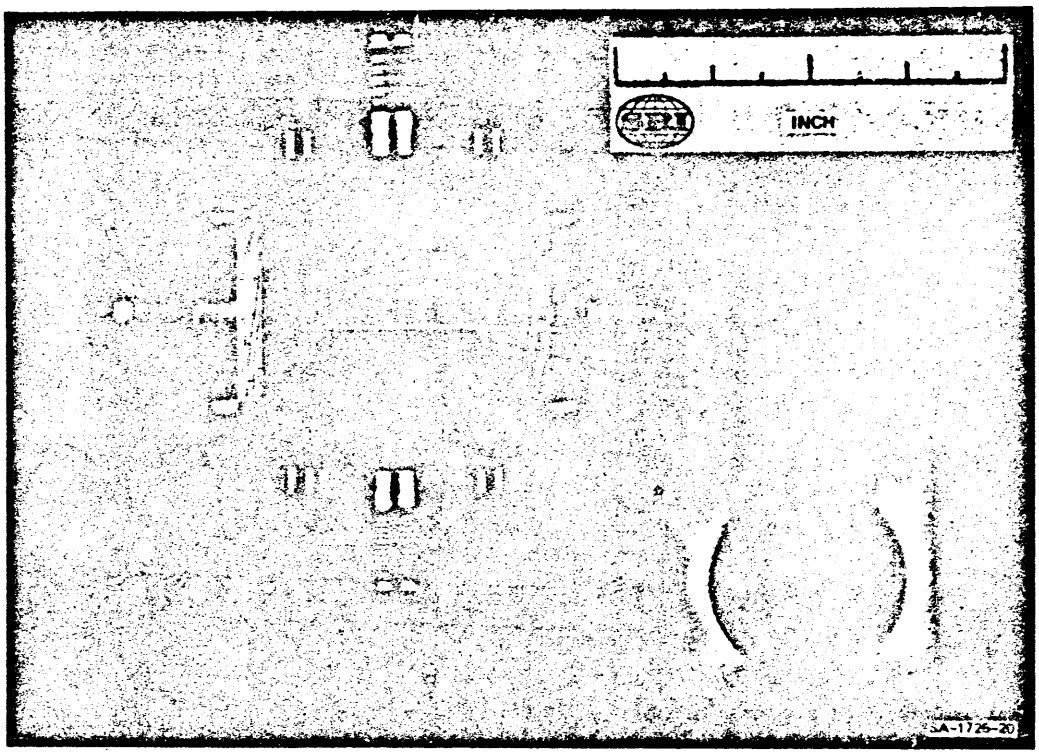

UNCLASSIFIED

FIGURE IV-13 WIDEBAND 20-dB W COUPLER (U)

(U)

capacitance has been increased. The isolation has been improved, presumably because the slight reduction in overall line widths results in a better even-to-odd-mode impedance ratio.

(U) The average gap between fingers of the large capacitance was 0.008 inch for unit 20-20-G and 0.0011 inch for unit 18-20-G.

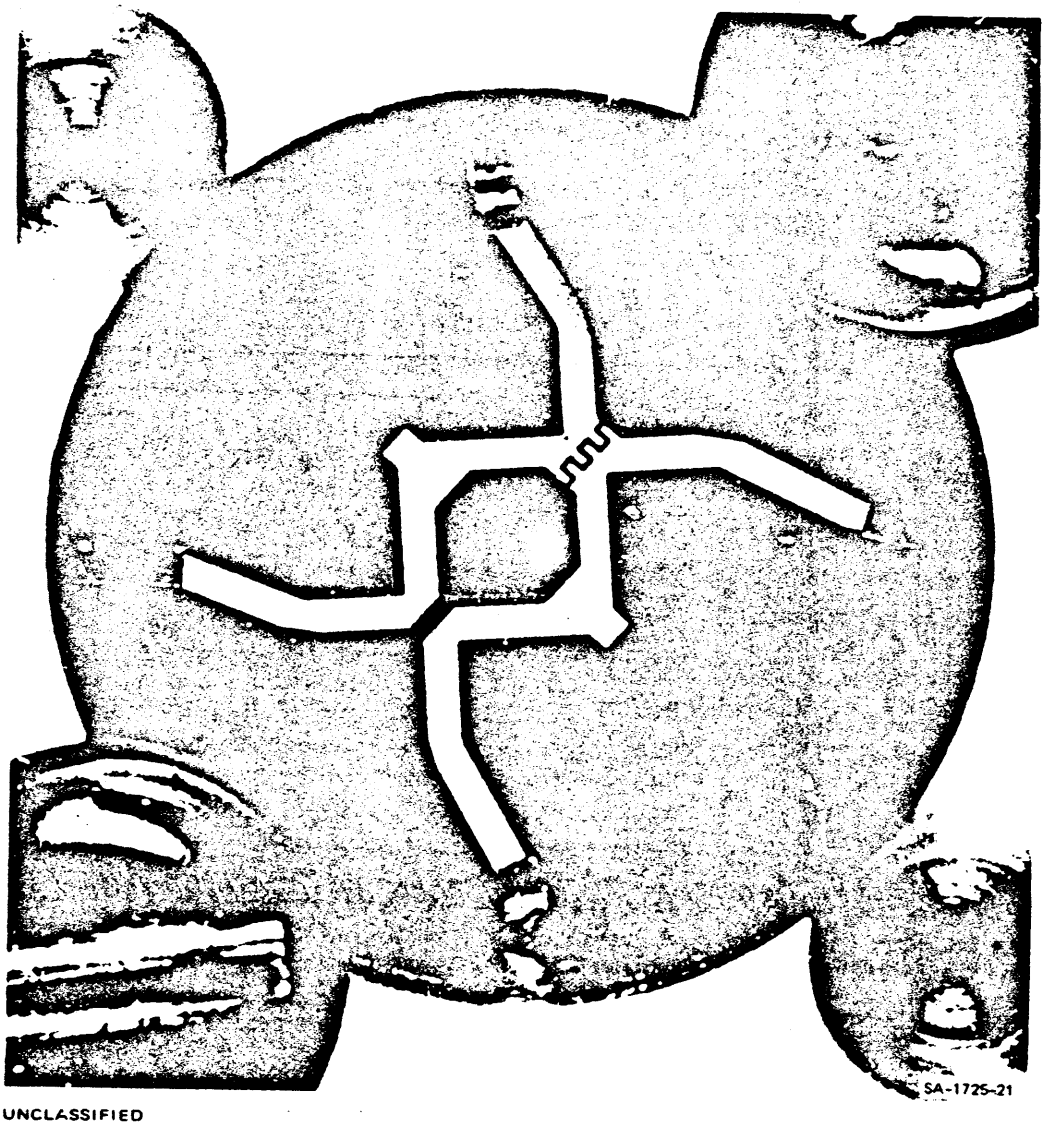

UNCLASSIFIED

FIGURE IV-14 CLOSEUP OF WIDEBAND 20-dB W COUPLER SHOWN IN FIGURE IV-13 (U)

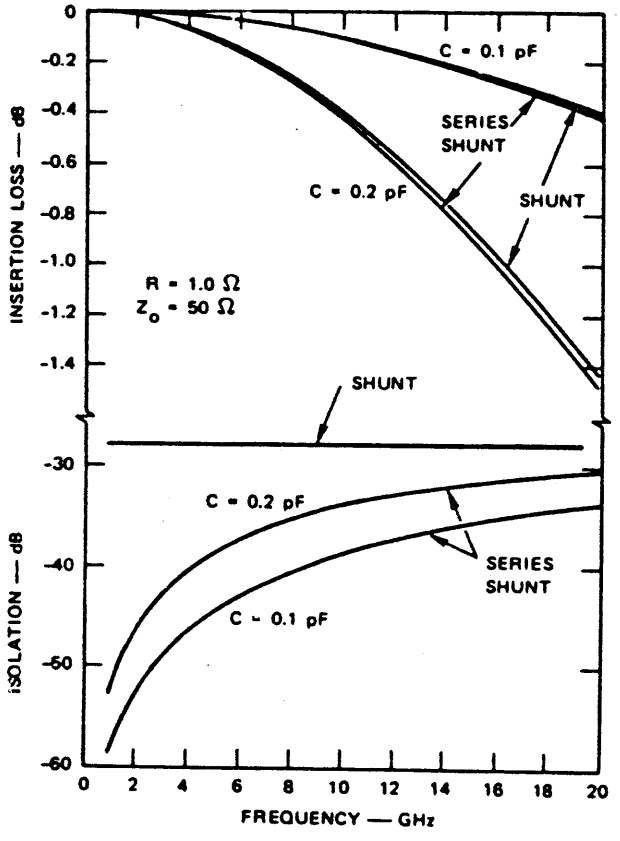

	ISOLATION	INSERTION LOSS	
SHUNT	$20 \log \left[1 + \frac{Z_o}{2 R_s}\right]$	$10 \log \left[1 + \left(\frac{Z_o}{2 X_c}\right)^2\right]$	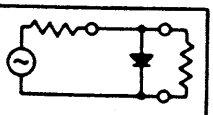
SERIES-SHUNT	$10 \log \left[\left(1 + \frac{Z_o}{2 R_s}\right) + \left(\frac{X_c}{2 Z_o}\right)^2 \left(1 + \frac{Z_o}{R_s}\right)^2\right]$	$10 \log \left[1 + \left(\frac{R_s}{2 Z_o}\right)^2 + \left(\frac{Z_o + R_s}{2 X_c}\right)^2\right]$	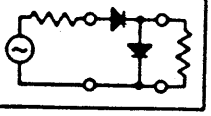

UNCLASSIFIED

SA-1725-48

FIGURE V-2 COMPARISON OF SHUNT AND SERIES-SHUNT SWITCH CONFIGURATIONS (U)

(U) [illegible] power

(U) [illegible] diodes in [illegible] the series diodes in the [illegible] the breakdown voltages can [illegible] from

$$V_{B} = [illegible] \quad \text{(shunt-connected diode)}$$

$$V_{B} = [illegible] \quad \text{(series-connected diode)}$$

where P_A is the [illegible] available [illegible] the load.

(U) A superficial comparison of power-handling capability would indicate that the series-shunt configuration is superior to either the shunt or shunt tandem configuration; however, in practice, the power dissipated per diode is about the same for all configurations. To illustrate, consider first identical diodes in both the shunt and series configuration. In the series-shunt configuration, the series diode has the greatest dissipation when the diode is forward-biased--i.e., when the switch arm is on. For this case, the ratio of power flowing through the switch arm to the power dissipated (P_D) in the diode is given by

(U)

$$\frac{P_A}{P_D} = \frac{R_s}{4Z_o}\left(\frac{2Z_o}{R_s} + 1\right)^2 \qquad \text{(series diode)}$$

and for a diode with R_s = 1 ohm in a 50-ohm system, P_A/P_D = 50.

(U) The shunt diode (in any configuration) has the greatest dissipation when the switch arm is off and the power ratio is given by

$$\frac{P_A}{P_D} = \frac{R_s}{Z_o}\left(\frac{Z_o}{2R_s} + 1\right)^2 \qquad \text{(shunt diode)},$$

and for a diode with R_s = 1 ohm in a 50-ohm system, P_A/P_D = 13.5.

(U) If the diodes are equal electrically, the series diode appears to be able to handle about four times the power of the shunt diode. In the series-shunt configuration, the shunt diode limits the switch power capability in the same way as in the shunt or shunt tandem configurations. Two additional considerations further limit the power-handling capability of the series diode, however. Because the series diode is generally selected to have a low value of capacitance, the series resistance will be greater than 1 ohm--on the order of 2 or 3 ohms minimum. If the series resistance is 3 ohms, the power ratio is reduced to approximately P_A/P_D = 50/3 = 13, which is nearly the power ratio for the shunt diode with 1 ohm series resistance. The most severe limitation on the use of the series diode arises from the method required to provide a heat sink. The CW dissipation of a typical beam-lead diode is about 1/4 watt, whereas a chip diode mounted on a stub or on a ground-plane heat sink will dissipate about 2.5 watts, or ten times as much.

TO: DAN
FRANK
Rene
Wayne
Brent
Randy

In 1972/1973 This was the report on my FIRST SP2T switch designed at Standford along with my partner Don Chamber Please see the Driver used in 1972

VI SPDT SWITCH (U)

A. General Design Approaches (U)

(U) Three approaches for the development of the SPDT switch were initially considered. One approach is to apply the circuit used by Nelson,[8] which meets all the specifications except switching time. Replacing the 200-ns-lifetime PIN diodes with Hewlett-Packard Type 5082-3258, 15-ns-lifetime devices will not degrade the performance of the switch, except that the higher ON resistance of the short-lifetime diodes will decrease the theoretical isolation by approximately 6 dB (to about 50 dB).

(U) The switch could be constructed in similar fashion to that applied by Nelson, except that no case and no glass-to-metal seals are required. Figure VI-1 shows the design of a switch constructed along the edge of a substrate in order to use both air and alumina dielectrics and to ground the diodes directly, thereby minimizing stray inductance. An alternative to drilling holes or using the edges of substrates would be to use shields to decrease stray coupling. However, shields are cumbersome and difficult to apply effectively in the configuration required for microstrip. Therefore, this approach would be problematical.

(U) The slot-line switch shown in Figure VI-2 is the second configuration considered because the shunt-diode configuration is ideally suited to this switch circuit, which effectively places the two arms in series with the common arm. However, the slot line also poses difficult problems of shielding between circuits and generally requires the use of shield partitions or absorbing material.

Pl see National Still makes these drivers in CHIP form [illegible]

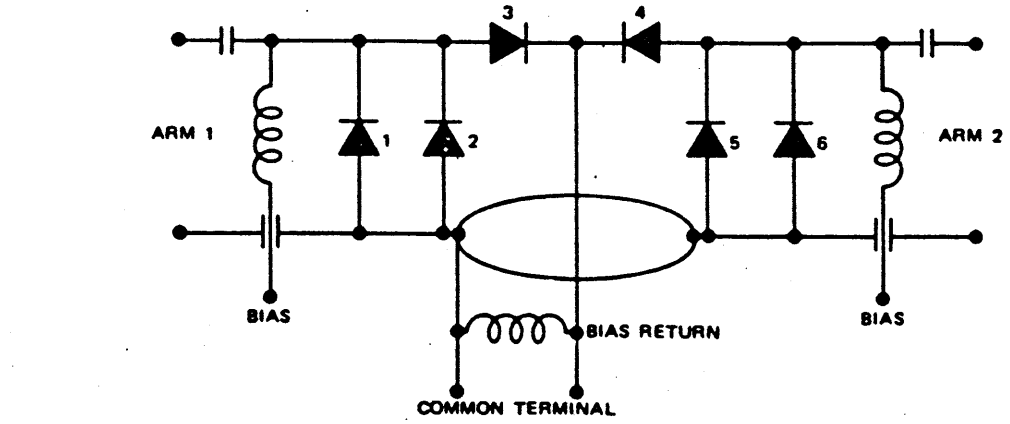

(a) SCHEMATIC DIAGRAM

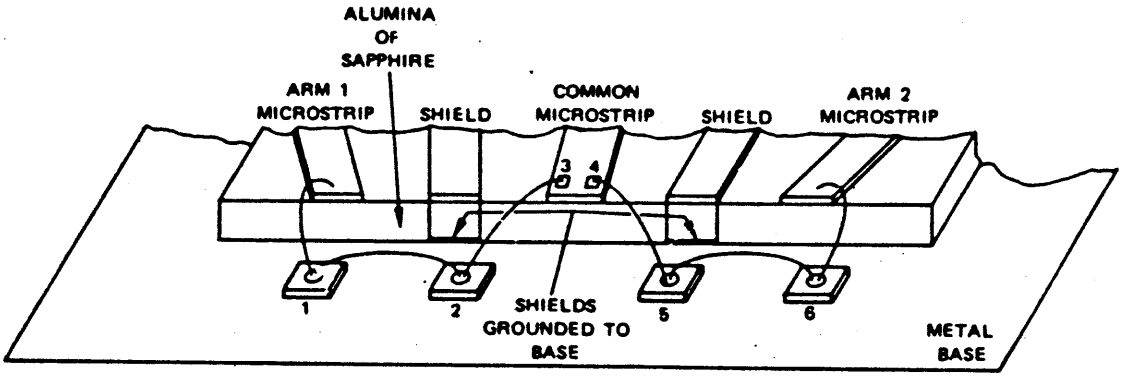

(b) DETAILS OF DIODE CONNECTIONS

UNCLASSIFIED

TA-651583-140

FIGURE VI-1 SPDT SWITCH (U)

(U) The preferred approach for the SPDT switch makes exclusive use of the shunt diodes throughout the circuit (Figure VI-3). This circuit is simpler to fabricate and has lower loss than the series-shunt switch. The computed VSWR of this circuit over most of the desired frequency range is 1.05:1 maximum.

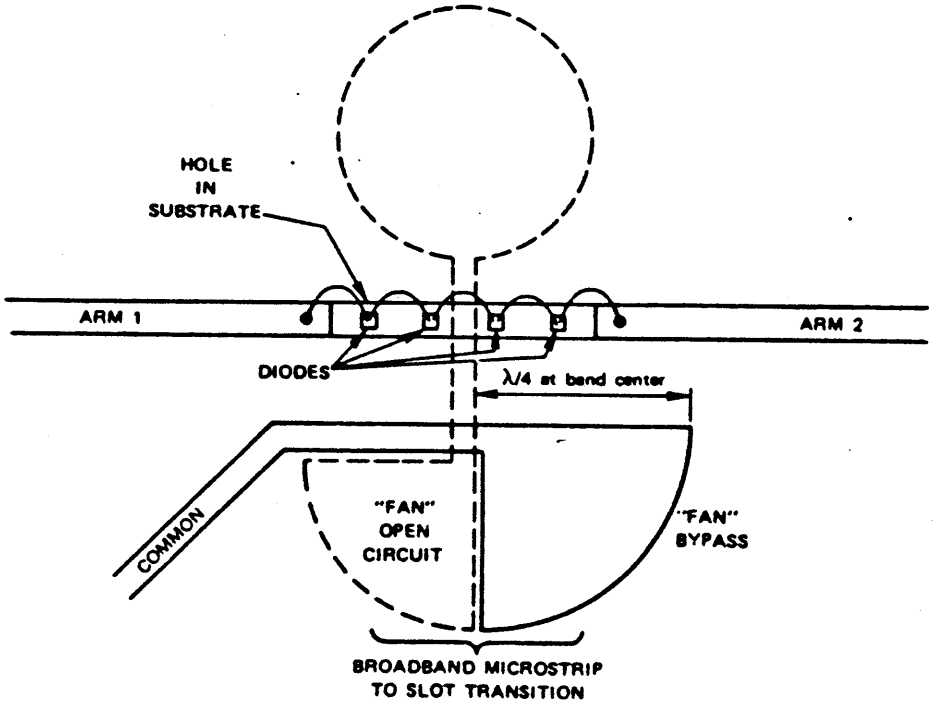

NOTE: Diodes are mounted on metal plates soldered to the bottom of the substrate.

UNCLASSIFIED

TA-661583-181

FIGURE VI-2 SLOT LINE AND MICROSTRIP SWITCH. Bypass capacitors and bias chokes not shown. (U)

(U) The switching signal to the diodes can be fed through a compensated high-impedance quarter-wavelength line section that acts as a choke. The reactance introduced by this choke can be used to obtain additional bandwidth from the circuit. The blocking capacitors can be installed in series with the RF ports. Either printed capacitors or beam-lead chip capacitors can be used to block the dc signals at the RF ports.

(U) As specified in the contract work statement, the switching time must be 15 ns from low loss to the 30-dB isolation state. The Hewlett-Packard 5082-3258 diodes have a 15-ns carrier lifetime; therefore,

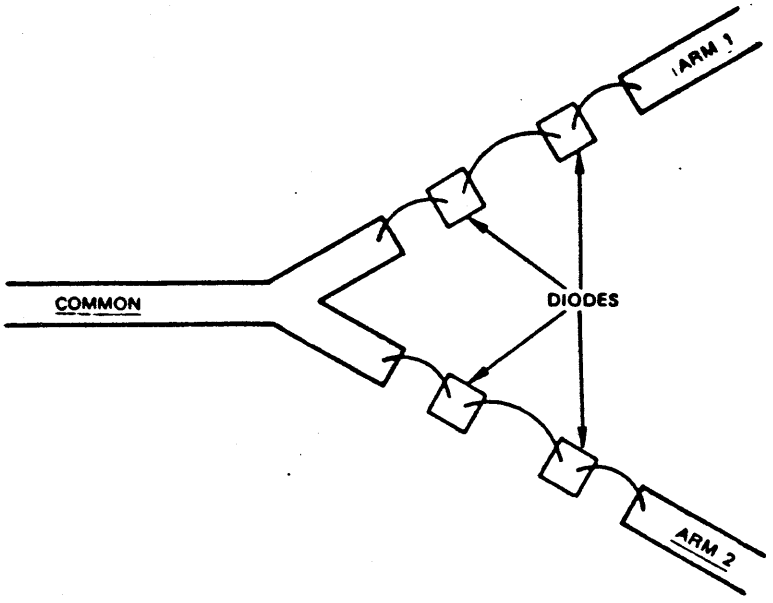

(a) TYPICAL LAYOUT

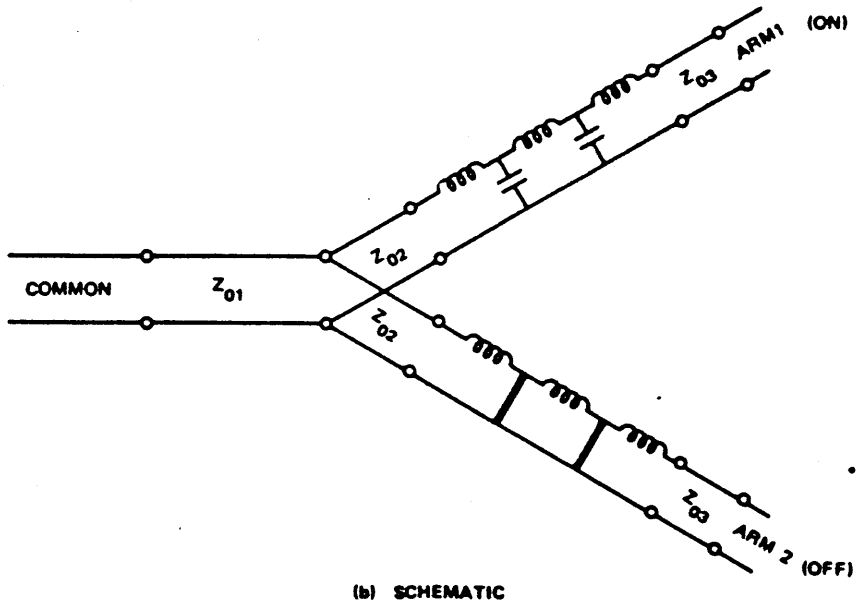

(b) SCHEMATIC

NOTE: Diodes mounted in holes in substrate on plate soldered to bottom, or the edge of substrate may be used to allow diodes to be mounted on the ground (see Figure 3).

UNCLASSIFIED TA-651583-152

FIGURE VI-3 SPDT SWITCH WITH ALL-SHUNT-DIODE CONFIGURATION (U)

(U)
with a proper drive circuit the fast switching can be achieved. Drivers for the SPDT switch are discussed separately in this section. The drivers will have transistor-transistor logic compatibility and can be constructed using hybrid thin film or monolithic integrated-circuit techniques.

B. Selected Design Approach (U)

(U) The preferred configuration for the SPDT switch is an arrangement whereby all diodes are connected in shunt. Packaged diodes are impractical because the package parasitics are very difficult to compensate over the broad bandwidth required. In addition, chip diodes allow better control of circuit values and fit the physical size of the circuit better. The all-diodes-in-shunt configuration greatly simplifies heat sinking and mechanical mounting of chips. Effective use of series diodes would require the use of a beam-lead configuration in most cases; however, the selection of available beam-lead diodes is much more limited at present than the selection of chips. The diode resistance, R_s, tends to be higher for beam-lead diodes, causing increased losses and more difficult heat removal since the main heat-conducting path is through the beam leads, whereas a shunt-mounted chip can be bonded directly to a large ground plane.

(U) The design principles of the SPDT switch are the same as those of the DPDT switch discussed in Section V. In fact, one-half of the DPDT shown in Figure V-3 could be used as a SPDT. All the design equations and information discussed in Section V are applicable to the SPDT switch designs. Therefore, no further details are discussed in this section.

1. PIN Diodes (U)

(U) The diode selected for the SPDT switch is the same as for the DPDT. Hewlett-Packard 5082-3258 diodes or Hewlett-Packard 5082-

(U)

3259 diodes are recommended for the design. These microstrip PIN diodes consist of a specially processed silicon chip of passivated design mounted on a gold-plated copper pedestal. The HP 5082-3258 uses a mesa-passivated chip optimized for fast switching or low-bias-currrent operation. The HP 5082-3259 uses a planar passivated chip optimized for medium power and high-Q circuits. The polarity of the 5982-3258 diodes is cathode on heat sink. The polarity of the 5082-3259 diode is anode on heat sink.

(U) The equivalent circuit for the diodes in forward- and reverse-bias conduction is shown in Figure VI-4. The important specifications for the diodes are as follows:

	HP 5082-3258	HP 5082-3259
Chip capacitance, C_T (pF)	0.3	0.15
Lead inductance, L_p (nH)	0.5	0.5
Residual series, R_S, resistance (ohms)	0.8	0.9
Carrier lifetime, τ (ns)	15.0	200.0
Reverse recovery time, t_{rr} (ns)	50.0	150.0
CW power switching capability (W)	150.0	35.0

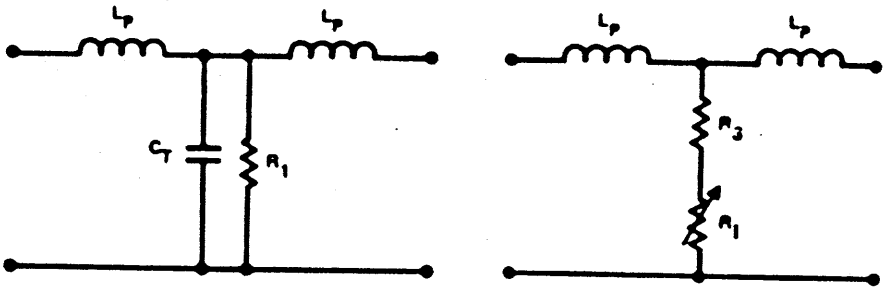

FIGURE VI-4 REVERSE- AND FORWARD-BIAS EQUIVALENT CIRCUITS (U)

2. Driver Circuit (U)

(U) The topology of the drive circuitry required for the SPDT switch is shown in Figure VI-5. The input logic signal is connected to two current drivers. One current driver is preceded by an inverter so that one set of diodes in the SPDT switch will be ON while the others are OFF.

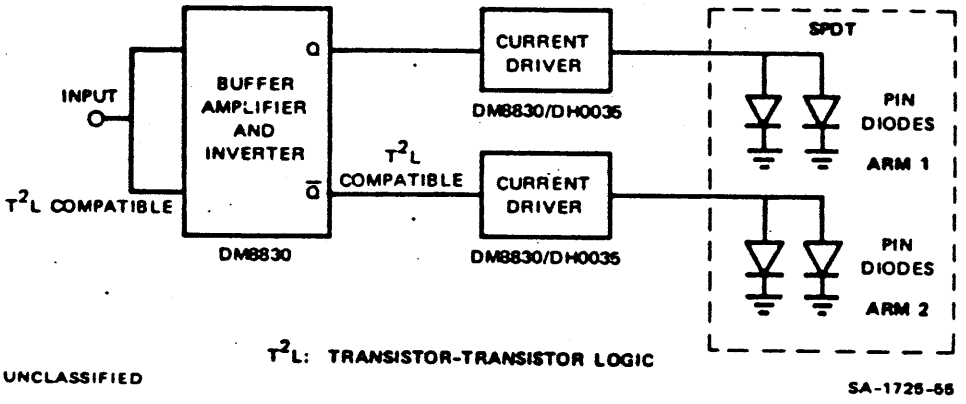

FIGURE VI-5 DRIVER TOPOLOGY FOR SPDT SWITCH (U)

(U) The current drivers recommended for the SPDT switch are DH0035/DH0035C manufactured by National Semiconductor. These are capable of delivering peak current in excess of one ampere at speeds up to 10 MHz. The next section explains how the National Semiconductor DH0035 may be applied to driving PIN diodes and comparable loads that require high peak currents at high repetition rates. The characteristics of the DH0035 are summarized in Table VI-1.

a. PIN-Diode Switching Requirements (U)

(U) Figure VI-6 shows a simplified schematic of a PIN-diode switch. Typically, the PIN diode is used in RF-through-microwave frequency moudlators and switches. Since the diode is in shunt with the RF path, the RF signal is attentuated when the diode is forward-biased (ON) and is passed unattenuated when the diode is reverse-biased (OFF).

(U)

There are essentially two considerations of interest in the ON condition. First, the amount of ON control current must be great enough to prevent the PF-signal current from significantly modulating the ON impedance of the diode. Second, the time required to achieve the ON condition must be minimized.

Table VI-1

(U) CHARACTERISTICS OF NATIONAL SEMICONDUCTOR DH0035 DRIVER (U)

Parameter	Conditions	Value
Differential supply voltage ($V^+ - V^-$)		30 V max
Output current		1,000 mA
Maximum power		1.5 W
t_{delay}	PRF = 5.0 MHz	10 ns
t_{rise}	$V^+ - V^- = 20$ V 10% to 90% .	15 ns
t_{fall}	$V^+ - V^- = 20$ V 90% to 10%	10 ns

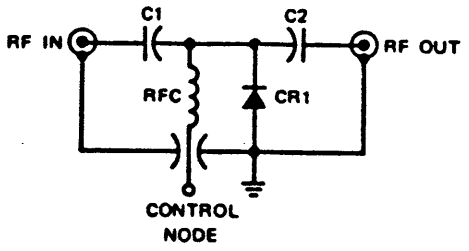

FIGURE VI-6 SIMPLIFIED PIN DIODE SWITCH (U)

(U) The charge-control model of a diode[9,10] leads to the charge continuity equation:

$$i = \frac{dQ}{dt} + \frac{Q}{\tau} \qquad (1)$$

where:

Q = Charge due to excess minority carriers

τ = Mean lifetime of the minority carriers.

Equation (1) implies a circuit model as shown in Figure VI-7. Under study conditions, dQ/dt = 0; hence:

$$I_{DC} = \frac{Q}{\tau} \text{ or } A = I_{DC}\tau \qquad (2)$$

where I_{DC} = steady-state "ON" current.

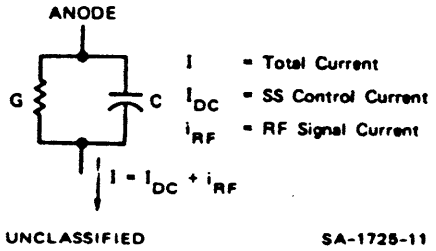

FIGURE VI-7 CIRCUIT MODEL FOR PIN SWITCH (U)

(U) The conductance is proportional to the current, I; hence, to minimize modulation caused by the RF signal, $I_{DC} \gg i_{RF}$. Typical values for I_{DC} range from 50 mA to 200 mA, depending on PIN-diode type and the amount of modulation that can be tolerated.

(U) The time response of the excess charge, Q, may be evaluated by taking the Laplace transform of Eq (1) and solving for Q:

$$Q(s) = \frac{\tau I(s)}{1 + s\tau} \qquad (3)$$

(U)

Solving Eq. (3) for Q(t) yields:

$$Q(t) = L^{-1}[Q(s)] = \tau\,[1 - \exp(-t/\tau)] \quad . \qquad (4)$$

(U) The time response of Q is shown in Figure VI-8(a). As can be seen, several carrier lifetimes are required to achieve the steadystate "on" condition ($Q = I_{DC} \cdot \tau$).

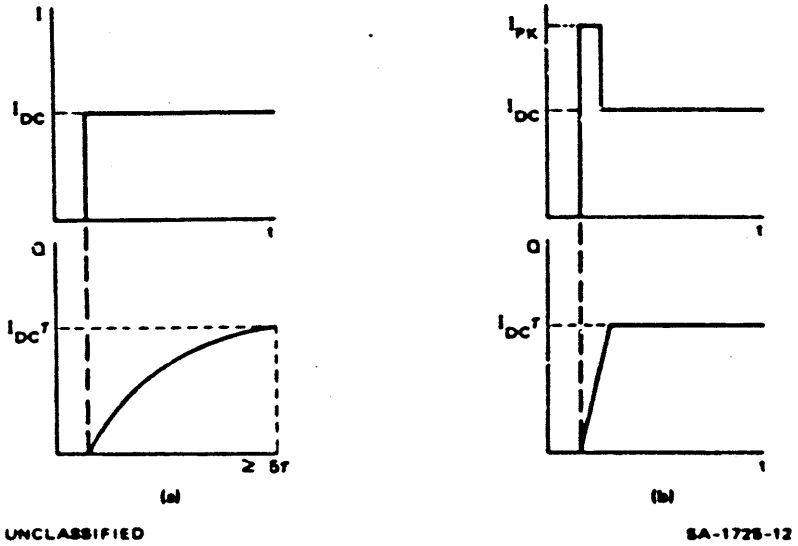

FIGURE VI-8 CHARGE AND TIME RESPONSE (U)

(U) The time response of the charge, and therefore the time for the diode to achieve the ON state, could be shortened by applying a current spike, I_{pk}, to the diode and then dropping the current to the steady-state value, I_{DC}, as shown in Figure VI-8(b). The optimum response would be dictated by:

$$(I_{pk})(t) = \tau\, I_{DC} \quad . \qquad (5)$$

(U) The turn-off requirements for the PIN diode are similar to the turn-on requirements, except that in the OFF condition this charge must be removed. Again, to remove the charge rapidly, a large peak current (in the opposite direction) must be applied to the PIN diode:

$$-I_{pk} \gg \frac{Q}{\tau} \quad . \tag{6}$$

(U) It is interesting to note an implication of Eq. (5). If the peak turn-on current were maintained for a period of time (say, equal to τ) then the diode would acquire an excess charge equal to $I_{pk} \cdot \tau$. This same charge must be removed at turn-off, instead of charge $I_{DC}\tau$, resulting in a considerably slower turn-off. Accordingly, control of the width of turn-on current peak is critical in achieving rapid turn-off.

b. Application of the DH0035 as a PIN Diode Driver (U)

(U) The DH0035 is specifically designed to provide both the current levels and the timing intervals required to optimally drive PIN-diode switches. Its schematic is shown in Figure VI-9. The device utilizes a complementary TTL input buffer such as the National Semiconductor DM7830/DM or DM5440/DM7440 for its input signals.

(U) Two configurations of PIN diode switch are possible--cathode grounded and anode grounded, as shown in Figures VI-10 and VI-11.

c. Repetition-Rate Considerations (U)

(U) Although ignored until now, the PRF--in particular, the OFF time of the PIN diode--is important in selection of C_2, R_M, and R_p. The capacitors must recharge completely during the diode OFF time. In short:

(U)

$$4\ R_M C_2 \leq t_{off}$$

$$4\ R_p C_1 \leq t_{off} \quad .$$

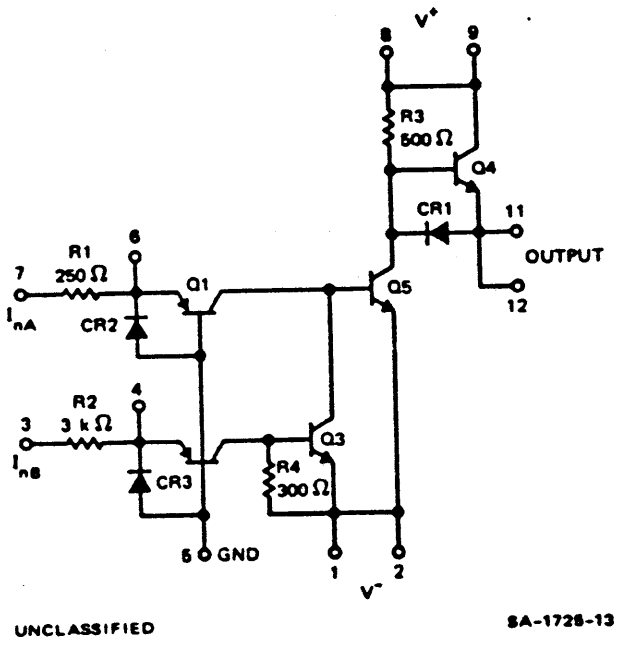

FIGURE VI-9 SCHEMATIC OF DH0035 PIN DIODE DRIVER (U)

d. Practical Results (U)

(U) A breadboard model of the circuit shown in Figure VI-10 has been tested in conjunction with an HP33622A PIN diode by National Semiconductor. I_{DC} was set at 100 mA, V^+ = 10.0 V, V^- = 10 V. Input signal to the DM8830 was a 100-kHz pulse train with pulses of 5 V peak amplitude and 5 μs in width. RF turn-on was accomplished in 10 to 12 ns; turn-off took approximately 5 ns.

(U) In practice, adjustment of C_2 (C_1) may be required to accomodate the particular PIN-diode minority-carrier lifetime.

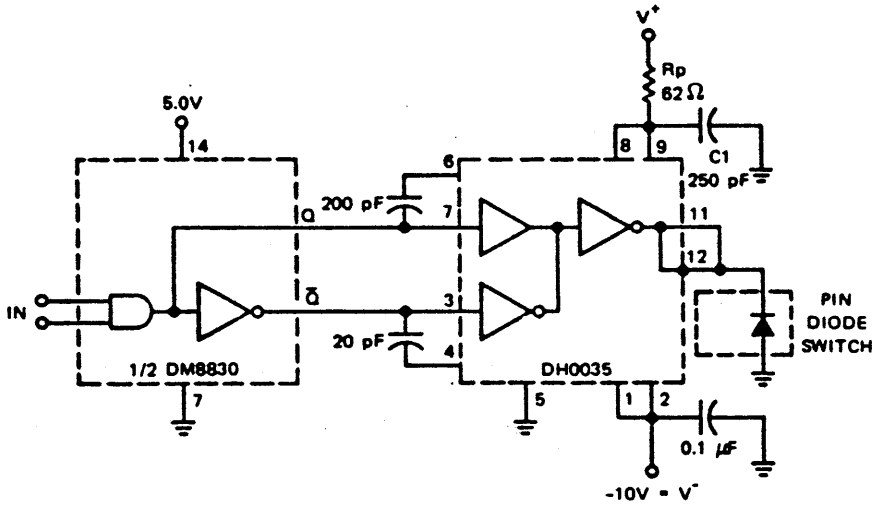

FIGURE VI-10 CATHODE-GROUNDED DESIGN OF TTL LOGIC COMPATIBLE PIN DIODE DRIVER (U)

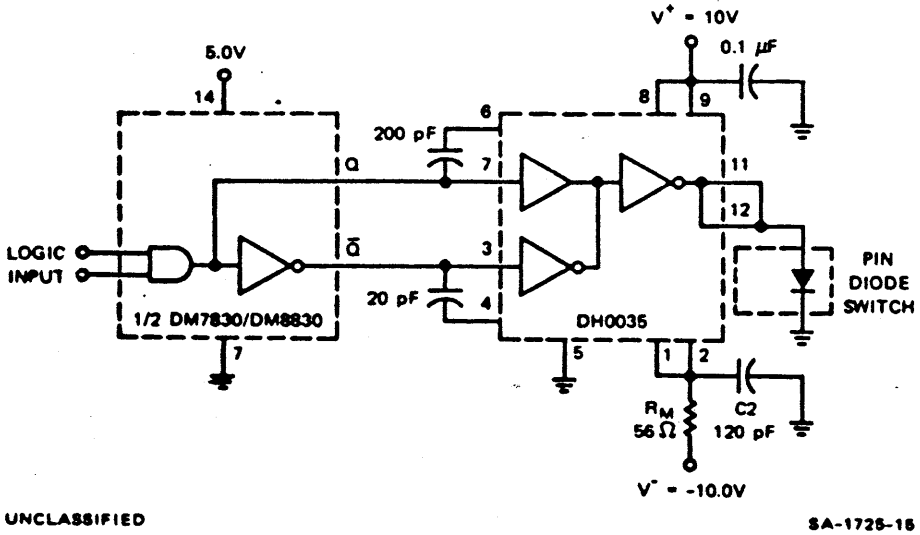

FIGURE VI-11 ANODE-GROUNDED DESIGN OF TTL-LOGIC-COMPATIBLE PIN DIODE DRIVER (U)

VII FREQUENCY TRANSLATOR (U)

A. Basic Approach (U)

(U) The frequency translator is based on development of a suitable DPDT transfer switch in order to solve the problems associated with spurious resonances of unterminated transmission-line elements. Conventional translator circuits do not provide for resistive loading of "switched-out" line sections, which, when open, can become relatively high-Q resonators at frequencies where their lengths are multiples of half-wavelengths. In wideband circuits particularly, the probability that large spurious responses will occur somewhere in the band due to weak coupling to one or more of the "switched-out" sections is great; therefore it is desirable to terminate all line sections for all phase-shift conditions of the translator. Figure VII-1 shows the translator circuit using four DPDT transfer switches that provides termination of all lines in their characteristic impedance.

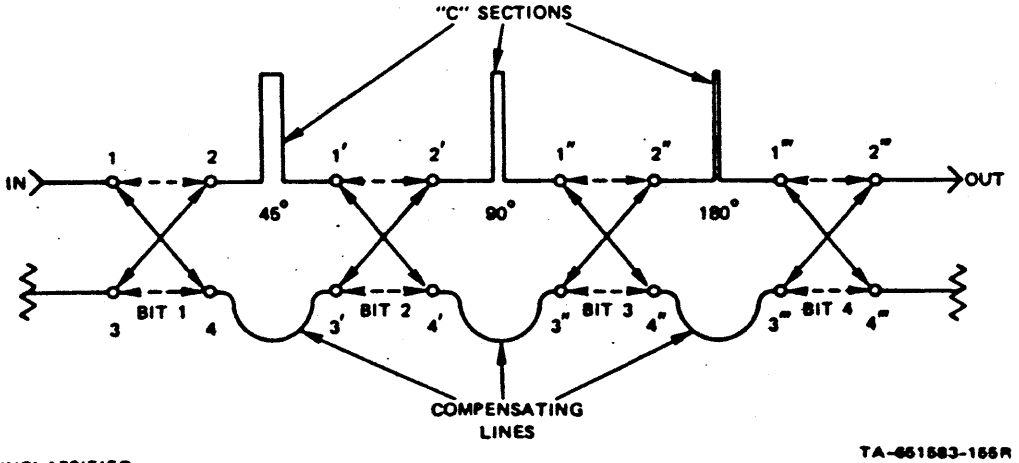

FIGURE VII-1 DIGITAL FREQUENCY TRANSLATOR (U)

(U) The design of the DPDT switch is the same as the one discussed in Section V. Three equivalent representations for the DPDT switches used in Figure VII-1 are shown in Figure VII-2. By use of the circuit

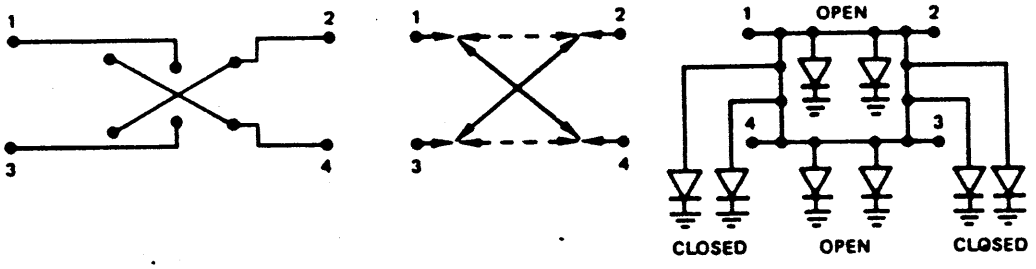

FIGURE VII-2 EQUIVALENT CIRCUITS FOR DPDT SWITCHES (U)

shown in Figure VII-2(c) the translator circuit can be redrawn into a practical configuration as shown in Figure VII-3, where the diodes have been omitted for simplicity. The frequency translator can be broken into the following components:

- DPDT switch
- 45° C-section
- Biasing circuits for the diodes
- Series capacitor for blocking dc currents
- 50-ohm terminations
- Crossovers
- Current drivers.

(U) Our approach was to design, fabricate, and test each of the above components first. It was decided that the translator switch should be developed and integrated only if the performance of each component was acceptable and within the design tolerances.

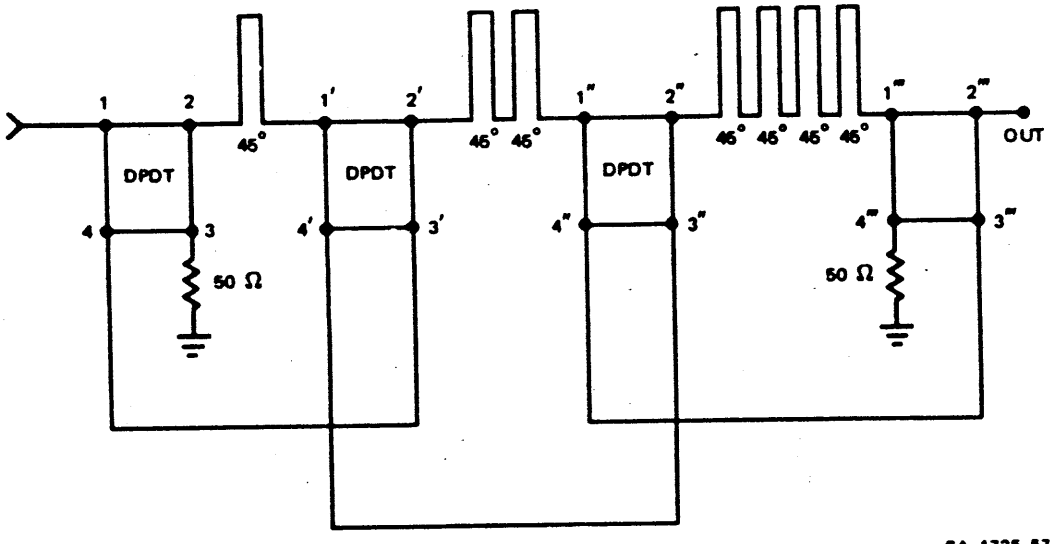

FIGURE VII-3 PRACTICAL FREQUENCY TRANSLATOR USING DPDT SWITCHES (U)

B. Isolation Requirement (U)

(U) Signal leakage through the "off" arms of the transfer switches can degrade the overall performance of the translator. The isolation requirements for the transfer switches derive directly from the amount of allowable phase shift and amplitude error than can be tolerated. The phase-shift error due to isolation leakage for the combination of a single phase-shift section and a compensating line can be calculated as shown in Figure VII-4. Because of the finite isolation of the transfer switches, a portion of the signal is shunt around the phase-shift section as indicated in Figure VII-4(a). The signal represented by V_ℓ in Figure VII-4(a) is attenuated first by the isolation of Switch S_1, and again by the isolation of Switch S_2 before it is recombined with the shifted signal.

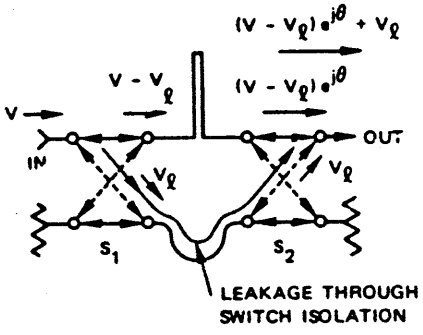

(a) SINGLE "C" SECTION AND COMPENSATING LINE SHOWING LEAKAGE PATH

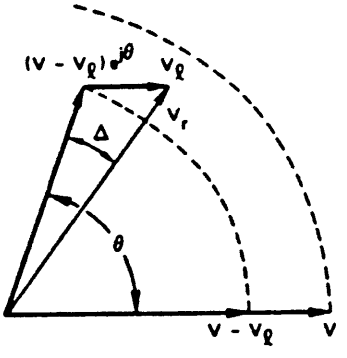

(b) PHASOR MODEL FOR DETERMINING PHASE SHIFT ERROR, Δ

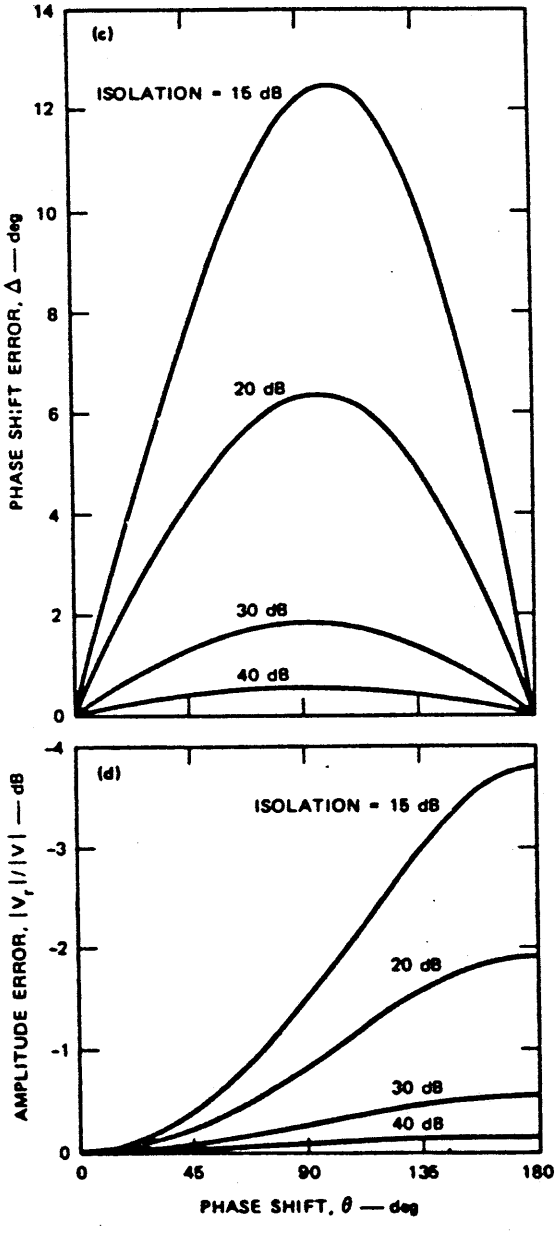

UNCLASSIFIED

SA-1725-68

FIGURE VII-4 PHASE-SHIFT ERRORS FOR SWITCHED C-SECTION (U)

(U)
The isolation values shown as parameters on the error curves in Figure VII-4(a) are the combined isolation of both switches--i.e., if each switch has 10 dB isolation by itself, the appropriate error curve would be the 20-dB curve.

(U) The phase-shift error adds or subtracts as shown in Figure VII-5 according to the total phase shift of the translator. Figure VII-5 shows the effect of the phase-shift error when the main signal path is through the phase shifters. Figure VII-5(b) shows the effect for zero phase shift when the main signal path is through the compensating-line sections.

(U) For the three phase-shift sections in series as shown in Figure VII-1, the phase-shift errors due to each section can be added. The 180° section adds no phase error--it only affects the amplitude of the transmitted signal. There is additional error contributed by leakage signals around two or three sections as well as around the sections taken individually. A summary of the possible leakage paths is shown in Figure VII-6 along with an approximate evaluation of the phase errors for the eight different phase positions of the translator. The phase errors due to leakage paths that span two or more phase-shift sections have been added to the total on the assumption that the leakage through the switch isolation does not significantly reduce the amplitude of the signal. This is only a fair approximation unless isolation values are 30 dB per switch or greater; however, it is useful to obtain a rough idea of the magnitude of errors to be expected.

(U) With only 15 dB isolation per switch, the maximum phase error is about 8°, as indicated in Figure VII-6. With 20 dB isolation per switch, the maximum phase error would be less than 3°. On the basis of this analysis, it appears that the 40-dB isolation requirement is much

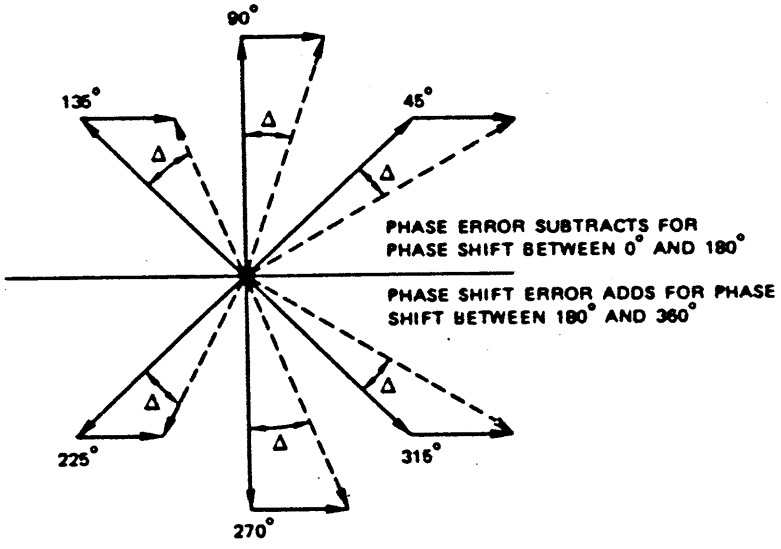

(a) PHASOR DIAGRAM SHOWING DIRECTION OF PHASE SHIFT ERRORS FOR LEAKAGE PATHS THROUGH COMPENSATING LINE SECTIONS

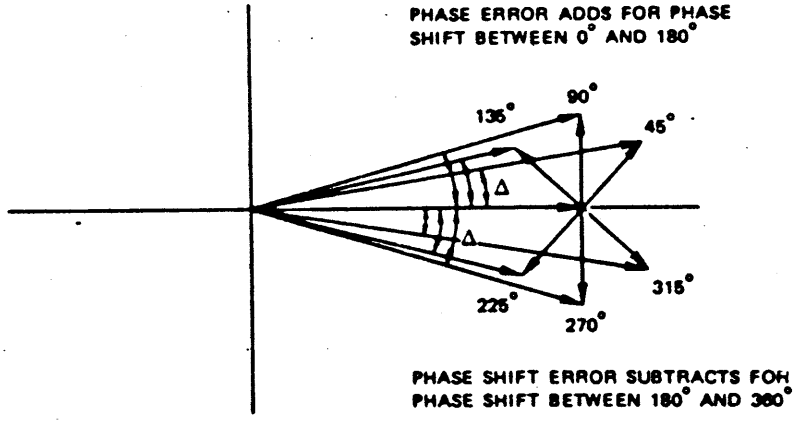

(b) PHASOR DIAGRAM SHOWING DIRECTION OF PHASE SHIFT ERRORS FOR LEAKAGE PATHS THROUGH "C" SECTIONS

UNCLASSIFIED SA-1726-69

FIGURE VII-5 PHASE-SHIFT ERRORS FOR THREE-BIT TRANSLATOR (U)

TOTAL PHASE SHIFT (deg)	PHASE ERROR PER PATH (deg)						TOTAL PHASE ERROR (deg)
	A	B	C	D	E	F	
45	-1.3	+1.9	0	-1.3	-1.9	-1.3	-3.9
90	+1.3	-1.9	0	-1.9	-1.9	-1.9	-6.3
45 + 90	-1.3	-1.9	0	-1.4	-1.9	-1.4	-7.7
180	+1.3	+1.9	0	+1.4	0	0	+4.6
45 + 180	-1.3	+1.9	0	-1.3	0	+1.4	+0.7
90 + 180	+1.3	-1.9	0	-1.9	+1.9	+1.9	+1.3
45 + 90 + 180	-1.3	-1.9	0	-1.4	+1.9	+1.3	-1.4
0	+1.3	+1.9	0	+1.4	-1.9	-1.4	+1.3

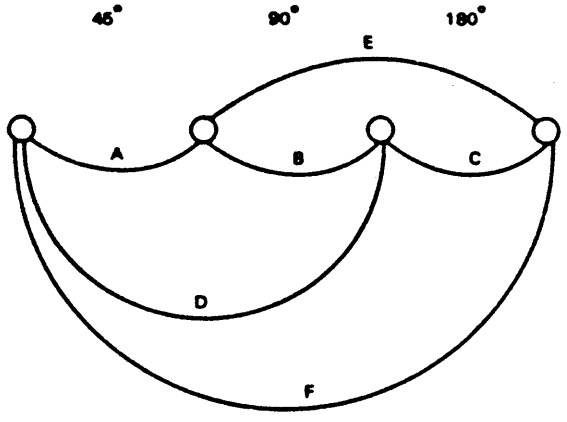

POSSIBLE LEAKAGE PATHS

UNCLASSIFIED

SA-1725-80

FIGURE VII-6 PHASE-ERROR SUMMARY — ISOLATION PER SWITCH = 15 dB (U)

(U)

greater than necessary, and that 20 dB isolation per switch would be adequate. Furthermore, a reduction of the isolation requirement from 40 to 20 dB would allow the transfer switch to be realized with one diode per arm rather than two, greatly simplifying production and reducing overall cost.

(U) In this case, because the isolation is not as critical as the DPDT switch discussed in Section VI and because the power-level requirements are low, beam-lead diodes can be used in realizing a one-diode-per-arm DPDT switch.

C. Design Approach for DPDT (U)

(U) The preferred configuration for the DPDT switch is an arrangement whereby all diodes are connected in shunt, as discussed in Section IV. Either packaged, chip, or beam-lead diodes can be used, depending on the frequency of operation and/or the power dissipation. Packaged diodes are impractical because the package parasitics are very difficult to compensate over the broad bandwidth required. Chip diodes allow better control of circuit values and fit the physical size of the circuit better. Earlier in the program, a decision was made not to use beam-lead diodes because of the limitation in electrical performance due mainly to a large R_s. Beam-lead PIN diodes were then in early stages of development. However, PIN diodes are now available in beam-lead form with characteristics equivalent to those of chip diodes. The only disadvantage is the limitation in power-handling capability (250 mW maximum). This limitation will not affect the operation of the DPDT switch used in the translator because the power-handling requirement is low (30 mW). Beam-lead diodes are ideally suited for microstrip fabrication techniques, and matching over broad bandwidths is greatly simplified. In addition, biasing shunt diodes can be easily done by using quarter-wavelength high-impedance lines and chip capacitors.

(U) The beam-lead diode that was considered as an alternative for the DPDT switch is the MA-47301 made by Microwave Associates, Burlington, Massachusetts. This particular diode has a C_p = 0.02 pF and R_s = 1.5 ohms at 100 mA bias current. In comparison, for the chip diodes HP 5082-3259 (considered earlier in this research program), C_p = 0.15 pF and R_s = 0.1 ohms at 100 mA bias. Since insertion loss and isolation depend ideally on C_p and R_s, respectively, the performance of the two diodes should be comparable. However, it is expected that the beam-lead diode would offer a large bandwidth, and matching problems would be easier to solve because the parasitics due to bonding wires are avoided. Breadboard

(U)
tests of insertion loss and isolation were performed on a single beam-lead diode MA-47301 but with no success because of time limitations and because the matching network was not optimum. We believe that with proper research it can be proven that beam-lead diodes offer better performance than chip diodes.

D. C-Section Design (U)

(U) The phase-shift elements for the frequency translator are based on the Type-A network described by Shiffman,[11] which is now commonly referred to as a "C-section" phase shifter. Figure VII-7 shows the theoretical response for several designs for the 45° and 90° bits. The parameter ρ is related to the coupling between the elements and determines the ripple bandwidth. The larger the value of ρ, the tighter the coupling and the smaller the physical spacing between the transmission-line elements for the C-section. For edge-coupled microstrip, a ρ of 3 is the maximum value that is practical on 0.010-inch-thick sapphire, and corresponds to a spacing of about 0.0008 inch, which can be etched with fairly good consistency in a production situation.

(U) The differential-phase responses* for the 45° shifter shown in Figure VII-7(a) indicates that a ρ of 1.80 equalizes the ripple variations over the desired band, with a maximum deviation of 2°. Smaller values of ρ produce more narrowband responses with increased phase deviation at the band-edges, while larger values increase the ripple. Similar characteristics are obtained for the 90° shifter shown in Figure VII-7(b) except

*(U) The differential phase response is the difference between the nominal phase response and the calculated response.

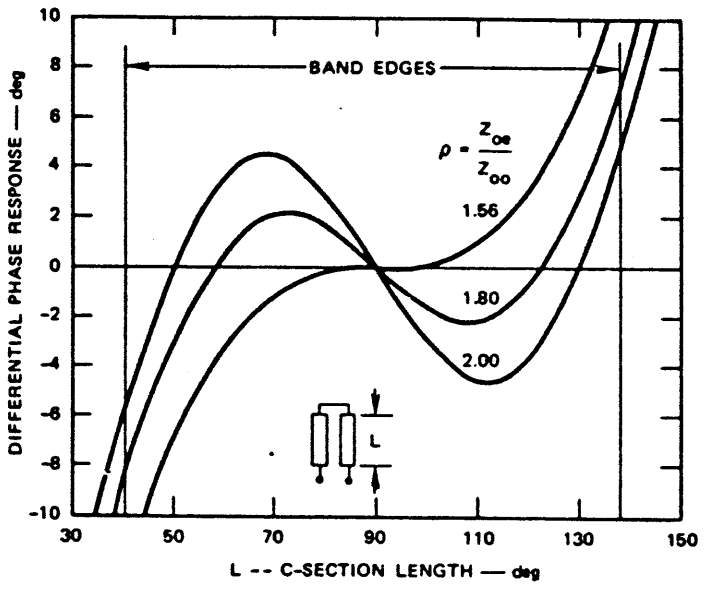

(a) 45° PHASE SHIFT — COMPENSATING LINE LENGTH = 225°

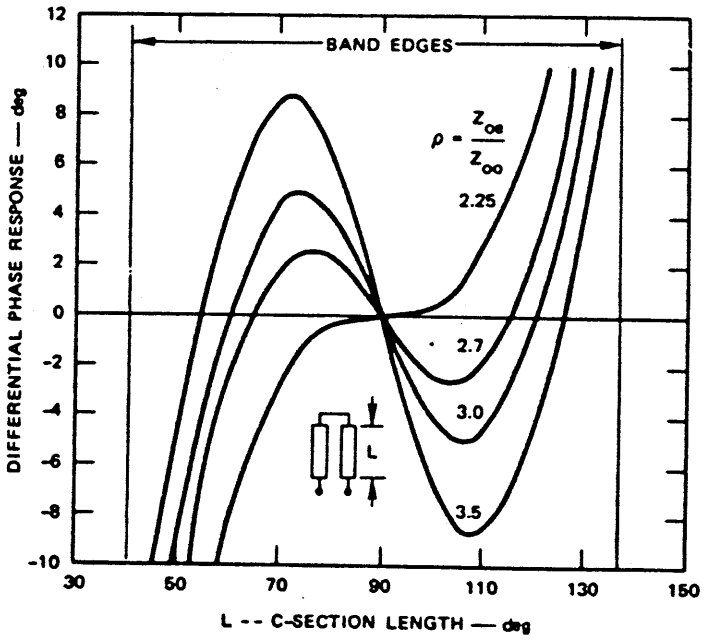

(b) 90° PHASE SHIFT — COMPENSATING LINE LENGTH = 270°

UNCLASSIFIED

SA-1725-61

FIGURE VII-7 THEORETICAL DIFFERENTIAL PHASE RESPONSE FOR C-SECTION PHASE SHIFTERS (U)

(U)

that the ripple is increased for the same bandwidth, and the equal-ripple coupling is also greater. For a maximum phase deviation of 5° for the 90° shifter, the value of ρ must be increased to 3, which is the practical maximum.

(U) A 90° shifter can also be realized by connecting two 45° shifters in tandem. For the examples outlined above, combining two 45° shifters, each with a ρ of 1.8, to obtain a total of 90° phase shift would result in a maximum phase deviation of 4°, whereas the single 90° shifter gives a maximum phase deviation of 5°. In addition, the 90° shifter requires much closer line spacing and consequently better control of tolerances, and would be somewhat more difficult to produce on a consistent basis in production. The only disadvantage of combining two 45° shifters is the extra circuit length required, which would tend to increase line losses somewhat. In all but the most critical situations, where loss is a major factor, the combination of two 45° shifters is considered a better approach than the single 90° shifter.

(U) It is possible to reduce the phase deviation of the 90° shifter by adding a phase-correcting network after the manner described by Schiffman[11] for the Type-B phase-shift network. The circuit configuration is shown in Figure VII-8(a) and the differential phase response for three corrected designs is shown in Figure VII-8(b). In general, the Type-B phase-shift network always consists of one tightly coupled C-section and a fairly loosely coupled correction network. In Figure VII-8 the tightly coupled C-section has $\rho_1 = 3$, the maximum practical value. The best value for ρ_2 is then between 1.20 and 1.25, and is determined mainly by the phase deviation at the band-edges, with a minimum between 1° and 2°. If ρ_1 could be increased to a value greater than 3, the corrected phase deviation could be reduced to below 1°.

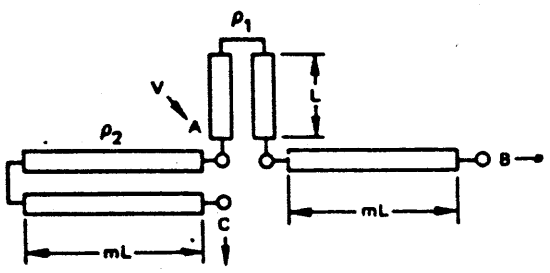

(a) TYPE B PHASE SHIFTER WITH CORRECTION SECTION

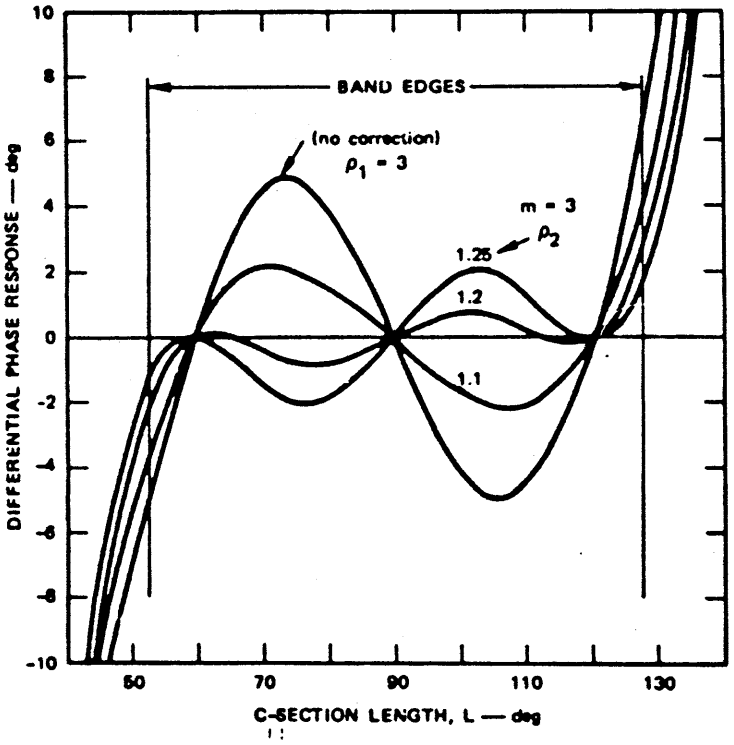

(b) THEORETICAL DIFFERENTIAL PHASE RESPONSE

UNCLASSIFIED SA-1725-62

FIGURE VII-8 TYPE-B PHASE SHIFTER (U)

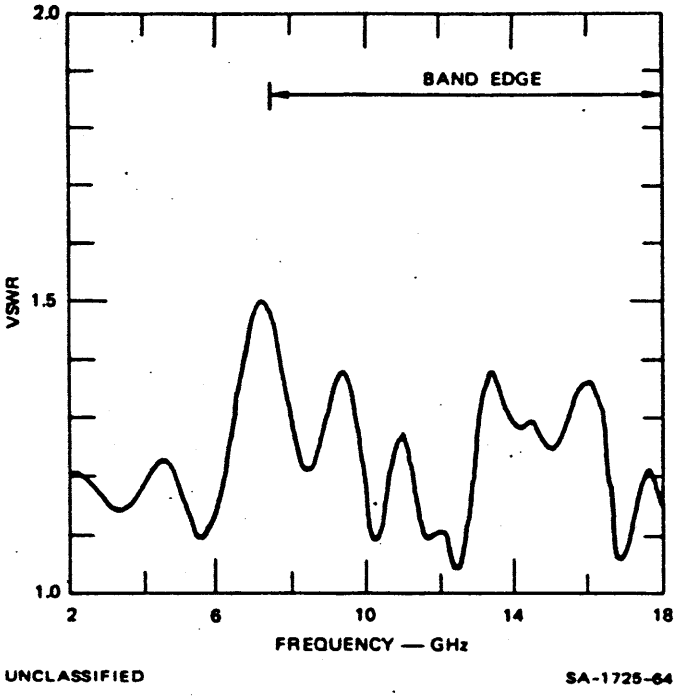

FIGURE VII-10 INPUT VSWR OF 45° C-SECTION (U)

(U)

transmission loss through a 45° C-section. The loss is equivalent to that of a six-inch-long, 0.085-inch-diameter coaxial cable with two SMA connectors. The loss data also include the effects of the reflections at the various ports and ribbon bonds.

(U) Figure VII-12 and VII-13 show the transmission phase of a 45° C-section taken at different line extensions of the network analyzer to compensate for the line transmission. The data shown in Figure VII-13 are much closer to the 25:1 scale-model data than the data shown in Figure VII-12. The center frequency of the C-section is about 10% lower than in theoretical design, which was expected because the model data were 8% lower than in the theoretical design. If the center frequency

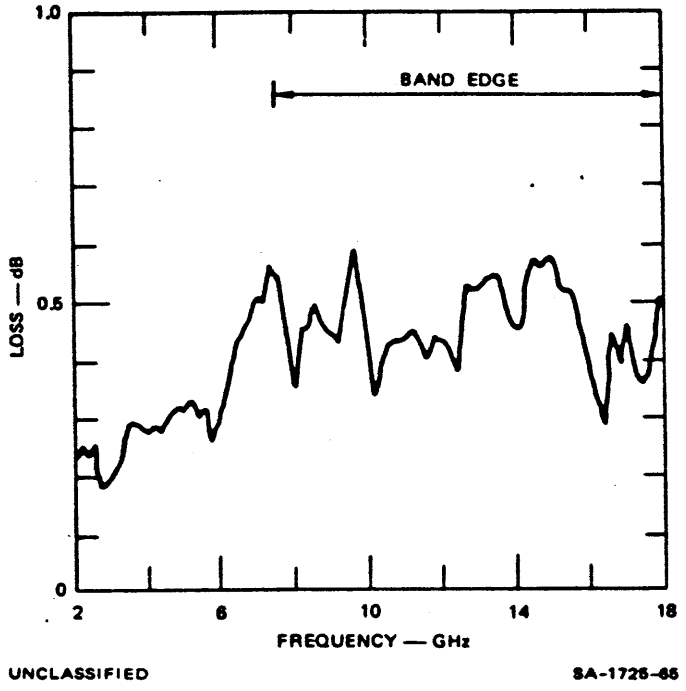

FIGURE VII-11 TRANSMISSION LOSS OF 45° C-SECTION (U)

(U)

is corrected, the phase-shift tolerance across the band will be ± 4° from a nominal phase shift of 45°. The data plots shown in Figures VII-10 through VII-13 were obtained from the data shown in Table VII-1.

E. Bias Tee (U)

(U) A 25:1 scale-model bias tee was designed and constructed. The bias tee consisted of a 50-ohm microstrip line with a quarter-wavelength (at midband) high-impedance line connected in the center. The other end of the high-impedance line was grounded. The high-impedance line was made of 25-mil-diameter copper wire, which corresponds to 1-mil-diameter gold wire at the actual size. Electrical tests were performed on the 50-ohm line with shortened stubs of various lengths. Plots of

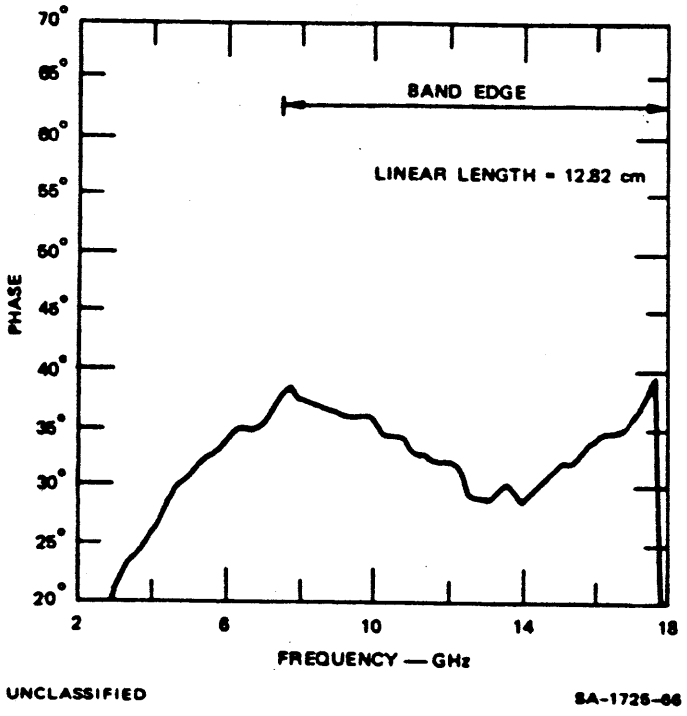

FIGURE VII-12 TRANSMISSION PHASE OF 45° C-SECTION. Linear length = 12.82 cm. (U)

(U)

transmission loss and return loss for two different conditions are shown in Figures VII-14 and VII-15. The results in Figure VII-14 were for a quarter-wavelength line suspended above the substrate in the air and in Figure VII-15 for a line taped to the substrate (dielectric constant of 10). The minor differences in the results are due to the differences in the electrical lengths of the high-impedance lines.

(U) It can be concluded from these results that a simple bias tee consisting of a quarter-wavelength high-impedance line terminated at one end by a bypass capacitor would be adequate for biasing individual diodes in DPDT switches. Also the results show that the useful bandwidth expected is larger than the bandwidth required.

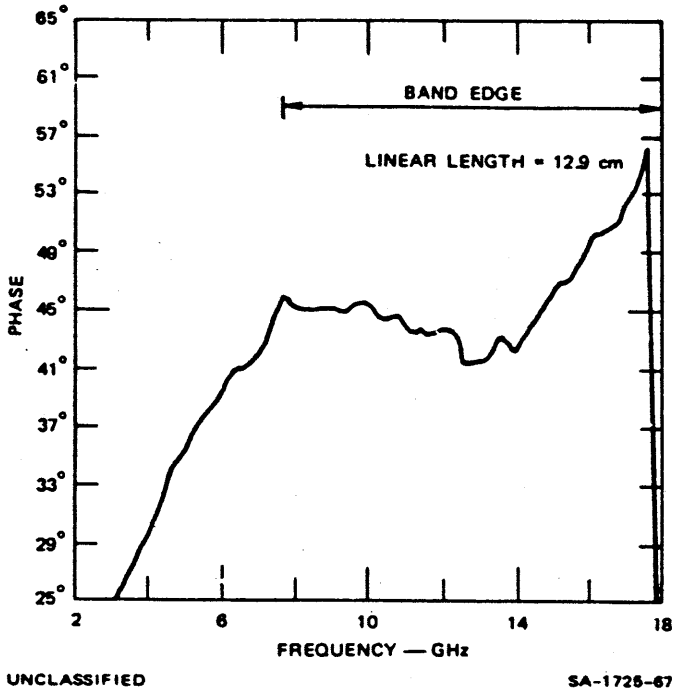

FIGURE VII-13 TRANSMISSION PHASE OF 45° C-SECTION. Linear length = 12.9 cm. (U)

(U) In order to obtain a bias tee at the actual frequencies using microstrip lines on 10-mil-thick sapphire substrates, the following development steps were taken:

- A 50-ohm line on sapphire substrate was fabricated and tested (see Figure VII-16 for mechanical details).
- A gold wire 0.001 inch in diameter and one-quarter wavelength long (at center frequency) was bonded from the center of the 50-ohm line to a short circuit at the edge of the substrate. (See Figure VII-17 for mechanical details.)
- The gold wire from the short circuit was disconnected, and a chip capacitor to ground was assembled at the edge of the substrate. The same 0.001-inch-diameter quarter-wavelength-long gold wire was bonded to the top of the chip capacitor. The capacitor acts as a bypass

Table VII-1

(U) MEASUREMENTS ON ACTUAL-SIZE 45° C-SECTION (U)

FREQ-MHZ	LOSS-DB MEAS 1	D-PHASE MEAS 1	REFL-MAG MEAS 1	VSWR MEAS 1	PHASE MEAS 1
2000.000	.22	-20.67	.094	1.21	14.14
2200.000	.26	-19.68	.094	1.21	14.94
2400.000	.23	-18.18	.091	1.20	16.24
2600.000	.26	-16.94	.086	1.19	17.28
2800.000	.18	-15.62	.080	1.17	18.43
3000.000	.19	-13.80	.073	1.16	20.05
3200.000	.22	-11.89	.068	1.15	21.77
3400.000	.25	-10.44	.067	1.14	23.03
3600.000	.30	-9.47	.068	1.15	23.81
3800.000	.29	-8.53	.073	1.16	24.56
4000.000	.28	-7.28	.083	1.18	25.61
4200.000	.29	-6.07	.093	1.21	26.63
4400.000	.27	-4.82	.099	1.22	27.70
4600.000	.30	-3.55	.103	1.23	28.79
4800.000	.32	-2.20	.097	1.22	29.96
5000.000	.32	-1.45	.083	1.18	30.51
5200.000	.34	-.70	.067	1.14	31.08
5400.000	.30	.33	.049	1.10	31.92
5600.000	.32	1.16	.042	1.09	32.57
5800.000	.26	1.54	.051	1.11	32.78
6000.000	.32	2.41	.065	1.14	33.44
6200.000	.35	3.38	.088	1.19	34.23
6400.000	.42	4.19	.119	1.27	34.86
6600.000	.45	4.34	.147	1.35	34.82
6800.000	.47	4.58	.173	1.42	34.87
7000.000	.51	5.14	.193	1.48	35.24
7200.000	.50	5.83	.202	1.50	35.75
7400.000	.57	7.12	.195	1.49	36.85
7600.000	.54	8.34	.179	1.44	37.89
7800.000	.45	9.16	.153	1.36	38.54
8000.000	.35	8.30	.126	1.29	37.47
8200.000	.46	8.34	.102	1.23	37.31
8400.000	.46	8.32	.093	1.21	37.10
8600.000	.50	8.20	.097	1.21	36.79
8800.000	.46	8.27	.114	1.26	36.68
9000.000	.44	8.27	.136	1.31	36.48
9200.000	.43	8.12	.152	1.36	36.16
9400.000	.53	8.08	.162	1.39	35.93
9600.000	.59	8.41	.150	1.35	36.07
9800.000	.53	8.63	.123	1.28	36.09
10000.00	.44	8.68	.085	1.19	35.96
10200.00	.34	7.71	.040	1.08	34.81
10400.00	.40	7.54	.048	1.10	34.45
10600.00	.43	7.79	.085	1.19	34.51
10800.00	.43	7.81	.109	1.24	34.33
11000.00	.45	7.02	.121	1.28	33.35

(U) Table VII-1 (continued) (U)

FREQ-MHZ	LOSS-DB MEAS 1	D-PHASE MEAS 1	REFL-MAG MEAS 1	VSWR MEAS 1	PHASE MEAS 1
11200.00	.45	6.53	.105	1.23	32.67
11400.00	.43	6.83	.074	1.16	32.76
11600.00	.40	6.49	.049	1.10	32.26
11800.00	.44	6.67	.046	1.10	32.25
12000.00	.44	6.91	.053	1.11	32.30
12200.00	.42	6.85	.046	1.10	32.05
12400.00	.38	6.40	.021	1.04	31.41
12600.00	.53	4.48	.021	1.04	29.31
12800.00	.52	4.61	.069	1.15	29.26
13000.00	.53	4.52	.110	1.25	28.97
13200.00	.54	4.65	.144	1.34	28.92
13400.00	.55	5.52	.164	1.39	29.59
13600.00	.53	6.46	.155	1.37	30.35
13800.00	.47	6.09	.140	1.32	29.79
14000.00	.45	5.25	.126	1.29	28.76
14200.00	.53	6.18	.124	1.28	29.51
14400.00	.57	6.67	.130	1.30	29.81
14600.00	.56	7.64	.128	1.29	30.59
14800.00	.57	8.25	.117	1.26	31.01
15000.00	.57	9.25	.110	1.25	31.81
15200.00	.52	10.02	.112	1.25	32.40
15400.00	.52	10.01	.124	1.28	32.21
15600.00	.51	10.82	.138	1.32	32.83
15800.00	.43	11.42	.153	1.36	33.25
16000.00	.38	12.58	.156	1.37	34.23
16200.00	.32	13.30	.149	1.35	34.76
16400.00	.28	13.57	.136	1.31	34.84
16600.00	.45	13.78	.085	1.18	34.85
16800.00	.39	14.10	.028	1.06	34.99
17000.00	.46	15.46	.033	1.07	36.17
17200.00	.38	16.10	.059	1.13	36.62
17400.00	.36	17.32	.084	1.18	37.64
17600.00	.39	19.45	.097	1.22	39.58
17800.00	.51	-160.31	.089	1.20	-140.37
18000.00	.49	-159.59	.066	1.14	-139.83

REF PLANE EXT(CM): INPUT= .00 TRAN= 12.82
LINEARIZED FROM 2000.00 TO 18000.00
SLOPE(S) (EQUIV CM)= .08

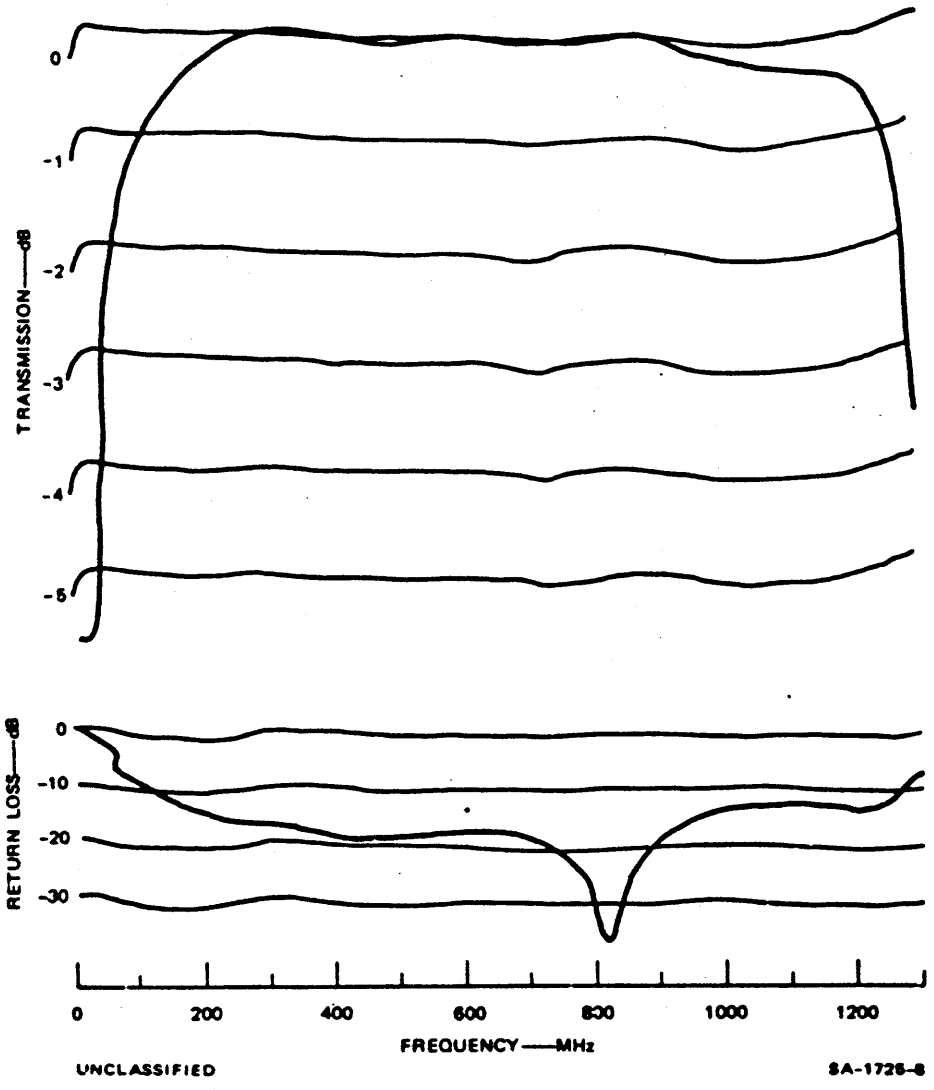

FIGURE VII-14 CHARACTERISTIC OF 25:1 SCALE BIAS TEE $\left[\frac{\lambda}{4}\right.$ (AIR) HIGH-IMPEDANCE LINE AT MIDBAND$\left.\right]$ (U)

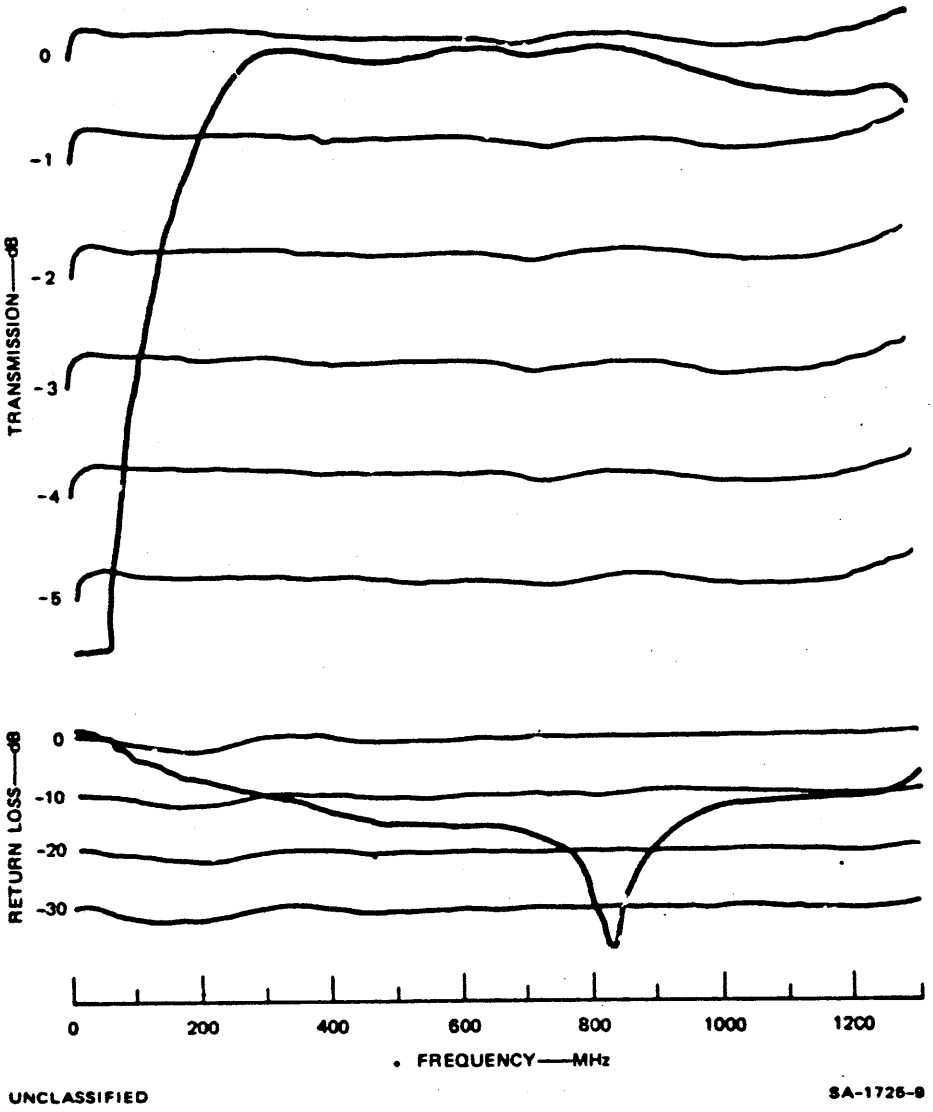

FIGURE VII-15 CHARACTERISTICS OF 25:1 SCALE BIAS TEE $\left[\frac{\lambda}{4}\right.$ (DIELECTRIC) HIGH-IMPEDANCE LINE AT MIDBAND$\left.\right]$ (U)

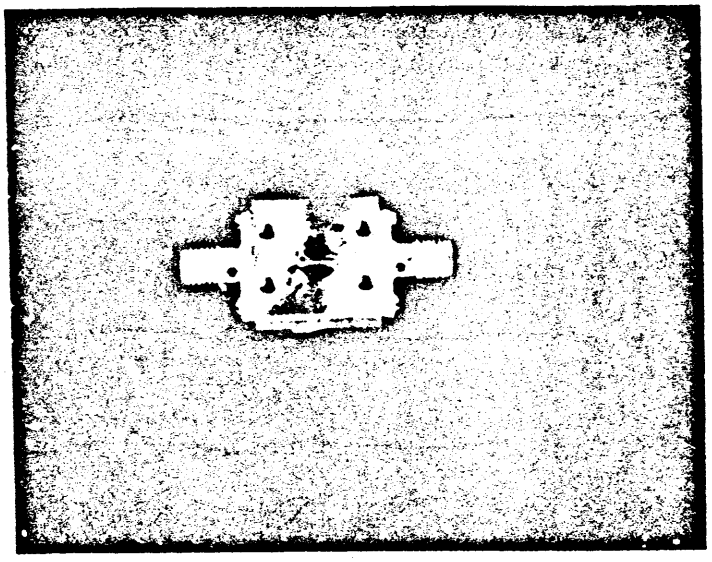

UNCLASSIFIED SA-1725-70

FIGURE VII-16 50-ohm MICROSTRIP TRANSMISSION LINE ON 10-mil-THICK SAPPHIRE SUBSTRATE (U)

(U)

or short-circuit to ground for RF signals and an open circuit for dc bias voltage. (See Figure VII-18 for mechanical details.)

1. Test Results for 50-ohm Microstrip Line (U)

(U) A 50-ohm microstrip line was fabricated on 10-mil-thick sapphire substrates using the processes discussed in Section X. The transmission line was first tested by using a time-domain reflectometer to see if all the ribbon bonds and connectors were in good condition (see Figure VII-19 for the TDR plots). Then the line was tested by the use of the 8541A automatic network analyzer. Both transmission and reflection tests were performed on the unit. The data are presented in Table VII-2 and the plots of transmission loss and input VSWR at Port 1 are shown in Figures VII-20 and VII-21, respectively. Tests were also performed by feeding the signal into Port 2. The results were similar to Port 1 data.

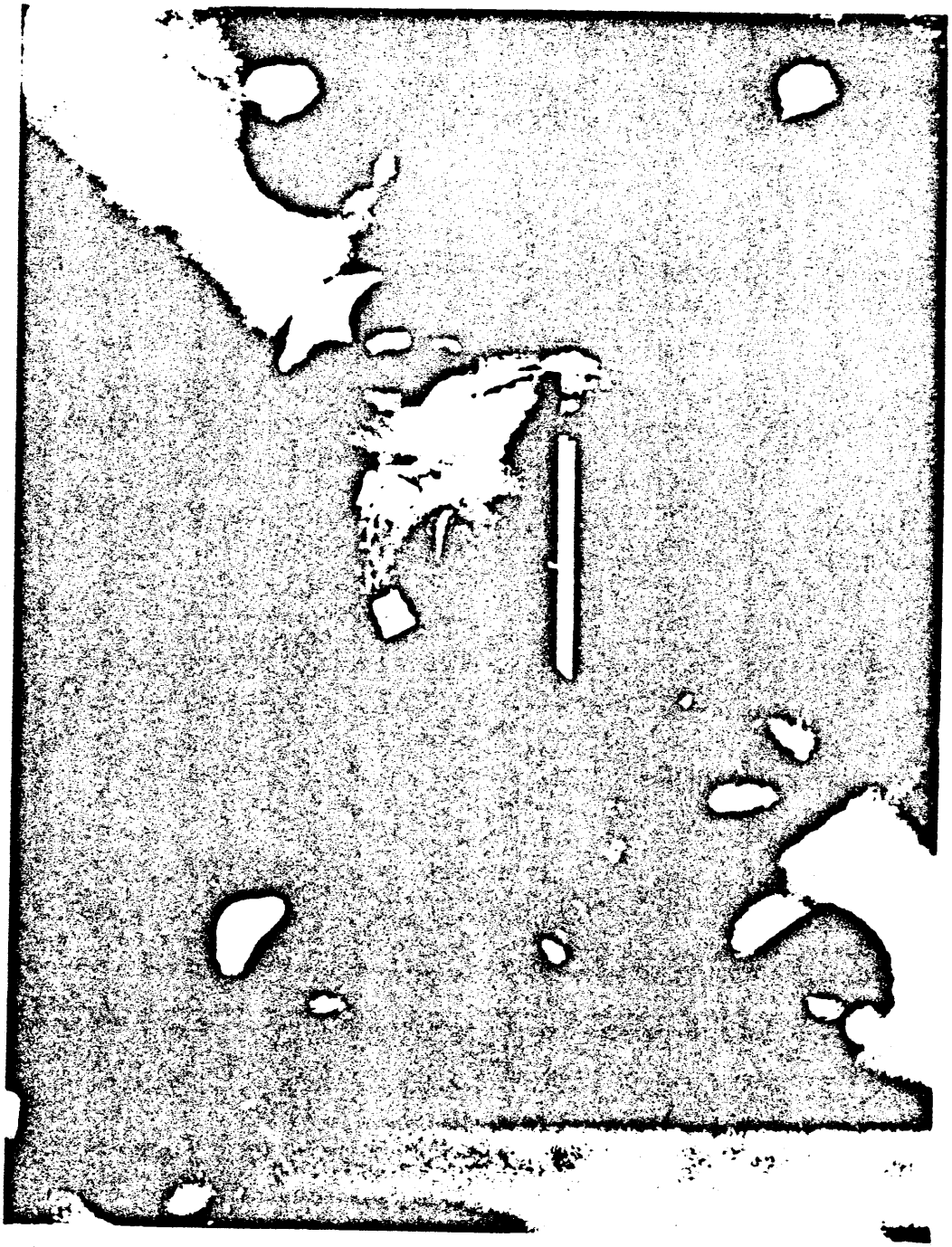

UNCLASSIFIED

SA-1725-71

FIGURE VII-17 BIAS TEE WITH ONE END GROUNDED (U)

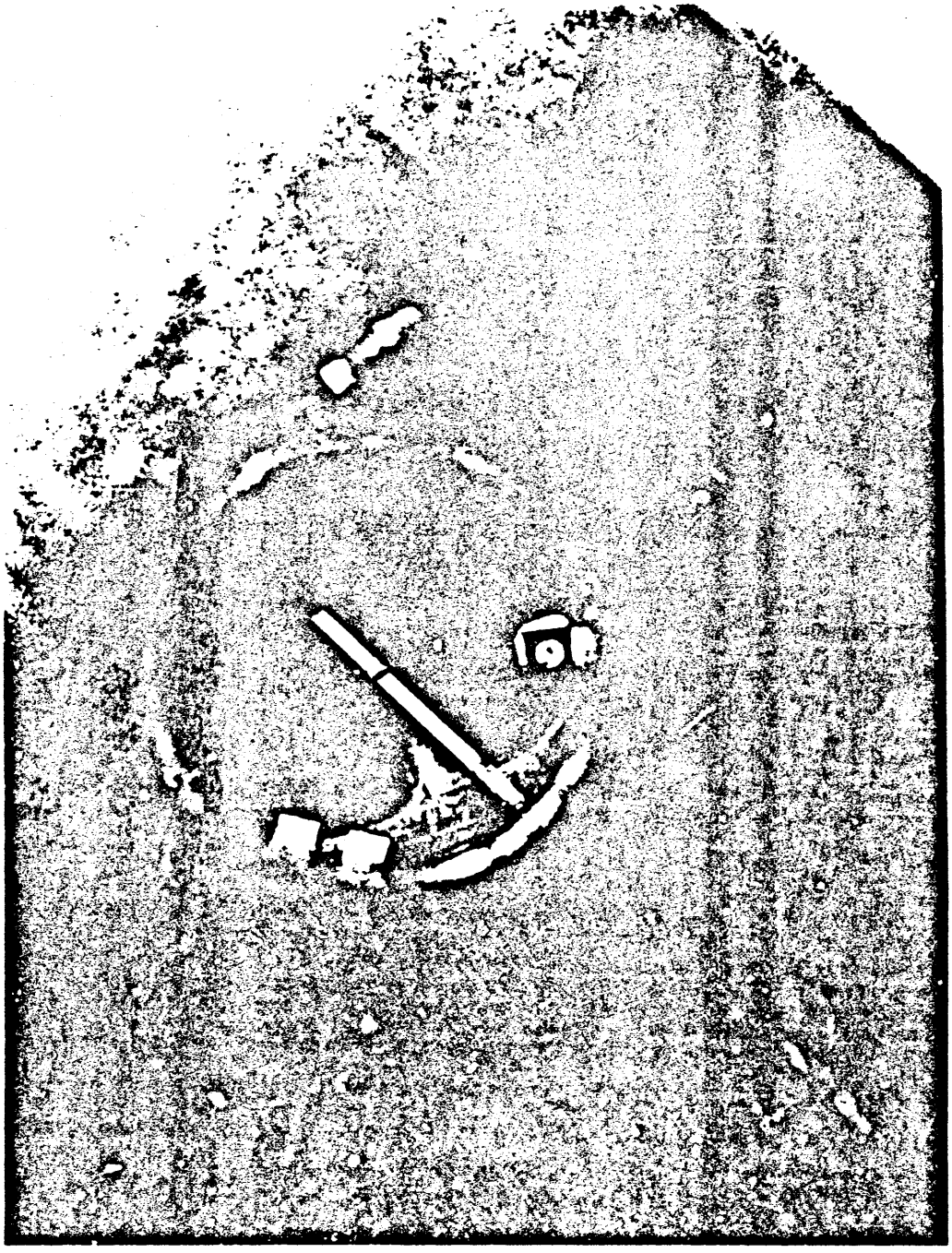

UNCLASSIFIED SA 1725-72

FIGURE VII-18 BIAS TEE WITH ONE END GROUNDED AT RF FREQUENCIES BY THE USE OF BYPASS CAPACITOR OPEN AT dc (U)

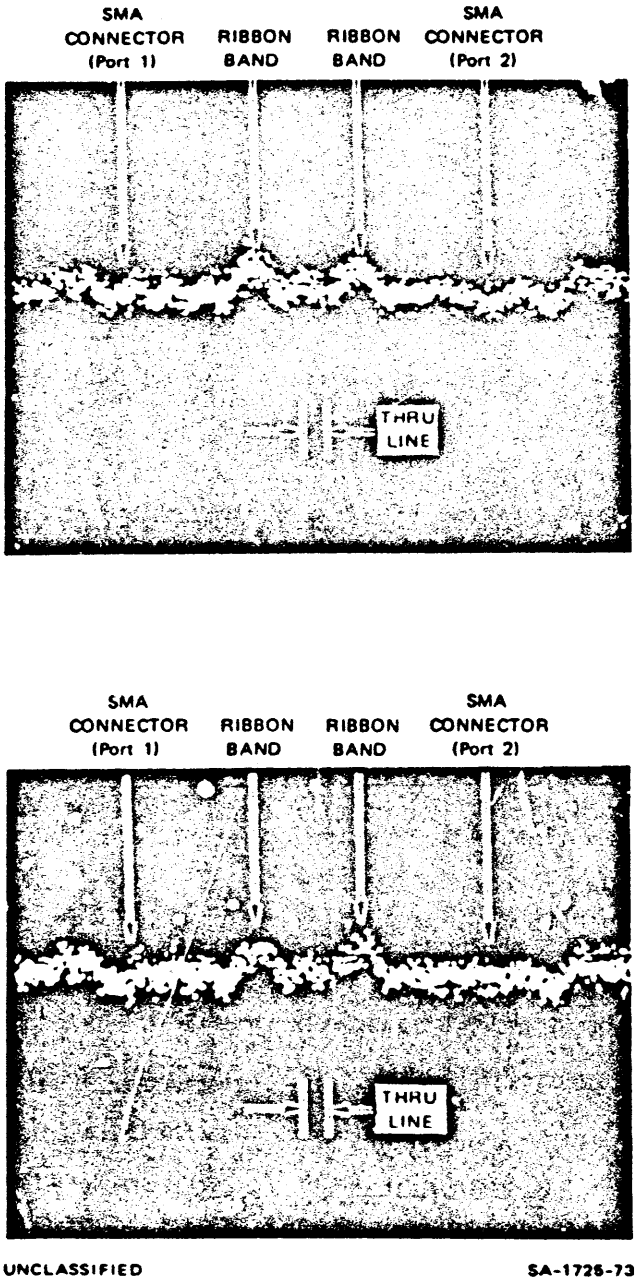

FIGURE VII-19 TDR PLOTS OF 50-ohm MICROSTRIP TRANSMISSION LINE ON 10-mil SAPPHIRE SUBSTRATE (U)

Table VII-2

(U) TRANSMISSION-LOSS AND REFLECTION TESTS OF MICROSTIP 50-OHM LINE ON 10-MIL-THICK SAPPHIRE SUBSTRATE (U)

FREQ-MHZ	LOSS-DB MEAS 1	D-PHASE MEAS 1	REFL-MAG MEAS 1	VSWR MEAS 1	PHASE MEAS 1
2000.000	.16	2.27	.003	1.01	-124.35
2200.000	.11	1.99	.002	1.00	-136.89
2400.000	.07	2.11	.003	1.01	-149.04
2600.000	.07	2.27	.003	1.01	-161.15
2800.000	.09	2.46	.005	1.01	-173.23
3000.000	.12	2.71	.005	1.01	174.76
3200.000	.14	2.71	.004	1.01	162.51
3400.000	.16	2.84	.006	1.01	150.36
3600.000	.18	2.67	.008	1.02	137.93
3800.000	.19	2.44	.010	1.02	125.43
4000.000	.23	2.12	.013	1.03	112.86
4200.000	.22	1.80	.018	1.04	100.27
4400.000	.19	1.91	.023	1.05	88.11
4600.000	.21	2.12	.029	1.06	76.06
4800.000	.23	2.18	.036	1.07	63.85
5000.000	.28	1.84	.042	1.09	51.25
5200.000	.25	1.45	.049	1.10	38.61
5400.000	.24	1.47	.052	1.11	26.35
5600.000	.24	1.40	.051	1.11	14.02
5800.000	.24	1.42	.050	1.10	1.77
6000.000	.26	1.49	.049	1.10	-10.42
6200.000	.24	1.62	.048	1.10	-22.56
6400.000	.25	1.60	.044	1.09	-34.83
6600.000	.21	1.21	.039	1.08	-47.49
6800.000	.20	.70	.033	1.07	-60.25
7000.000	.24	.09	.027	1.06	-73.13
7200.000	.22	-.28	.023	1.05	-85.78
7400.000	.23	-.34	.017	1.04	-98.10
7600.000	.24	-.43	.013	1.03	-110.45
7800.000	.27	-.21	.009	1.02	-122.49
8000.000	.29	-.57	.005	1.01	-135.11
8200.000	.21	-.44	.007	1.01	-147.25
8400.000	.20	-.49	.012	1.02	-159.57
8600.000	.22	-.41	.018	1.04	-171.75
8800.000	.21	.01	.020	1.04	176.42
9000.000	.19	.22	.021	1.04	164.36
9200.000	.21	.26	.024	1.05	152.14
9400.000	.28	-.08	.028	1.06	139.54
9600.000	.28	-.54	.030	1.06	126.81
9800.000	.32	-1.00	.029	1.06	114.09
10000.00	.32	-1.35	.027	1.06	101.48
10200.00	.30	-1.54	.030	1.06	89.02
10400.00	.28	-1.77	.036	1.08	76.52
10600.00	.28	-1.73	.044	1.09	64.31
10800.00	.32	-2.22	.052	1.11	51.56
11000.00	.33	-2.24	.062	1.13	39.28

(U) Table VII-2 (continued) (U)

FREQ-MHZ	LOSS-DB MEAS 1	D-PHASE MEAS 1	REFL-MAG MEAS 1	VSWR MEAS 1	PHASE MEAS 1
11200.00	.34	-2.10	.074	1.16	27.16
11400.00	.36	-2.11	.087	1.19	14.89
11600.00	.34	-2.04	.101	1.23	2.69
11800.00	.34	-2.38	.116	1.26	-9.91
12000.00	.38	-2.46	.128	1.29	-22.25
12200.00	.46	-2.47	.140	1.33	-34.52
12400.00	.50	-2.93	.151	1.35	-47.24
12600.00	.51	-4.75	.154	1.36	-61.32
12800.00	.49	-5.19	.156	1.37	-74.02
13000.00	.41	-5.61	.155	1.37	-86.71
13200.00	.40	-6.23	.152	1.36	-99.59
13400.00	.43	-6.14	.149	1.35	-111.77
13600.00	.46	-6.48	.143	1.33	-124.37
13800.00	.42	-6.06	.131	1.30	-136.21
14000.00	.48	-5.18	.122	1.28	-147.60
14200.00	.39	-5.02	.116	1.26	-159.70
14400.00	.36	-4.69	.109	1.24	-171.63
14600.00	.33	-4.50	.100	1.22	176.29
14800.00	.37	-4.86	.094	1.21	163.66
15000.00	.35	-5.11	.094	1.21	151.14
15200.00	.32	-5.93	.097	1.21	138.06
15400.00	.25	-6.67	.100	1.22	125.05
15600.00	.17	-7.30	.103	1.23	112.17
15800.00	.17	-7.73	.105	1.23	99.47
16000.00	.24	-8.04	.104	1.23	86.89
16200.00	.33	-8.10	.102	1.23	74.57
16400.00	.37	-8.27	.106	1.24	62.14
16600.00	.46	-7.74	.098	1.22	50.40
16800.00	.37	-8.33	.083	1.18	37.54
17000.00	.41	-8.39	.070	1.15	25.21
17200.00	.39	-9.09	.058	1.12	12.29
17400.00	.47	-9.44	.050	1.10	-.37
17600.00	.37	-10.33	.037	1.08	-13.52
17800.00	.45	-10.91	.018	1.04	-26.36
18000.00	.34	168.85	.012	1.02	141.13

REF PLANE EXT(CM): INPUT= .00 TRAN= .00
LINEARIZED FROM 2000.00 TO 18000.00
SLOPE(S) (EQUIV CM)= 5.11

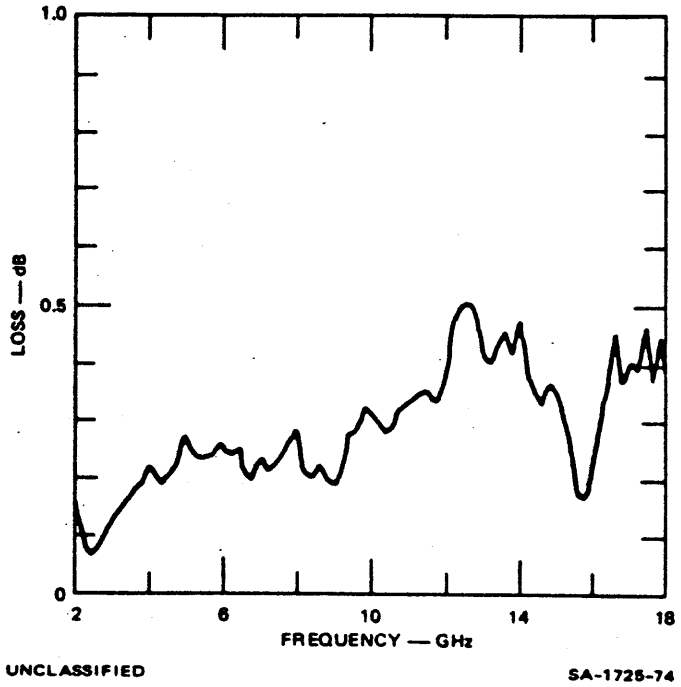

FIGURE VII-20 TRANSMISSION LOSS OF MICROSTRIP 50-ohm TRANSMISSION LINE ON 10-mil-THICK SAPPHIRE SUBSTRATE (Input to Port 1) (U)

2. Test Results for Microstrip Bias Tee with RF and dc Grounded (U)

(U) A quarter-wavelength-long, 0.001-inch diameter gold wire was bonded from the center of the microstrip 50-ohm transmission line discussed above to a pad shorted to the ground plane at the edge of the sapphire substrate. Both transmission and reflection tests were performed on the assembled unit using the 8541A automatic network analyzer. The first set of data were taken for a high-impedance quarter-wavelength line 0.240 inch long. The results showed that the line needed to be shortened to compensate for the extra line length that is introduced by the wrap-around to the ground plane. The best results were obtained for a high-impedance line 0.189 inch long. These results are shown in Figures

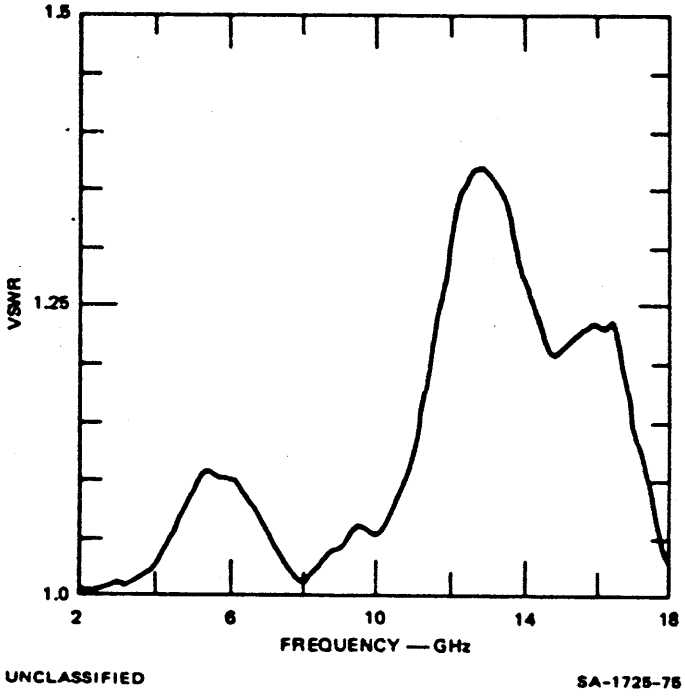

FIGURE VII-21 INPUT VSWR (Port 1) OF MICROSTRIP 50-ohm TRANSMISSION LINE ON 10-mil-THICK SAPPHIRE SUBSTRATE (U)

(U)

VII-22 and VII-23, respectively. The data for Port 1 input are tabulated in Table VII-3. The measurements here also are repeated for the second port with similar results.

3. Test Results for Microstrip Bias Tee with RF Grounded, dc Open (U)

(U) A 22-pF chip capacitor made by Alpha Industries was attached to the shorted pad and the gold wire was bonded on top of the capacitor. Transmission-loss and reflection tests were performed on the assembled unit using the same automatic network analyzer. The initial review of the data indicated that the 0.189-inch-long high-impedance line needed to be shorted. This was necessary because of an extra

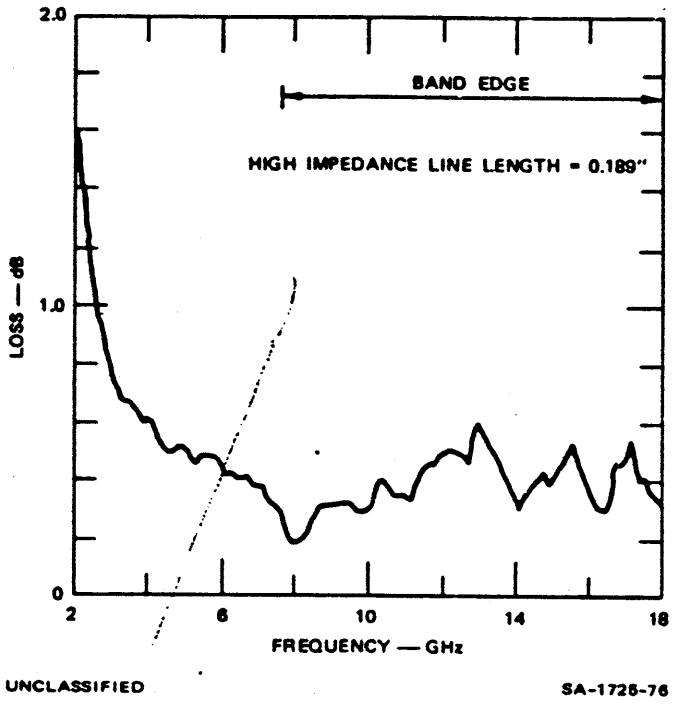

FIGURE VII-22 TRANSMISSION LOSS OF BIAS TEE (RF and dc grounded) INPUT AT PORT 1 (U)

(U)

inductance introduced by the chip capacitor. The best results were obtained for a line length 0.170 inch long. The transmission-loss results are plotted in Figure VII-24, and VSWR results are plotted in Figure VII-25, respectively. The data is tabulated in Table VII-4.

4. Conclusions (U)

(U) A broadband bias tee has been designed and fabricated for biasing the PIN diodes used in the DPDT switch. The transmission and VSWR characteristics are comparable to those of a single 50-ohm microstrip transmission line over the band of operation.

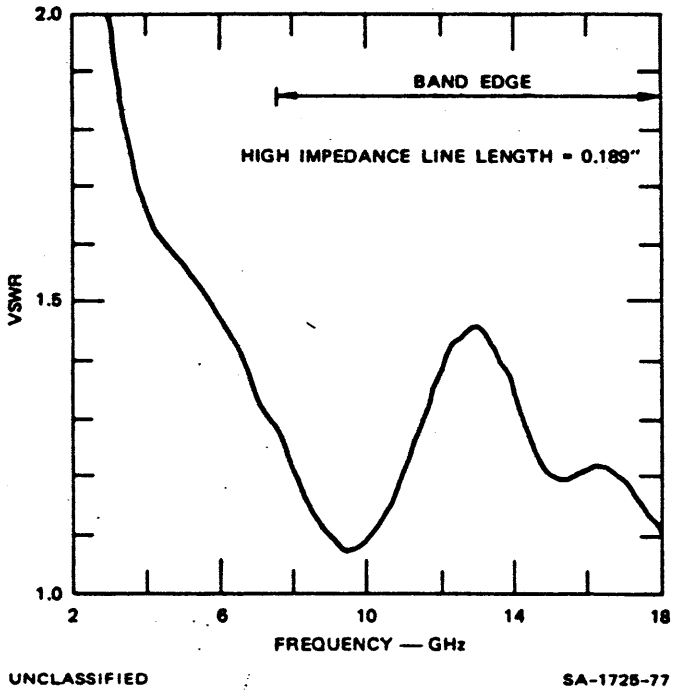

FIGURE VII-23 VSWR AT PORT 1 OF BIAS TEE (RF and dc grounded) (U)

F. Blocking Capacitors (U)

(U) A blocking capacitor is required in the design of a frequency translator to pass the RF signals but block all the dc bias currents to the PIN diodes. In order to achieve a low series impedance, a very high capacitance is required. The physical size of the capacitor is proportional to the value of the capacitance. Therefore, limitation of the size is dependent on the dimensions of the transmission line. Since 50-ohm lines on microstrip are 0.010-inch wide, beam-lead capacitors with 0.010-inch-wide tabs will cause the minimum impedance discontinuity.

(U) Another limitation in the selection of the capacitor is the lead inductance introduced. The rule of thumb is to select a capacitor that has an adequately low impedance for the application. It was decided

Table VII-3

(U) TRANSMISSION AND REFLECTION MEASUREMENTS ON BIAS TEE (RD AND dc GROUNDED) (U)

FREQ-MHZ	LOSS-DB MEAS 1	D-PHASE MEAS 1	REFL-MAG MEAS 1	VSWR MEAS 1	PHASE MEAS 1
2000.000	1.62	15.61	.495	2.96	-94.25
2200.000	1.36	12.94	.454	2.66	-109.47
2400.000	1.12	11.20	.419	2.44	-123.76
2600.000	.97	9.73	.387	2.26	-137.78
2800.000	.83	8.44	.359	2.12	-151.61
3000.000	.74	7.14	.333	2.00	-165.46
3200.000	.68	5.97	.311	1.90	-179.17
3400.000	.68	5.09	.293	1.83	167.41
3600.000	.64	3.89	.277	1.76	153.66
3800.000	.60	3.10	.263	1.71	140.33
4000.000	.61	2.36	.252	1.67	127.04
4200.000	.54	1.93	.242	1.64	114.07
4400.000	.50	1.40	.235	1.61	101.00
4600.000	.50	.93	.231	1.60	87.98
4800.000	.53	.12	.227	1.59	74.64
5000.000	.51	-.54	.223	1.57	61.43
5200.000	.46	-.96	.217	1.56	48.46
5400.000	.49	-1.05	.212	1.54	35.83
5600.000	.48	-1.01	.207	1.52	23.33
5800.000	.48	-1.09	.201	1.50	10.70
6000.000	.43	-.98	.195	1.48	-1.73
6200.000	.43	-1.40	.188	1.46	-14.70
6400.000	.40	-1.88	.181	1.44	-27.73
6600.000	.43	-2.58	.172	1.41	-40.97
6800.000	.38	-2.92	.160	1.38	-53.85
7000.000	.38	-2.83	.149	1.35	-66.30
7200.000	.33	-2.92	.140	1.32	-78.93
7400.000	.32	-2.42	.130	1.30	-90.97
7600.000	.27	-2.68	.121	1.28	-103.78
7800.000	.18	-2.67	.112	1.25	-116.31
8000.000	.19	-2.79	.098	1.22	-128.97
8200.000	.20	-2.88	.083	1.18	-141.60
8400.000	.26	-2.96	.071	1.15	-154.23
8600.000	.31	-2.99	.062	1.13	-166.80
8800.000	.32	-2.49	.054	1.11	-178.84
9000.000	.32	-2.75	.047	1.10	168.36
9200.000	.33	-2.96	.042	1.09	155.60
9400.000	.33	-3.40	.039	1.08	142.62
9600.000	.29	-3.71	.039	1.08	129.78
9800.000	.30	-3.78	.041	1.09	117.16
10000.00	.32	-3.75	.046	1.10	104.65
10200.00	.41	-3.87	.052	1.11	91.98
10400.00	.38	-4.05	.060	1.13	79.26
10600.00	.35	-4.20	.071	1.15	66.58
10800.00	.35	-4.06	.083	1.18	54.17
11000.00	.34	-4.13	.096	1.21	41.55

(U) Table VII-3 (continued) (U)

FREQ-MHZ	LOSS-DB MEAS 1	D-PHASE MEAS 1	REFL-MAG MEAS 1	VSWR MEAS 1	PHASE MEAS 1
11200.00	.37	-4.34	.109	1.25	28.79
11400.00	.44	-4.28	.122	1.28	16.31
11600.00	.46	-4.28	.137	1.32	3.76
11800.00	.48	-4.48	.150	1.35	-8.97
12000.00	.51	-5.03	.161	1.38	-22.07
12200.00	.50	-5.22	.171	1.41	-34.80
12400.00	.49	-4.96	.179	1.44	-47.08
12600.00	.46	-6.69	.181	1.44	-61.36
12800.00	.58	-6.71	.186	1.46	-73.92
13000.00	.58	-6.19	.187	1.46	-85.95
13200.00	.52	-5.53	.182	1.45	-97.82
13400.00	.47	-4.58	.175	1.42	-109.42
13600.00	.43	-3.84	.166	1.40	-121.22
13800.00	.38	-3.76	.160	1.38	-133.69
14000.00	.31	-3.79	.150	1.35	-146.26
14200.00	.36	-4.16	.135	1.31	-159.17
14400.00	.39	-4.64	.122	1.28	-172.20
14600.00	.44	-4.87	.108	1.24	175.03
14800.00	.39	-4.93	.099	1.22	162.43
15000.00	.43	-4.94	.093	1.20	149.88
15200.00	.47	-5.20	.088	1.19	137.08
15400.00	.53	-5.53	.088	1.19	124.20
15600.00	.45	-5.45	.092	1.20	111.74
15800.00	.40	-5.36	.094	1.21	99.28
16000.00	.32	-5.43	.097	1.21	86.67
16200.00	.30	-5.56	.099	1.22	74.00
16400.00	.32	-5.80	.099	1.22	61.23
16600.00	.46	-6.37	.095	1.21	48.11
16800.00	.47	-6.20	.092	1.20	35.74
17000.00	.54	-6.17	.088	1.19	23.23
17200.00	.41	-6.07	.079	1.17	10.80
17400.00	.41	-6.37	.073	1.16	-2.04
17600.00	.36	-6.10	.063	1.13	-14.31
17800.00	.33	-7.23	.058	1.12	-27.99
18000.00	.32	172.94	.050	1.11	139.63

REF PLANE EXT(CM): INPUT= .00 TRAN= .00
LINEARIZED FROM 2000.00 TO 18000.00
SLOPE(S) (EQUIV CM)= 5.23

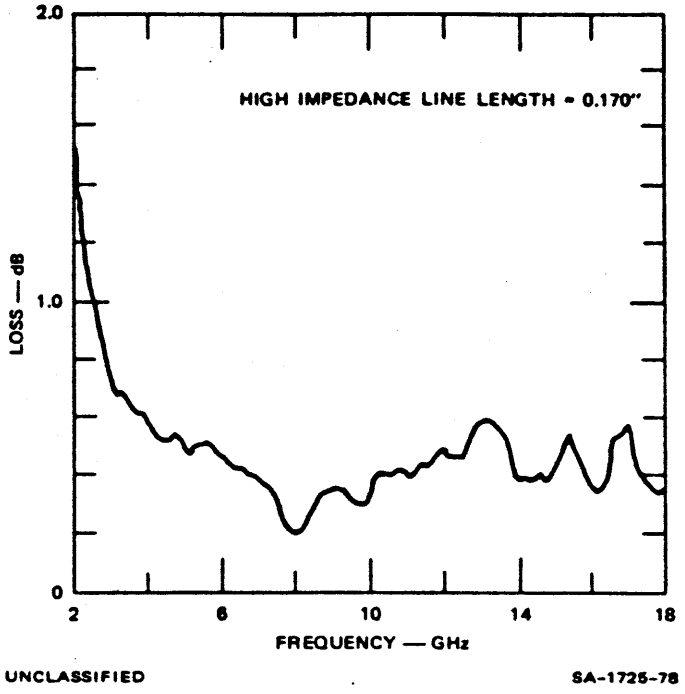

FIGURE VII-24 TRANSMISSION LOSS OF BIAS TEE (RF grounded and dc open) INPUT AT PORT 1 (U)

(U)

to investigate the relative merits of 4.5-pF beam-lead capacitors (SC-9001C) and 47-pF beam-lead capacitors, both manufactured by Alpha Industries. At 7.5 GHz, 4.7-pF capacitors will introduce an additional impedance of 5 ohms in series with the 50-ohm line impedance. This small change in impedance is acceptable and will not change the VSWR of the line too much.

(U) Our approach in fabricating and testing a blocking capacitor was to first fabricate a 50-ohm microstrip transmission line, obtain complete test results, and then open a gap in the line and bond a 4.7-pF beam-lead capacitor across it (see Figure VII-26). The tests on the 50-ohm microstrip transmission line used are shown in Figures VII-27 and VII-28. The data are tabulated in Table VII-5.

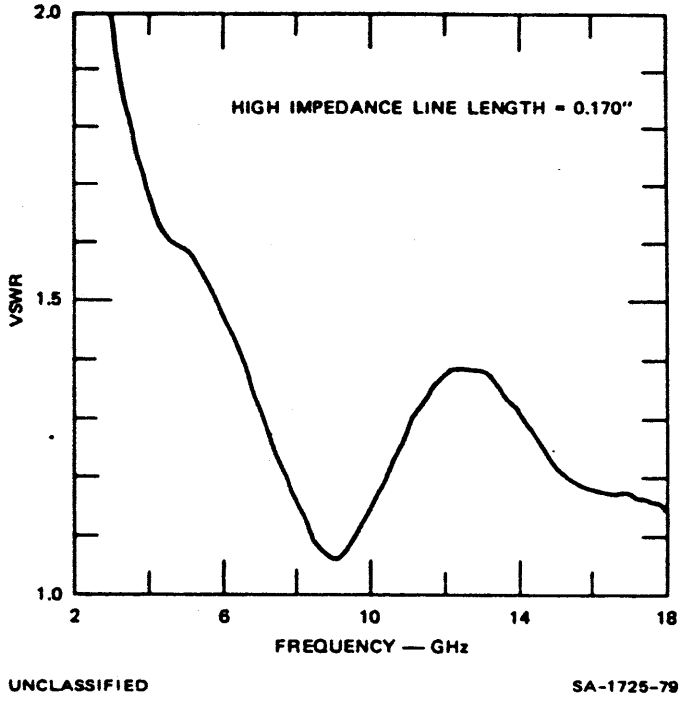

FIGURE VII-25 VSWR AT PORT 1 OF BIAS TEE (RF grounded and dc open) (U)

(U) The transmission and reflection tests on a series 4.7-pF beam-lead capacitor mounted in a 50-ohm microstrip transmission line are shown in Figures VII-29 and VII-30, respectively. The data are tabulated in Table VII-6. Similar tests on a series 4.7-pF beam-lead capacitor are shown in Figures VII-31 and VII-32, respectively. The data for the 47-pF series capacitor are tabulated in Table VII-7.

(U) Comparing the results of the series capacitor with those of a straight 50-ohm transmission line shows that the series capacitor does not introduce any major changes to transmission or reflection characteristics. Although minor changes in VSWR and transmission loss were expected, it appears that the series capacitor is useful over a much broader bandwidth than indicated theoretically from considering the capacitance

Table VII-4

(U) TRANSMISSION AND REFLECTION MEASUREMENTS ON BIAS TEE (RF GROUNDED AND dc OPEN) (U)

FREQ-MHZ	LOSS-DB MEAS 1	D-PHASE MEAS 1	REFL-MAG MEAS 1	VSWR MEAS 1	PHASE MEAS 1
2000.000	1.63	15.76	.495	2.96	-94.12
2200.000	1.37	13.03	.455	2.67	-109.40
2400.000	1.14	11.23	.418	2.44	-123.74
2600.000	1.00	9.77	.386	2.26	-137.74
2800.000	.86	8.56	.359	2.12	-151.49
3000.000	.76	7.20	.333	2.00	-165.39
3200.000	.68	6.07	.311	1.90	-179.06
3400.000	.69	5.11	.294	1.83	167.43
3600.000	.64	3.92	.279	1.77	153.70
3800.000	.60	3.14	.266	1.72	140.37
4000.000	.62	2.30	.256	1.69	126.99
4200.000	.55	1.90	.245	1.65	114.05
4400.000	.52	1.42	.238	1.63	101.03
4600.000	.51	.97	.233	1.61	38.04
4800.000	.54	.19	.230	1.60	74.71
5000.000	.51	-.49	.228	1.59	61.49
5200.000	.46	-.99	.224	1.58	48.45
5400.000	.50	-1.22	.218	1.56	35.68
5600.000	.51	-1.32	.211	1.54	23.04
5800.000	.51	-1.30	.204	1.51	10.52
6000.000	.46	-1.12	.196	1.49	-1.84
6200.000	.46	-1.50	.187	1.46	-14.78
6400.000	.42	-1.98	.178	1.43	-27.79
6600.000	.43	-2.56	.167	1.40	-40.91
6800.000	.39	-2.97	.153	1.36	-53.87
7000.000	.40	-2.95	.139	1.32	-66.39
7200.000	.36	-2.95	.125	1.29	-78.93
7400.000	.35	-2.45	.112	1.25	-90.98
7600.000	.31	-2.66	.102	1.23	-103.73
7800.000	.22	-2.49	.092	1.20	-116.11
8000.000	.20	-2.68	.078	1.17	-128.85
8200.000	.20	-2.78	.064	1.14	-141.48
8400.000	.25	-3.00	.051	1.11	-154.24
8600.000	.32	-3.17	.041	1.09	-166.95
8800.000	.34	-2.68	.036	1.07	-179.00
9000.000	.35	-2.86	.032	1.07	168.29
9200.000	.35	-3.06	.032	1.07	155.54
9400.000	.34	-3.35	.037	1.08	142.71
9600.000	.30	-3.53	.046	1.10	129.99
9800.000	.30	-3.58	.056	1.12	117.39
10000.00	.30	-3.66	.067	1.14	104.77
10200.00	.39	-3.92	.079	1.17	91.98
10400.00	.41	-4.26	.091	1.20	79.10
10600.00	.40	-4.36	.101	1.22	66.46
10800.00	.42	-4.05	.111	1.25	54.24
11000.00	.40	-4.03	.121	1.28	41.71

(U) Table VII-4 (continued) (U)

FREQ-MHZ	LOSS-DB MEAS 1	D-PHASE MEAS 1	REFL-MAG MEAS 1	VSWR MEAS 1	PHASE MEAS 1
11200.00	.39	-4.02	.131	1.30	29.19
11400.00	.44	-4.07	.140	1.33	16.59
11600.00	.42	-4.13	.146	1.34	3.98
11800.00	.46	-4.30	.155	1.37	-8.72
12000.00	.49	-4.88	.159	1.38	-21.85
12200.00	.47	-4.94	.162	1.39	-34.45
12400.00	.46	-4.77	.164	1.39	-46.83
12600.00	.46	-6.57	.162	1.39	-61.26
12800.00	.55	-6.89	.162	1.39	-74.02
13000.00	.60	-6.73	.161	1.38	-86.40
13200.00	.60	-6.16	.158	1.38	-98.38
13400.00	.57	-4.93	.152	1.36	-109.68
13600.00	.55	-4.03	.146	1.34	-121.32
13800.00	.48	-3.51	.141	1.33	-133.34
14000.00	.38	-3.34	.138	1.32	-145.71
14200.00	.39	-3.88	.130	1.30	-158.79
14400.00	.38	-4.39	.123	1.28	-171.85
14600.00	.42	-4.74	.115	1.26	175.27
14800.00	.37	-4.93	.108	1.24	162.55
15000.00	.42	-4.97	.102	1.23	149.97
15200.00	.47	-5.21	.096	1.21	137.18
15400.00	.55	-5.68	.090	1.20	124.16
15600.00	.47	-5.56	.088	1.19	111.74
15800.00	.40	-5.61	.085	1.19	99.15
16000.00	.36	-5.66	.083	1.18	86.57
16200.00	.33	-5.92	.083	1.18	73.77
16400.00	.37	-5.88	.082	1.18	61.27
16600.00	.53	-6.52	.080	1.17	48.08
16800.00	.54	-6.11	.082	1.18	35.94
17000.00	.58	-5.85	.082	1.18	23.67
17200.00	.43	-5.74	.077	1.17	11.24
17400.00	.39	-6.20	.076	1.17	-1.77
17600.00	.36	-6.15	.074	1.16	-14.25
17800.00	.34	-7.20	.073	1.16	-27.85
18000.00	.35	172.95	.067	1.14	139.75

REF PLANE EXT(CM): INPUT= .00 TRAN= .00
LINEARIZED FROM 2000.00 TO 18000.00
SLOPE(S) (EQUIV CM)= 5.23

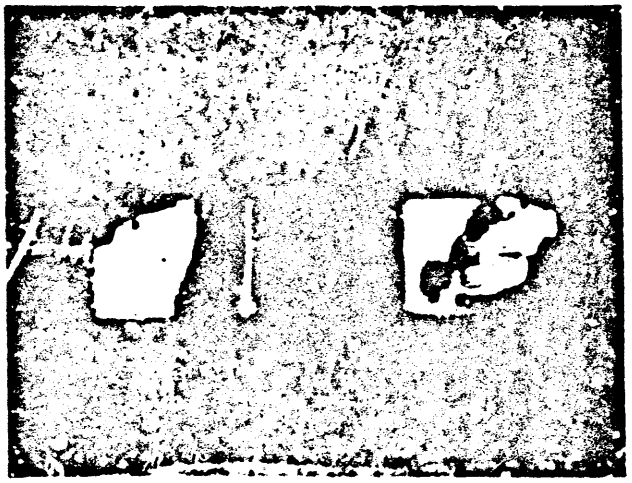

UNCLASSIFIED 8A-1725-80

FIGURE VII-26 ASSEMBLY OF 4.7-pF SERIES CAPACITOR (SC-8001C) ON MICROSTRIP TRANSMISSION LINE (U)

(U)

alone. Broadband operation occurs primarily because the inductance of the beam leads has a cancelling effect and resonates with the capacitive reactance of the capacitor. Based on the test results on the series capacitor, it can be concluded that the beam-lead capacitor is suitable for application in the frequency translator.

G. 50-ohm Termination. (U)

(U) Several different design approaches were considered for realizing a 50-ohm termination. The approaches were:

- Use external chip resistors on 25-mil-by-25-mil substrates
- Etch a resistor using the chrome layer under the gold metallization on 10-mil-thick sapphire substrate.
- Etch a resistor using the tantalum nitride layer on 10-mil-thick alumina substrate.

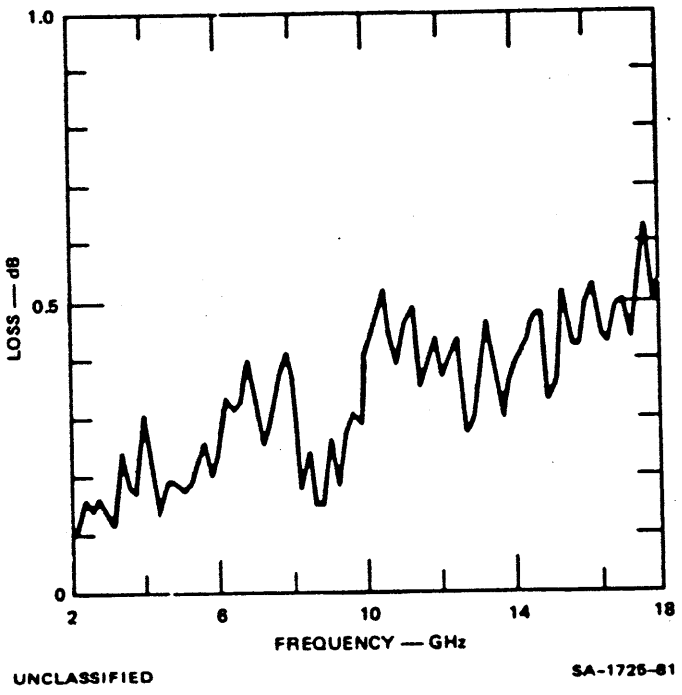

FIGURE VII-27 TRANSMISSION-LOSS MEASUREMENTS ON 50-ohm MICROSTRIP LINE ON 10-mil-THICK SAPPHIRE SUBSTRATE (U)

(U) Of the above three approaches, the chip resistor and tantalum nitride etched-resistor termination were selected for our application. The chrome etched resistor was not considered because the thickness of the thin layer of chrome on sapphire substrate is generally unpredictable and the resistivity value is very high. Also the chrome resistors have a tendency to change in value with age if they are not properly heat-treated.

(U) Considerable research in processing and testing was performed in making tantalum nitride resistors from gold on tantalum-nitride-plated, 10-mil-thick alumina substrates supplied by Electrotec, Garland, Texas. The VSWR of the resistor was high because of a shunt capacitance effect across the resistor. A plot of the TDR data on a typical shunt resistor

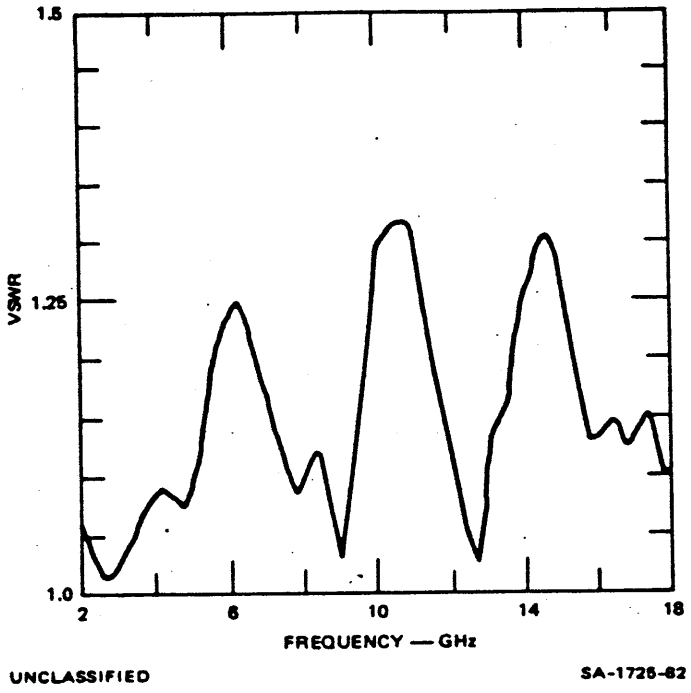

FIGURE VII-28 VSWR AT PORT 1 OF 50-ohm MICROSTRIP LINE ON 10-mil-THICK SAPPHIRE SUBSTRATE (U)

(U)

is shown in Figure VII-33. Attempts were made to isolate the shunt capacitance, without success. It appears that the shunt capacitance is due to the input connector assembly. Further experiments were cancelled primarily because of the difficulty in controlling the value of the resistors and the adherence of the gold to the alumina substrate. In order to stabilize the resistors, the etched substrates had to be heat-treated. During the heat-treating process, the chrome layer that is under the tantalum nitride layer diffused into the tantalum and gold layer, eliminating the bonding action. Many times during the testing, the gold layer would lift up, causing unpredictable data.

Table VII-5

(U) TRANSMISSION AND REFLECTION TESTS OF 50-OHM MICROSTRIP LINE ON 10-MIL-THICK SAPPHIRE SUBSTRATE (U)

FREQ-MHZ	LOSS-DB MEAS 1	PHASE MEAS 1	VSWR MEAS 1	FLATNESS MEAS 1
2000.000	.18	80.73	1.06	-.16
2200.000	.10	52.63	1.04	-.24
2400.000	.16	25.06	1.03	-.18
2600.000	.15	-2.83	1.01	-.19
2800.000	.16	-30.50	1.01	-.18
3000.000	.14	-59.04	1.02	-.20
3200.000	.12	-86.78	1.03	-.22
3400.000	.25	-113.95	1.05	-.09
3600.000	.19	-142.91	1.06	-.15
3800.000	.17	-170.05	1.07	-.17
4000.000	.31	162.38	1.08	-.03
4200.000	.21	133.31	1.09	-.13
4400.000	.14	106.14	1.08	-.20
4600.000	.20	78.04	1.08	-.14
4800.000	.19	49.80	1.07	-.15
5000.000	.18	22.48	1.09	-.16
5200.000	.19	-5.61	1.12	-.15
5400.000	.22	-33.47	1.16	-.12
5600.000	.26	-61.75	1.20	-.08
5800.000	.21	-89.47	1.22	-.13
6000.000	.25	-117.00	1.24	-.09
6200.000	.34	-144.98	1.25	.00
6400.000	.32	-173.37	1.24	-.02
6600.000	.34	159.57	1.22	-.00
6800.000	.40	131.92	1.20	.06
7000.000	.32	103.15	1.17	-.02
7200.000	.26	76.65	1.14	-.08
7400.000	.29	47.68	1.12	-.05
7600.000	.37	19.53	1.10	.03
7800.000	.42	-8.02	1.08	.08
8000.000	.36	-35.59	1.09	.02
8200.000	.19	-63.15	1.12	-.15
8400.000	.25	-92.28	1.12	-.09
8600.000	.15	-120.27	1.10	-.19
8800.000	.15	-147.34	1.06	-.19
9000.000	.27	-176.38	1.03	-.07
9200.000	.19	154.71	1.07	-.15
9400.000	.28	128.21	1.13	-.06
9600.000	.32	99.81	1.19	-.02
9800.000	.29	70.63	1.25	-.05
10000.00	.42	43.79	1.30	.08
10200.00	.46	16.62	1.31	.12
10400.00	.52	-11.32	1.32	.18
10600.00	.43	-39.29	1.32	.09
10800.00	.39	-67.44	1.32	.05
11000.00	.47	-94.73	1.29	.13

(U) Table VII-5 (continued) (U)

FREQ-MHZ	LOSS-DB MEAS 1	PHASE MEAS 1	VSWR MEAS 1	FLATNESS MEAS 1
11200.00	.50	-123.96	1.24	.16
11400.00	.36	-151.00	1.19	.02
11600.00	.40	-178.37	1.17	.06
11800.00	.44	152.49	1.14	.10
12000.00	.37	124.16	1.10	.04
12200.00	.41	97.10	1.07	.07
12400.00	.45	68.67	1.04	.11
12600.00	.28	39.76	1.02	-.06
12800.00	.29	12.40	1.07	-.04
13000.00	.40	-15.90	1.13	.06
13200.00	.47	-43.49	1.15	.13
13400.00	.40	-71.50	1.16	.06
13600.00	.30	-99.86	1.21	-.04
13800.00	.38	-127.52	1.25	.04
14000.00	.42	-157.18	1.27	.08
14200.00	.44	175.66	1.30	.10
14400.00	.48	148.77	1.31	.14
14600.00	.49	120.55	1.30	.15
14800.00	.33	92.02	1.28	-.01
15000.00	.37	64.32	1.24	.03
15200.00	.53	36.21	1.20	.19
15400.00	.44	7.77	1.16	.10
15600.00	.43	-19.87	1.13	.09
15800.00	.50	-48.01	1.13	.16
16000.00	.54	-76.01	1.14	.20
16200.00	.46	-104.54	1.15	.12
16400.00	.43	-132.72	1.14	.09
16600.00	.49	-160.40	1.12	.15
16800.00	.51	170.02	1.13	.17
17000.00	.45	142.88	1.14	.11
17200.00	.53	115.36	1.15	.19
17400.00	.64	86.22	1.13	.30
17600.00	.51	57.77	1.10	.17
17800.00	.56	29.94	1.10	.22

REF PLANE EXT(CM): INPUT= .00 TRAN= .00
LINEARIZED FROM 2000.00 TO 17800.00
LINEARIZED FROM 2000.00 TO 17800.00

GPM1 TASK=7A

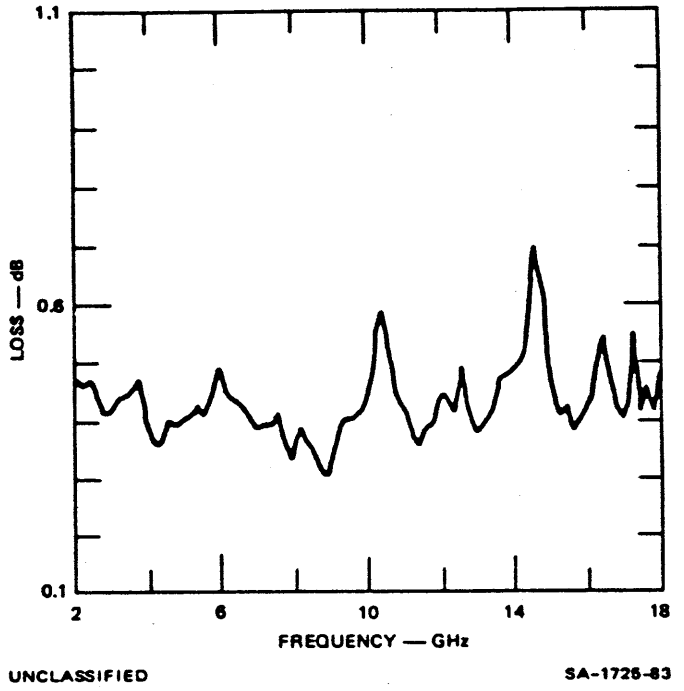

FIGURE VII-29 TRANSMISSION-LOSS MEASUREMENTS OF SERIES 4.7-pF BEAM LEAD CAPACITOR MOUNTED IN 50-ohm MICROSTRIP LINE (U)

(U) The best results on the 50-ohm termination were obtained by using a 25-mil-by-25-mil thin-film chrome resistor supplied by FMI, Burlington, Massachusetts. A test jig was fabricated that consisted of a 50-ohm microstrip transmission line that was shunted by a 50-ohm chip resistor at one end. The short circuit for the resistor was made by either silver epoxy or gold paste. The data for such a 50-ohm termination are shown in Figure VII-34 and tabulated in Table VII-8.

H. Driver-Circuit Topology for the Translater (U)

(U) There are four DPDT switches used in a translator. Each DPDT type is discussed in Section VI. Each has a pair of diodes that are ON while the other pair are OFF. (This is assuming that one diode is used

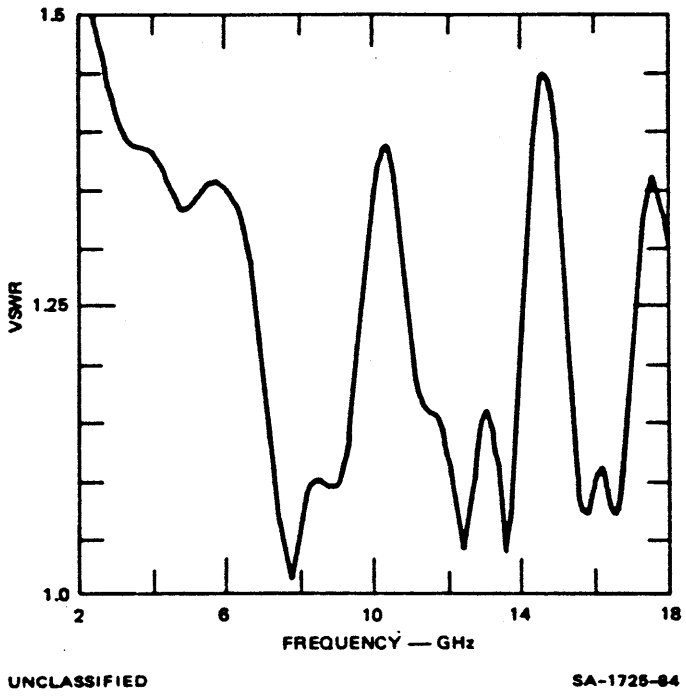

FIGURE VII-30 VSWR AT PORT 1 OF SERIES 4.7-pF BEAM-LEAD CAPACITOR MOUNTED IN 50-ohm MICROSTRIP LINE (U)

(U)

in each arm.) The drivers required for the DPDT are the same as those required for the SPDT in Section VI. A topology layout of the driver circuits that will satisfy the needs for the complete translator is shown in Figure VII-35.

I. The Hybrid Switch--An Alternative Transfer-Switch Technique (U)

(U) In the frequency translator, the transfer switch is the critical performance-determining element. A new approach for realizing this component that has several advantages over the conventional DPDT switch combines two 3-dB hybrids and two PIN diodes as shown in Figure VII-36. The physical structure is identical to the amplitude modulator. However,

Table VII-6

(U) TRANSMISSION AND REFLECTION TESTS ON SERIES 4.7-pF BEAM-LEAD CAPACITOR MOUNTED IN 50-OHM MICROSTRIP LINE (U)

FREQ-MHZ	LOSS-DB MEAS 1	FLATNESS MEAS 1	VSWR MEAS 1	REFL-MAG MEAS 1	D-PHASE MEAS 1
2000.000	.47	.04	1.65	.246	13.48
2200.000	.46	.03	1.58	.226	12.05
2400.000	.46	.04	1.53	.208	11.10
2600.000	.45	.03	1.48	.193	10.36
2800.000	.41	-.02	1.45	.182	9.09
3000.000	.41	-.02	1.42	.172	7.85
3200.000	.43	-.00	1.39	.164	6.54
3400.000	.44	.01	1.38	.161	5.88
3600.000	.44	.02	1.38	.161	5.31
3800.000	.46	.04	1.38	.161	4.56
4000.000	.40	-.03	1.38	.160	4.04
4200.000	.35	-.08	1.37	.157	4.14
4400.000	.35	-.08	1.36	.152	3.70
4600.000	.39	-.04	1.34	.146	3.40
4800.000	.39	-.04	1.33	.141	3.30
5000.000	.39	-.04	1.33	.143	2.63
5200.000	.41	-.02	1.34	.146	2.19
5400.000	.42	-.01	1.35	.149	1.59
5600.000	.40	-.03	1.36	.151	1.09
5800.000	.44	.01	1.35	.150	.66
6000.000	.48	.06	1.35	.148	.37
6200.000	.44	.01	1.34	.145	-.19
6400.000	.43	.01	1.32	.140	.02
6600.000	.42	-.01	1.30	.130	.08
6800.000	.40	-.02	1.26	.115	.03
7000.000	.38	-.05	1.21	.094	.01
7200.000	.39	-.04	1.14	.067	-.47
7400.000	.39	-.04	1.09	.041	-.98
7600.000	.41	-.02	1.03	.016	-1.19
7800.000	.36	-.06	1.02	.008	-1.41
8000.000	.33	-.10	1.06	.027	-1.87
8200.000	.38	-.04	1.09	.041	-2.39
8400.000	.36	-.07	1.10	.048	-3.14
8600.000	.34	-.09	1.10	.047	-2.79
8800.000	.31	-.12	1.09	.044	-2.96
9000.000	.30	-.13	1.09	.044	-3.28
9200.000	.36	-.07	1.11	.050	-3.48
9400.000	.40	-.03	1.14	.067	-3.77
9600.000	.40	-.03	1.20	.092	-4.16
9800.000	.41	-.02	1.27	.120	-4.65
10000.00	.42	-.00	1.33	.142	-5.23
10200.00	.49	.06	1.37	.155	-5.66
10400.00	.58	.15	1.39	.162	-5.43
10600.00	.52	.09	1.36	.152	-5.86
10800.00	.44	.01	1.30	.131	-5.57
11000.00	.42	-.01	1.23	.105	-5.50

(U) Table VII-6 (continued) (U)

FREQ-MHZ	LOSS-DB MEAS 1	FLATNESS MEAS 1	VSWR MEAS 1	REFL-MAG MEAS 1	D-PHASE MEAS 1
11200.00	.38	-.05	1.18	.083	-5.52
11400.00	.35	-.08	1.16	.074	-5.64
11600.00	.38	-.04	1.16	.073	-6.34
11800.00	.39	-.04	1.15	.069	-6.85
12000.00	.45	.02	1.12	.058	-7.53
12200.00	.44	.01	1.08	.039	-7.83
12400.00	.41	-.02	1.04	.020	-8.12
12600.00	.49	.06	1.06	.031	-9.40
12800.00	.41	-.02	1.13	.060	-9.79
13000.00	.37	-.06	1.16	.074	-9.71
13200.00	.39	-.03	1.15	.068	-9.74
13400.00	.43	.00	1.10	.050	-9.50
13600.00	.47	.04	1.03	.016	-9.54
13800.00	.47	.04	1.07	.035	-9.60
14000.00	.48	.05	1.20	.093	-10.02
14200.00	.50	.07	1.32	.139	-10.66
14400.00	.56	.13	1.41	.169	-11.02
14600.00	.69	.26	1.45	.183	-11.00
14800.00	.58	.16	1.44	.179	-10.95
15000.00	.44	.01	1.38	.161	-11.36
15200.00	.41	-.02	1.27	.121	-11.52
15400.00	.42	-.01	1.16	.073	-12.11
15600.00	.38	-.05	1.08	.036	-12.22
15800.00	.41	-.02	1.07	.032	-13.29
16000.00	.42	-.00	1.10	.048	-13.77
16200.00	.49	.06	1.11	.052	-14.87
16400.00	.53	.11	1.08	.038	-14.66
16600.00	.46	.04	1.06	.031	-14.98
16800.00	.41	-.02	1.13	.061	-15.83
17000.00	.40	-.03	1.21	.096	-16.40
17200.00	.54	.11	1.29	.128	-15.80
17400.00	.41	-.02	1.34	.147	-15.57
17600.00	.46	.03	1.36	.152	-16.22
17800.00	.40	-.03	1.34	.144	162.56
18000.00	.51	.08	1.29	.127	161.36

REF PLANE EXT(CM): INPUT= .00 TRAN= 5.15
LINEARIZED FROM 2000.00 TO 18000.00
SLOPE(S) (EQUIV CM)= 6.39

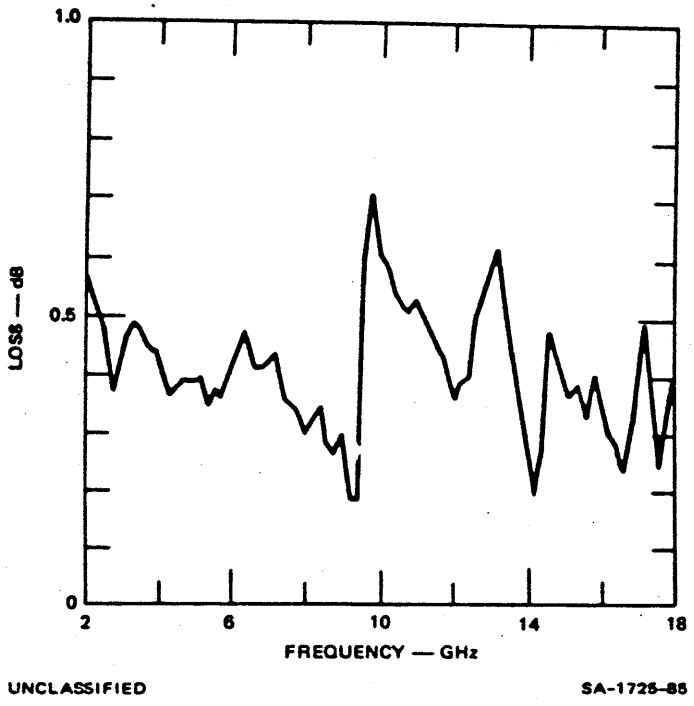

FIGURE VII-31 TRANSMISSION-LOSS MEASUREMENTS OF SERIES 4.7-pF BEAM-LEAD CAPACITOR MOUNTED IN 50-ohm MICROSTRIP LINE (U)

(U)

the diodes are fully switched on or off and intermediate levels of attenuation are not required.

(U) Figure VII-36 depicts the ideal situation when the diodes are conducting. Terminals 1 and 2 are connected and Terminals 3 and 4 are connected. A signal entering Terminal 1 is split into equal powers by the hybrid, and each is reflected by the short circuit due to the conducting diodes. Each reflected signal is reversed in phase so that when recombined by the hybrid the sum leaves by way of the other terminal. A signal entering any port undergoes a similar split and recombination.

(U) In the situation when the diodes are back-biased, the two hybrids are connected in tandem to form a 0-dB coupler--i.e., signal

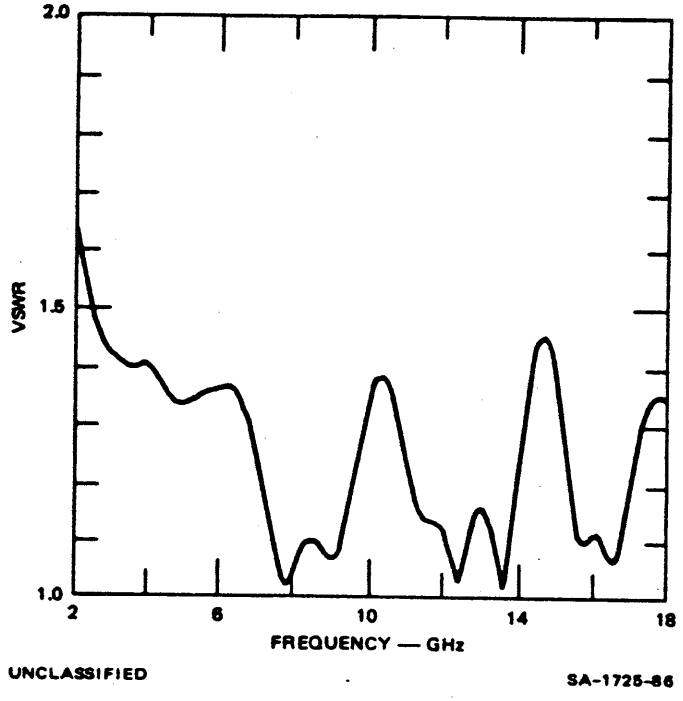

FIGURE VII-32 VSWR AT PORT 1 OF SERIES 4.7-pF BEAM-LEAD CAPACITOR MOUNTED IN 50-ohm MICROSTRIP LINE (U)

(U)

paths are between Terminals 1 and 4 and between Terminals 2 and 3.

(U) The advantages of the hybrid switch technique over the conventional DPDT approach are:

- External crossovers in the frequency translator are not required. The crossover is built into the hybrid switch.
- Only two diodes per switch are required.
- The driver circuits are identical to those for the modulator. (No shaping circuits are required.)
- Low VSWR is inherent in the design.
- Filter design techniques are not required.

Table VII-7

(U) TRANSMISSION AND REFLECTION TESTS ON SERIES 4.7-pF BEAM-LEAD CAPACITOR MOUNTED IN 50-OHM MICROSTRIP LINE (U)

FREQ-MHZ	LOSS-DB MEAS 1	REFL-MAG MEAS 1	VSWR MEAS 1	PHASE MEAS 1
2000.000	.55	.245	1.65	37.08
2200.000	.54	.224	1.58	37.39
2400.000	.49	.206	1.52	38.53
2600.000	.47	.191	1.47	39.84
2800.000	.36	.181	1.44	41.26
3000.000	.40	.173	1.42	43.02
3200.000	.46	.169	1.41	44.67
3400.000	.48	.165	1.39	46.28
3600.000	.46	.168	1.40	47.45
3800.000	.44	.169	1.41	48.95
4000.000	.43	.168	1.40	50.88
4200.000	.39	.162	1.39	52.34
4400.000	.36	.156	1.37	54.13
4600.000	.38	.149	1.35	56.22
4800.000	.38	.144	1.34	58.68
5000.000	.38	.143	1.33	60.28
5200.000	.39	.146	1.34	61.98
5400.000	.34	.148	1.35	63.92
5600.000	.37	.153	1.36	66.05
5800.000	.35	.153	1.36	67.74
6000.000	.41	.152	1.36	70.18
6200.000	.42	.154	1.36	72.56
6400.000	.47	.150	1.35	74.89
6600.000	.41	.140	1.33	76.85
6800.000	.40	.126	1.29	78.79
7000.000	.42	.104	1.23	80.75
7200.000	.43	.077	1.17	82.63
7400.000	.36	.048	1.10	84.26
7600.000	.34	.021	1.04	86.61
7800.000	.33	.008	1.02	89.14
8000.000	.30	.028	1.06	90.45
8200.000	.31	.042	1.09	92.45
8400.000	.34	.047	1.10	94.05
8600.000	.28	.044	1.09	95.39
8800.000	.26	.038	1.08	97.19
9000.000	.30	.030	1.06	99.63
9200.000	.18	.038	1.08	101.92
9400.000	.18	.064	1.14	102.49
9600.000	.64	.095	1.21	103.88
9800.000	.71	.121	1.27	107.92
10000.00	.61	.145	1.34	110.49
10200.00	.59	.160	1.38	112.65
10400.00	.53	.160	1.38	114.69
10600.00	.52	.148	1.35	117.59
10800.00	.50	.127	1.29	120.54
11000.00	.53	.101	1.22	122.65

(U) Table VII-7 (continued) (U)

FREQ-MHZ	LOSS-DB MEAS 1	REFL-MAG MEAS 1	VSWR MEAS 1	PHASE MEAS 1
11200.00	.50	.077	1.17	124.21
11400.00	.47	.064	1.14	125.60
11600.00	.44	.062	1.13	127.57
11800.00	.42	.061	1.13	128.96
12000.00	.36	.055	1.12	131.01
12200.00	.38	.036	1.07	133.13
12400.00	.40	.014	1.03	135.21
12600.00	.50	.041	1.09	136.17
12800.00	.54	.065	1.14	138.28
13000.00	.58	.073	1.16	140.48
13200.00	.60	.063	1.14	143.66
13400.00	.50	.041	1.09	146.26
13600.00	.43	.008	1.02	148.70
13800.00	.33	.050	1.10	150.82
14000.00	.25	.103	1.23	152.55
14200.00	.18	.148	1.35	153.20
14400.00	.29	.176	1.43	154.86
14600.00	.48	.187	1.46	157.40
14800.00	.43	.181	1.44	159.13
15000.00	.38	.159	1.38	161.40
15200.00	.36	.121	1.27	163.17
15400.00	.39	.079	1.17	164.79
15600.00	.33	.048	1.10	165.95
15800.00	.40	.046	1.10	167.13
16000.00	.35	.053	1.11	170.06
16200.00	.30	.050	1.11	171.88
16400.00	.28	.034	1.07	174.52
16600.00	.23	.032	1.07	176.90
16800.00	.30	.056	1.12	178.45
17000.00	.43	.088	1.19	179.99
17200.00	.48	.121	1.28	-177.40
17400.00	.33	.139	1.32	-175.08
17600.00	.24	.150	1.35	6.17
17800.00	.35	.150	1.35	7.70
18000.00	.40	.146	1.34	9.98

REF PLANE EXT(CM): INPUT= .00 TRAN= 12.50

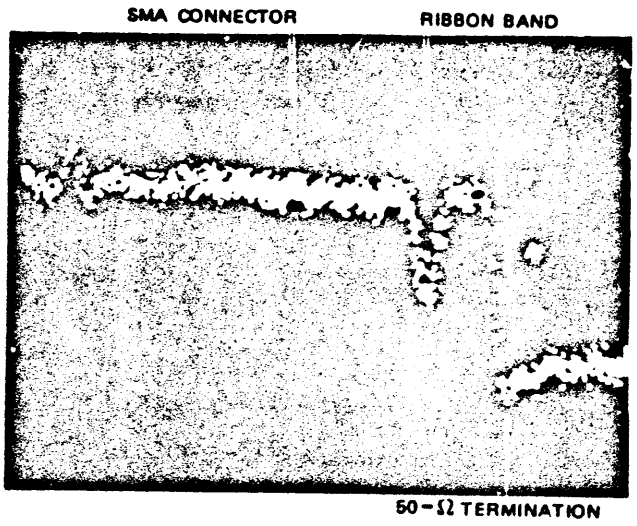

FIGURE VII-33 50-ohm TANTALUM NITRIDE TERMINATION ETCHED ON 10-mil-THICK ALUMINA SUBSTRATE (U)

(U) The disadvantages of the hybrid switch techniques over the conventional DPDT approach are:

- The diodes must be electrically balanced.
- The diodes must be positioned accurately in the circuit.
- The hybrid switch structure requires more substrate area than the DPDT structure, as discussed in Section VI.
- Very low diode ON resistance is required for low crosstalk.

(U) Overall performance of the hybrid switch, including isolation and VSWR, will depend on the imbalance of the hybrids. The isolation should be about 20-dB for one diode per leg. This is comparable to the isolation obtained with one diode per arm in the DPDT switch. The bandwidth is determined by the bandwidth of the hybrids. The signal-path lengths are about the same or slightly longer, depending on the final layout in the hybrid switch, than the path lengths through the DPDT switch. However, internal VSWRs in the DPDT switch are expected to be

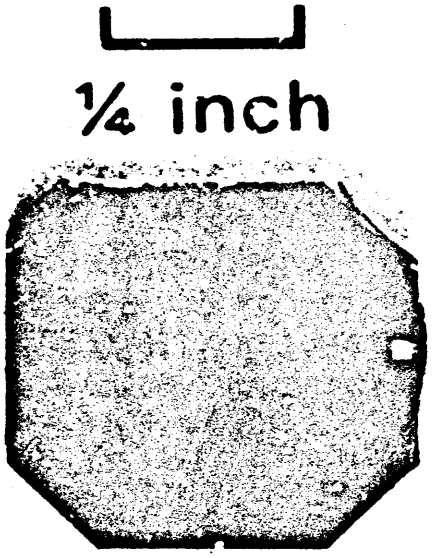

UNCLASSIFIED SA-1726-63

FIGURE VII-34 50-ohm MICROWAVE TERMINATION (25 mils x 25 mils) (U)

(U)

large because of the bandpass-filter nature of the design. Therefore, the conductor losses for the hybrid switch are expected to be less and at the most no more than for the DPDT switch.

(U) Further theoretical research and experimental evidence are required to confirm all the assumed advantages of using such a switch. No further work was performed in this program because the research was beyond the scope of the work statement and time limitations.

Table VII-8

(U) TEST RESULTS ON 50-OHM MICROWAVE CHIP TERMINATION
(25 MILS X 25 MILS) (U)

FREQ-MHZ	VSWR MEAS 1	RTN LOSS MEAS 1	R-OHMS MEAS 1	X-OHMS MEAS 1	Z-OHMS MEAS 1
300.000	1.02	41.26	50.63	.59	50.64
500.000	1.03	38.14	51.15	.49	51.15
700.000	1.03	36.75	51.46	-.10	51.46
900.000	1.03	36.66	51.27	-.78	51.28
1100.000	1.03	37.23	50.54	-1.29	50.55
1300.000	1.03	37.94	49.61	-1.21	49.62
1500.000	1.03	37.45	48.84	-.62	48.84
1700.000	1.03	35.99	48.46	.32	48.46
1900.000	1.04	34.54	48.63	1.25	48.65
2100.000	1.05	32.92	49.23	2.11	49.28
2300.000	1.05	32.69	49.99	2.31	50.04
2500.000	1.05	32.91	50.49	2.22	50.54
2700.000	1.05	33.13	50.59	2.15	50.63
2900.000	1.05	32.13	50.44	2.44	50.50
3100.000	1.07	29.72	50.61	3.22	50.71
3300.000	1.09	27.16	51.44	4.22	51.61
3500.000	1.12	25.11	53.15	4.79	53.36
3700.000	1.14	23.62	55.40	4.39	55.57
3900.000	1.16	22.71	57.47	2.49	57.52
4100.000	1.16	22.52	58.08	-.63	58.08
4300.000	1.16	22.65	56.86	-3.88	56.99
4500.000	1.15	23.35	54.00	-5.83	54.32
4700.000	1.13	24.55	50.56	-5.96	50.91
4900.000	1.11	25.95	47.71	-4.36	47.90
5100.000	1.09	27.11	46.12	-1.72	46.15
5300.000	1.09	27.36	46.06	1.17	46.07
5500.000	1.10	26.62	47.34	3.70	47.48
5700.000	1.11	25.73	49.57	5.15	49.84
5900.000	1.12	25.24	52.05	5.20	52.31
6100.000	1.11	25.32	53.91	4.08	54.06
6300.000	1.11	25.94	54.64	2.51	54.70
6500.000	1.10	26.86	54.52	1.46	54.54
6700.000	1.09	27.34	54.32	1.22	54.34
6900.000	1.10	26.45	54.79	1.39	54.80
7100.000	1.13	24.58	56.15	1.12	56.16
7300.000	1.16	22.57	58.01	-.46	58.01
7500.000	1.20	20.91	59.08	-3.78	59.20
7700.000	1.23	19.75	57.76	-7.98	58.31
7900.000	1.25	18.97	53.88	-11.11	55.01
8100.000	1.26	18.79	48.78	-11.35	50.08
8300.000	1.26	18.71	44.31	-9.42	45.30
8500.000	1.25	18.95	41.39	-5.69	41.78
8700.000	1.24	19.36	40.36	-1.18	40.37
8900.000	1.22	20.02	41.47	3.25	41.59
9100.000	1.20	20.87	44.62	6.68	45.11

(U) Table VII-8 (continued) (U)

FREQ-MHZ	VSWR MEAS 1	RTN LOSS MEAS 1	R-OHMS MEAS 1	X-OHMS MEAS 1	Z-OHMS MEAS 1
9300.000	1.18	21.88	49.26	7.98	49.90
9500.000	1.15	22.90	53.96	6.35	54.33
9700.000	1.14	23.78	56.57	2.08	56.61
9900.000	1.13	24.41	55.83	-2.59	55.89
10100.00	1.12	24.69	52.69	-5.35	52.96
10300.00	1.12	24.99	49.32	-5.55	49.63
10500.00	1.11	25.73	47.07	-4.05	47.24
10700.00	1.09	27.13	46.39	-2.22	46.44
10900.00	1.07	29.48	46.96	-1.14	46.97
11100.00	1.05	31.80	47.91	-1.40	47.93
11300.00	1.08	28.82	47.81	-2.81	47.90
11500.00	1.13	24.51	45.98	-4.09	46.17
11700.00	1.19	21.21	42.92	-3.92	43.10
11900.00	1.25	18.95	39.99	-1.75	40.03
12100.00	1.31	17.49	38.38	1.95	38.43
12300.00	1.35	16.62	38.68	6.62	39.25
12500.00	1.35	16.56	41.77	11.01	43.20
12700.00	1.33	16.87	47.08	13.76	49.05
12900.00	1.29	17.95	54.27	12.60	55.72
13100.00	1.23	19.61	59.69	6.18	60.01
13300.00	1.18	21.45	58.81	-2.61	58.87
13500.00	1.18	21.76	52.27	-8.06	52.89
13700.00	1.23	19.64	44.53	-8.23	45.28
13900.00	1.32	17.29	38.78	-4.68	39.06
14100.00	1.40	15.61	35.79	.72	35.80
14300.00	1.46	14.62	35.57	6.84	36.22
14500.00	1.48	14.20	37.89	12.39	39.86
14700.00	1.46	14.60	42.60	15.86	45.46
14900.00	1.38	15.99	48.60	15.77	51.09
15100.00	1.27	18.50	53.00	11.96	54.34
15300.00	1.16	22.41	53.15	7.18	53.63
15500.00	1.11	25.89	49.65	5.05	49.90
15700.00	1.17	22.09	45.72	6.21	46.14
15900.00	1.27	18.55	43.97	9.40	44.96
16100.00	1.34	16.72	45.64	13.40	47.57
16300.00	1.39	15.70	50.61	16.70	53.29
16500.00	1.40	15.51	57.47	16.63	59.83
16700.00	1.33	16.88	62.23	10.55	63.12
16900.00	1.20	20.65	60.08	1.68	60.11
17100.00	1.09	26.99	52.91	-3.56	53.03
17300.00	1.11	25.34	45.50	-2.54	45.57
17500.00	1.25	18.96	40.31	3.16	40.43
17700.00	1.47	14.41	37.67	11.44	39.37
17900.00	1.69	11.82	38.28	20.04	43.21

REF PLANE EXT(CM): INPUT= .00 TRAN= .00

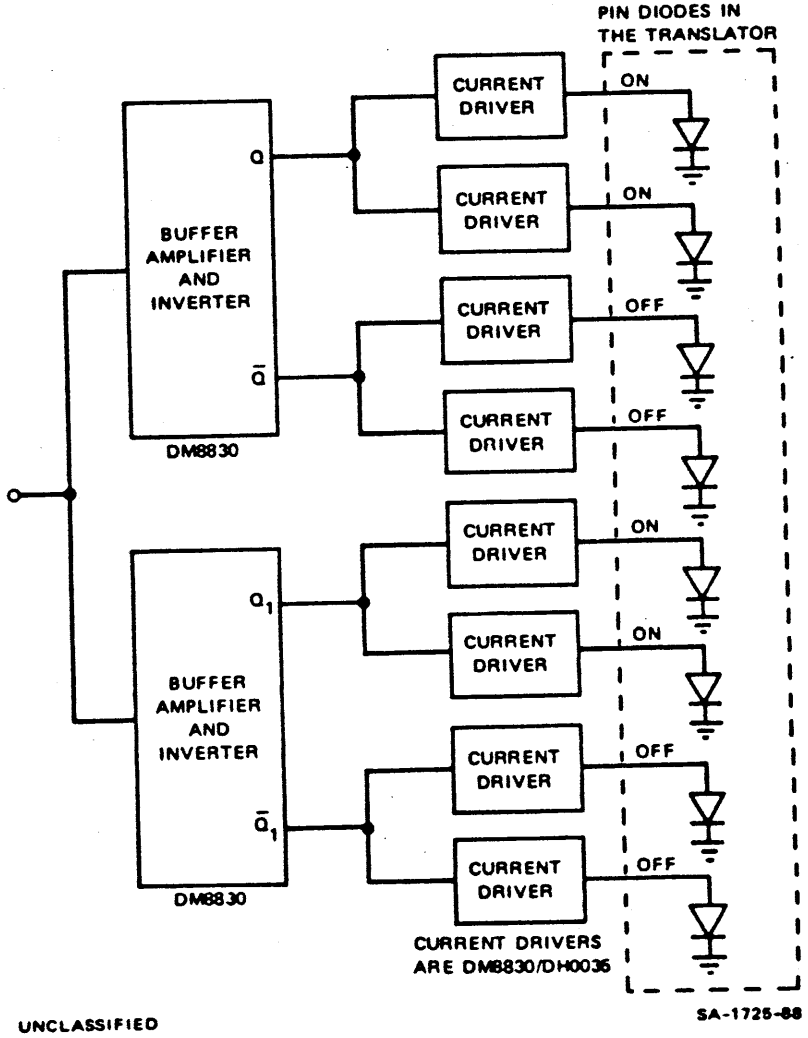

FIGURE VII-35 DRIVER-CIRCUIT TOPOLOGY FOR THE TRANSLATOR (U)

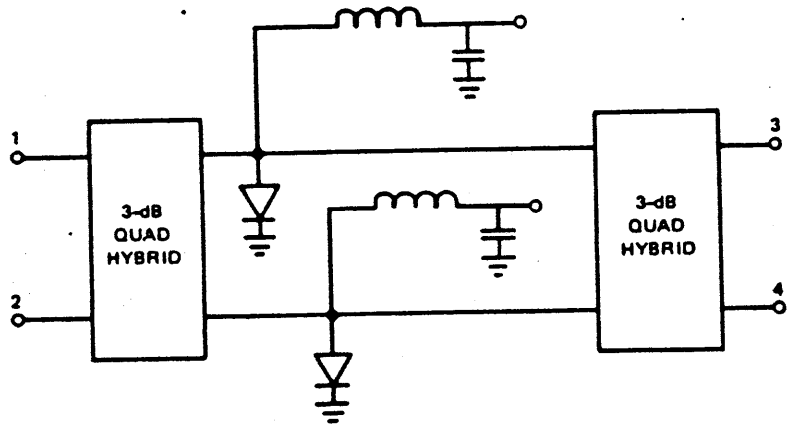

FIGURE VII-36 THE HYBRID SWITCH (U)

IX LIMITER-DETECTOR (U)

A. Basic Design (U)

(U) The basic schematic of the limiter-detector is depicted in Figure IX-1. Chip diodes for the limiter are arranged in such a manner that the connecting wires form series inductances while the diodes appear as shunt capacitances. The resulting circuit is a low-pass filter with very broadband characteristics. The Schottky-barrier diode is mounted on a feedthrough capacitor and is dc-isolated from the limiter by means of a series capacitor. In addition, the diode is loaded with a series RL circuit that provides a dc return and facilitates matching the diode at the RF frequency.

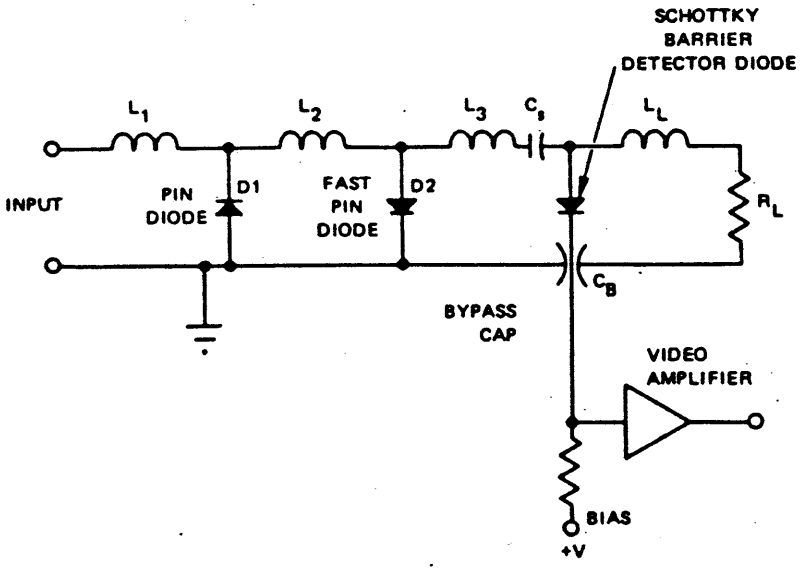

FIGURE IX-1 SCHEMATIC OF HIGH-POWER LIMITER-DETECTOR VIDEO-AMPLIFIER CONFIGURATION (U)

(U) The limiter is of the self-bias type. The first diode is a pin diode (HP 5082-0012) with good power capabilities. The second diode is a fast-switching pin diode (HP 5082-0001) to limit the spike leakage. The two diodes are mounted in opposite directions, to provide a dc return path for each other. The diodes for the limiter are chips in order to reduce the series inductance to an absolute minimum for fast-switching operation.

B. Small-Signal Sensitivity (U)

(U) The most important characteristic of the detector itself is its small-signal sensitivity. This is given by

$$TS(dBm) = TS_o + TS_f + 5 \log B \qquad \text{(IX-1)}$$

where

$$TS_o = 10 \log \left[\frac{5\sqrt{4KT}}{4 \cdot 10^3} \cdot \frac{\sqrt{R_s + R_j}}{R_j} \sqrt{\frac{R_j + R_A}{R_u}} \right]$$

$$TS_f = 10 \log \left[\frac{P_{in}}{P_d} \right]$$

$$u = \frac{e}{nKT}$$

n = Ideality factor of the Schottky-barrier diode = 1.05

k = Boltzman's constant

e = Charge of an electron

T = Absolute temperature of the junction

R_s = Series resistance of the diode

$R_u = \frac{u}{I}$ = Junction resistance of the diode

(U)

I = Diode current

R_A = Equivalent video-amplifier noise resistance

B = Video bandwidth

P_{in} = Power delivered to the detector

P_j = Power dissipated in the junction resistance.

The behavior of TS_o as a function of R_A and I is depicted in Figure IX-2. Most important is that TS_o increases with bias current by 10 dB per decade when $R_A \geq 100$ ohms and the bias current is reasonably large. The increase of TS_o with larger currents is due to increasing 1/f noise in the diode.

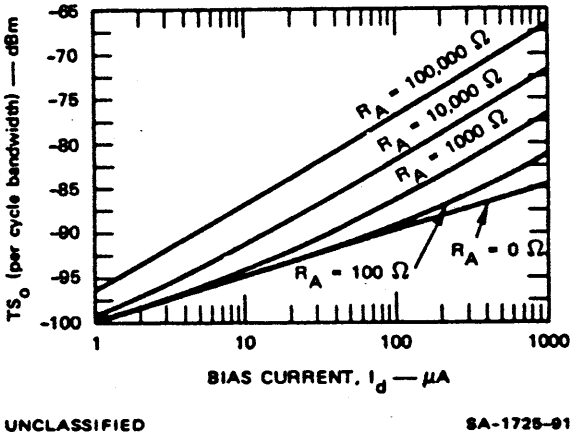

FIGURE IX-2 VARIATION OF TS_o WITH BIAS-CURRENT PARAMETER, R_A, EQUAL TO EQUIVALENT NOISE RESISTANCE OF VIDEO AMPLIFIER. Source: Ref. 12. (U)

On the other hand, a larger bias current reduces the junction resistance R_j and facilitates matching the diode at the RF frequency. Another benefit of a low R_j is that the detector square-law characteristic extends over a larger range. The limit increases 10 dB per decade change in bias

(U)

current and reaches a level of about -10 dBm at 200 μA, where the departure is only -1.5 dB from the square-law characteristic.

(U) The term TS_f is the ratio of the power delivered to the diode, to the power dissipated in the junction resistance. To be precise, this value must be computed from the insertion loss. The last term in Eq. (IX-1) is determined by the video bandwidth.

C. Optimized Impedance Matching (U)

(U) Figure IX-3 shows the equivalent circuit of only the detector part of the complete circuit. The HP 5082-2716 Schottky-barrier diode has been specially selected because it has the typical parameters C_j = 0.07 pF, R_s = 10 ohms, L_s = 0.1 nH, and C_p = 0.04 pF. These values guarantee a high cutoff frequency. The series combination of R_L and L_L is now adjusted to give as good a match to 50 ohms as possible.

(U) The values of R_j from 100 to 1000 ohms a few cases were analyzed. The capacitor C_B is most easily realized from an open-circuited

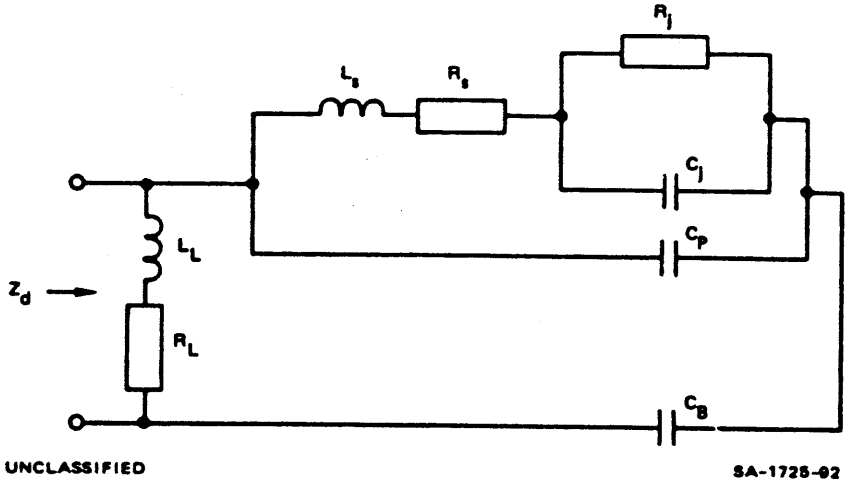

FIGURE IX-3 EQUIVALENT CIRCUIT OF THE SCHOTTKY-BARRIER DIODE WITH BYPASS CAPACITOR AND ADDITIONAL LOAD RESISTOR (U)

(U)

stub (or two stubs in parallel) of a low-impedance line λ/4 long at some frequency around the center of the band. The diode in series with C_B complements R_L and L_L. Impedance matches over the full band were found possible with VSWR ≤ 1.25. The loss ratio, TS_f, decreases slightly at higher frequencies, because less input power is lost in R_L. The sensitivity components TS_f and TS_o as functions of R_j for the selected diode are shown in Figure IX-4. The slope of the curve for TS_f declines as a function of frequency in the band of interest. The curve for TS_o is given for $R_A \geq 1000$ ohms, and is not quite as steep for lower noise resistances. The main result of this is that th· sum of TS_o and TS_f is virtually independent of R_j, so that R_j can be chosen independently.

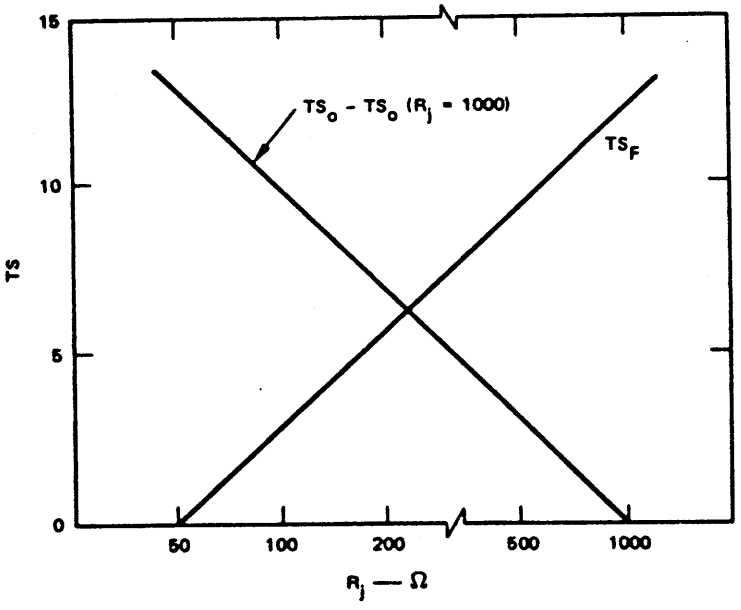

FIGURE IX-4 TS_o AND TS_f vs JUNCTION RESISTANCE R_j. The curve for TS_f is given for f = 10 GHz. The other curve is for $R_A > 1000$ ohms.

(U) Using an optimization technique for microwave networks, configurations with the following values were analyzed and optimized for a best match to the input line:

(1) R_j = 200 ohms. This value gives a reasonable range for the square-law characteristic, and it is fairly easy to achieve a good impedance match. All bonding wires were modeled in the program as transmission lines of high impedance. The calculated maximum VSWR for the complete limiter-detector is 1.25.

(2) R_j = 50 ohms. This requires a high bias current, but has the advantage that R_L can be left out. In addition, the series capacitor can be omitted, and L_L provides a dc return for the Schottky barrier as well as for the limiter diodes. However, the VSWR increases to a maximum of 1.5. But the elimination of two elements facilitates the fabrication and in practice may turn out to give results equivalent to R_j = 200 ohms.

An approximate layout and the corresponding values of the circuit elements are given in Figure IX-5. The capacitance values for the diodes obtained by the optimization should easily be realizable with at least two types of pin diodes.

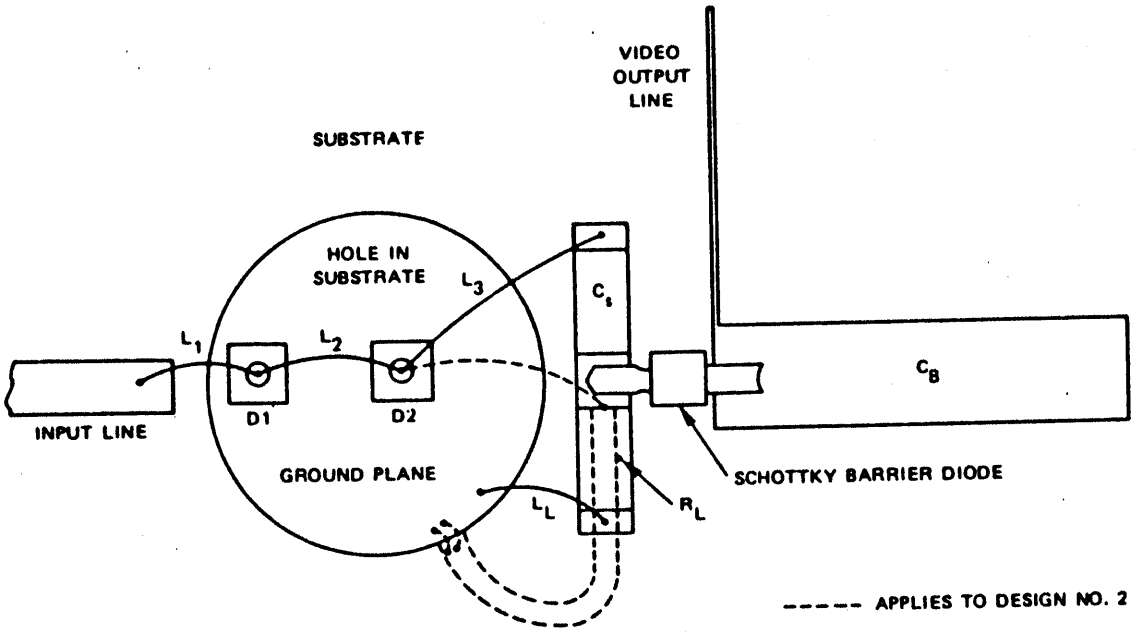

DESIGN NO.	R_j	L_1^* ℓ (in.)	C (D1) (pF)	L_2^* ℓ (in.)	C (D2) (pF)	L_3^* ℓ (in.)	C_s (pF)	R_L (Ω)	L_L ℓ (in.)	C_B Z_o	C_B ℓ (in.)
1	200	0.019	0.105	0.027	0.11	0.05	0.41	60	0.03	25	0.25
2	50	0.022	0.10	0.028	0.12	0.036	—	—	88 Ω/0.25"	24	0.28

* Wire diameter = 1 mil.

UNCLASSIFIED

SA-1725-84

FIGURE IX-5 APPROXIMATE LAYOUT OF THE LIMITER-DETECTOR ON MICROSTRIP (U)

(U)

Four screw and washer assemblies at the substrate corners are sufficient to provide adequate compressive force to eliminate air gaps from under the substrate and provide some shock mounting. The mode-suppressor pin engages the top and bottom ground planes by means of the holes visible in the center of the base and top cover.

B. Coaxial-to-Microstrip Transitions (U)

(U) At the beginning of the development of the wideband components, no commercially produced coaxial-to-microstrip transitions could be found that operated with suitably low VSWR through the upper end of P-band. A simple transition with the necessary performance was constructed from semirigid coaxial cable as shown in Figure X-2. A length of cable was used between the box and the connector in order to provide enough friction to effectively capture the center conductor. At the time of this development, commercial connectors with captured center pins had consistently high VSWR when compared to cable assemblies without center-pin capture. The coaxial structure was extended into the box wall and stepped down at constant impedance to a final size of 0.007 inch for attachment to the stripline circuit. This approach suffered somewhat from the variability from batch to batch of the semirigid coaxial cable. Some cables had significantly more friction than others between the conductors and the solid dielectric material. As a result, some of the transitions constructed in this manner allowed movement of the center conductor and subsequent breakage of the coaxial-to-microstrip joint.

(U) Toward the latter part of the component development, a suitable captured connector became available from Micromode Products, Inc. (Santee, California) that combined a flange and cable assembly. The transition was then shortened into a compact unit as shown in Figure X-1.

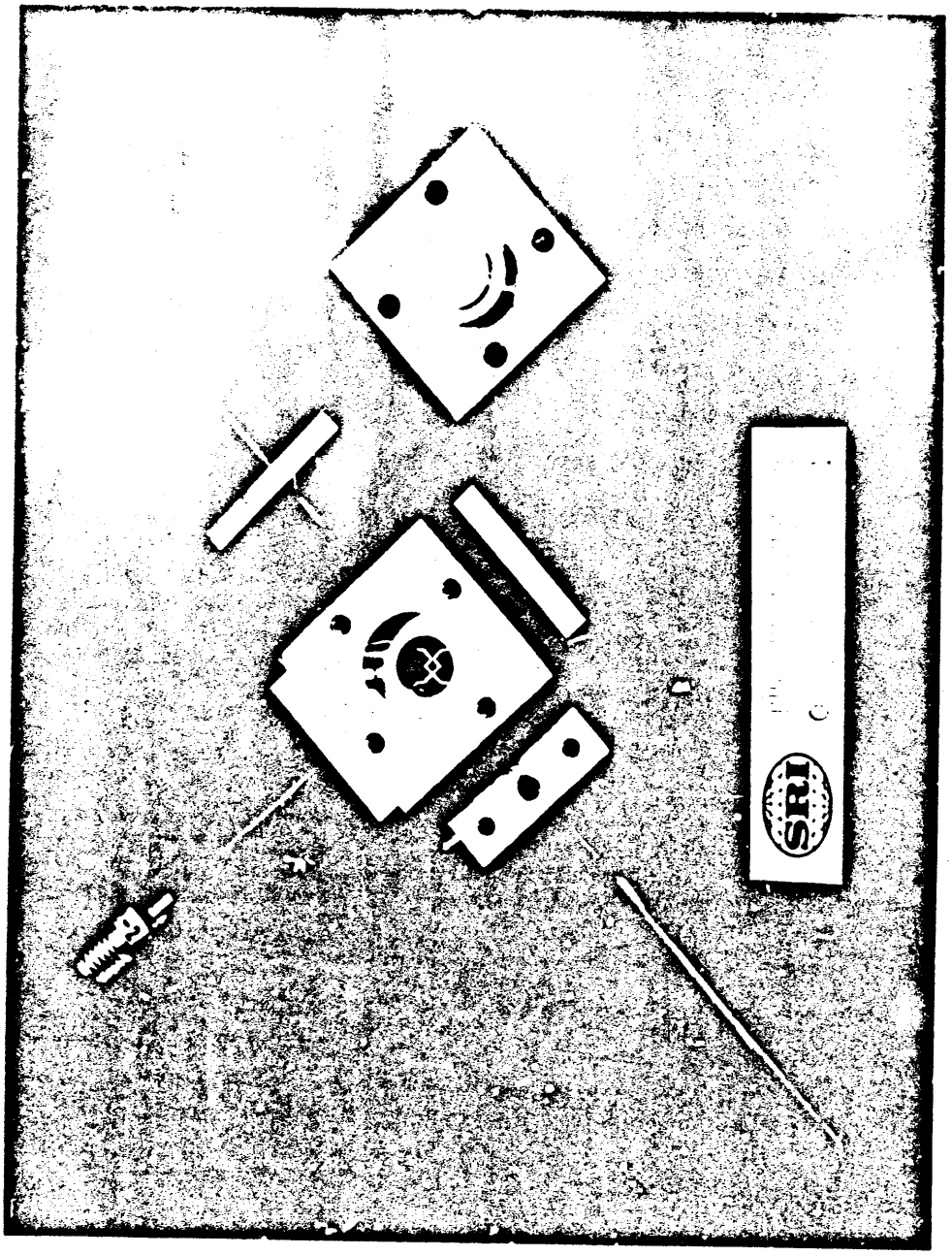

FIGURE X-2 EXPLODED VIEW OF 20 dB COUPLER SHOWING DETAILS OF COAXIAL-TO-MICROSTRIP TRANSITION (U)

(U) Figure X-3 shows the loss and VSWR for a Microcode cable assembly. The cyclic characteristic of the VSWR indicates that the major reflections are due to the connectors at the ends as expected. Overall, the cable assembly has good performance with a maximum average VSWR of less than 1.5 up to 18 GHz.

(U) A microstrip through-line assembly is shown in Figure X-4 (one connector is removed in the photograph); its measured characteristics are shown in Figure X-5. Presumably the peak in the VSWR curve is due to the sum of the reflections from the transitions plus connectors. On this basis, the VSWR per transition-connector combination is about 1.17. If a conservative VSWR value of 1.05 is used for the SMA connector from Figure X-3 at $f \approx 13$ GHz, the maximum VSWR of the coax-to-microstrip transition is 1.10. The electrical length of the total assembly is 5.1 cm. The mechanical distance across the microstrip substrate is 0.25 inch.

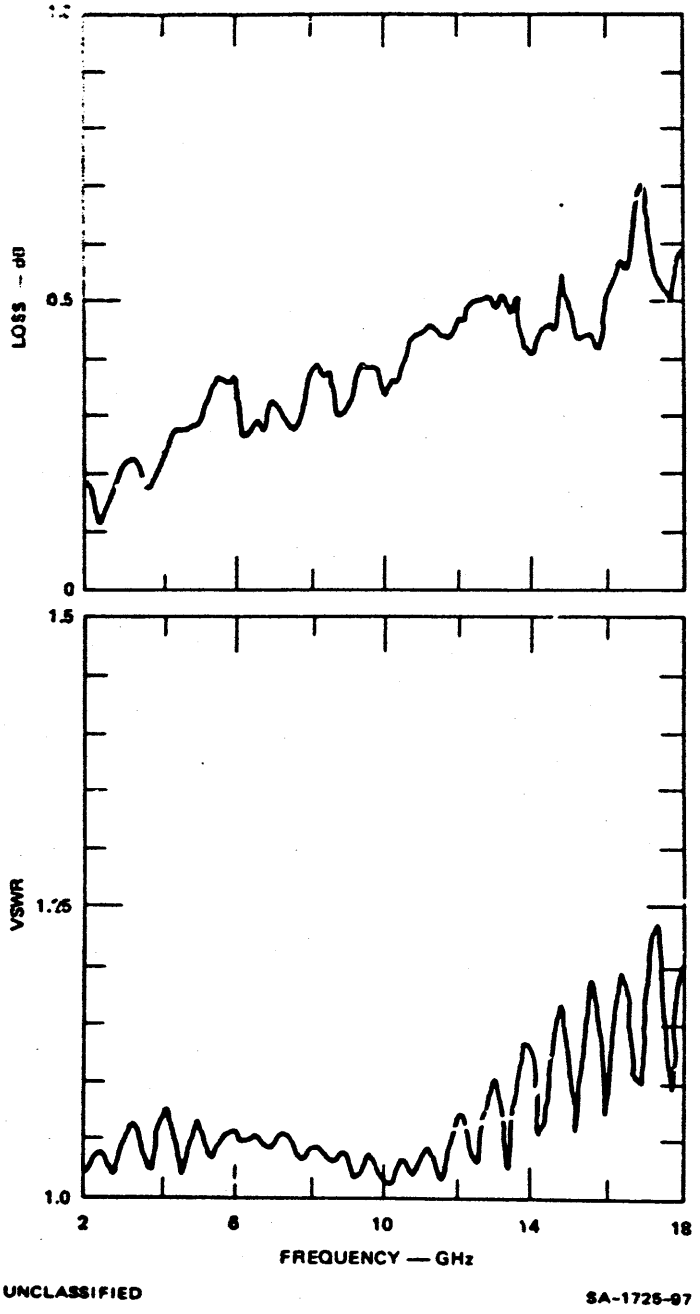

FIGURE X-3 TRANSMISSION AND REFLECTION CHARACTERISTICS OF 5-INCH-LONG, 0.084-INCH-DIAMETER SEMIRIGID COAXIAL CABLE WITH SMA CONNECTORS ON EACH END (Micromode Products, Inc.) (U)

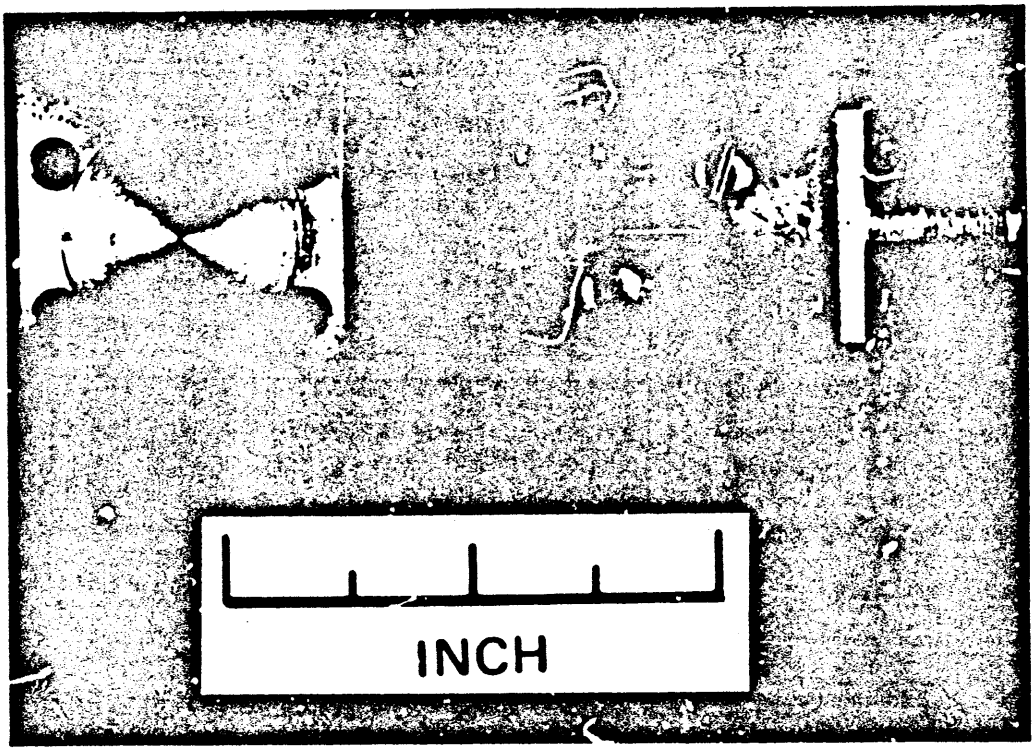

UNCLASSIFIED SA-1725-68

FIGURE X-4 MICROSTRIP THROUGH-LINE ASSEMBLY (one connector removed) (U)

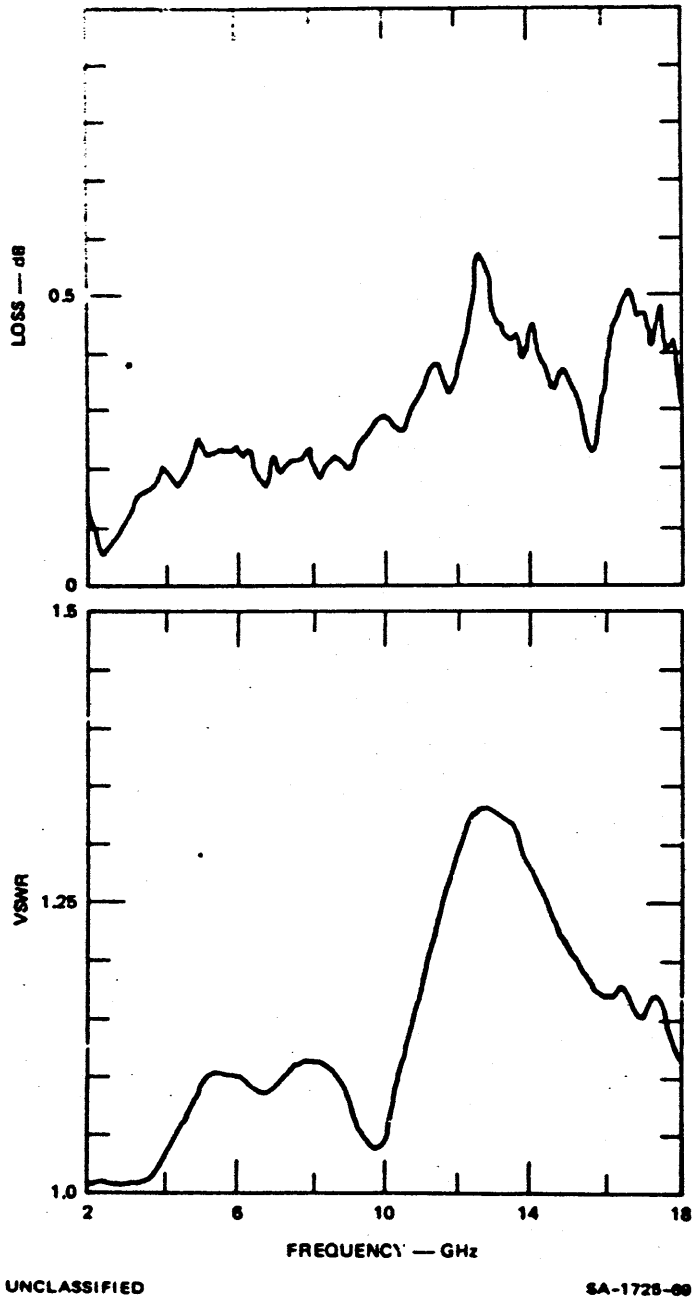

FIGURE X-5 TRANSMISSION AND REFLECTION CHARACTERISTICS FOR MICROSTRIP THROUGH-LINE AND SMA CONNECTORS (U)

REFERENCES

1. S. P. Hartwig, D. J. Masse, and R. A. Pucel, "Frequency Dependant Behavior of Microstrip," GMTT Symposium Digest, pp. 110-116 (May 1968), UNCLASSIFIED.

2. J. K. Shimizu and E. M. T. Jones, "Coupled-Transmission Line Directional Couplers," IRE Trans., Vol. PGMTT-6, pp. 403-410 (October 1958), UNCLASSIFIED.

3. G. Matthaei, L. Young, and E. M. T. Jones, Microwave Filters, Impedance-Matching Networks, and Coupling Structures, pp. 812-815, (McGraw-Hill Book Company, New York, N.Y.), UNCLASSIFIED.

4. T. J. Bryant and J. A. Weiss, "Parameters of Microstrip Transmission Lines and of Coupled Pairs of Microstrip Lines," IEEE Trans. on Microwave Theory and Techniques, Vol. MTT-16, pp. 1021-1027 (December 1968), UNCLASSIFIED.

5. R. Levy, "Directional Couplers," Advances in Microwaves, Vol. 1, p. 124 (Academic Press, New York, N.Y., 1966), UNCLASSIFIED.

6. A. F. Podell, "A High-Directivity Microstrip Coupler Technique," G-MTT 1970 International Microwave Symposium, May 11-14, 1970, IEEE Cat. No. 70C10-MTT, pp. 33-36, UNCLASSIFIED.

7. J. F. White and K. E. Mortenson, "Diode SPDT Switching at High Power with Octave Microwave Bandwidth," IEEE Trans. on Microwave Theory and Techniques, Vol. MTT-16, No. 1, pp. 30-36 (January 1968), UNCLASSIFIED.

8. W. Nelson, "Hybrid Circuits for Multioctave Multiple-Throw Microwave Switches," IEEE J. Solid-State Circuits, Vol. SC-3, No. 3, pp. 243-246 (September 1968), UNCLASSIFIED.

9. J. Millman and H. Taub, Pulse, Digital, and Switching Waveforms (McGraw-Hill Book Company, Inc., New York, N. Y., 1965), UNCLASSIFIED.

10. J. G. Linvill, Models of Transistors and Diodes (McGraw-Hill Book Company, Inc., New York, N.Y., 1963) UNCLASSIFIED.

11. B. M. Schiffman, "A New Class of Broad-Band Microwave 90-Degree Phase Shifters," IRE Trans. on Microwave Theory and Techniques, Vol. MTT-6. No. 4, pp. 232-237 (April 1958), UNCLASSIFIED.

12. "The Hot Carrier Diode, Theory, Design, and Application," HPA Application Note 907, Hewlett-Packard Associates, Palo Alto, Calif., UNCLASSIFIED.

END

DATE
FILMED
1-75